UNIVERSITY
OF MICHIGAN
APR -1
PHYSICS
LIBRARY

REGISTERED No. M. 3121

PROCEEDINGS

OF THE

INDIAN ACADEMY

OF SCIENCES

VOL. XXXVI] *SECTION A* [No. 6

DECEMBER 1952

Price Rs. 2 or 3 Sh. *Annual Subscription Rs. 18*

PRINTED AT THE BANGALORE PRESS, BANGALORE CITY, BY G. SRINIVASA RAO, SUPERINTENDENT, AND PUBLISHED BY THE INDIAN ACADEMY OF SCIENCES, BANGALORE.

ON THE POLARISATION AND SPECTRAL CHARACTER OF THE IRIDESCENCE OF POTASSIUM CHLORATE CRYSTALS

By Sir C. V. Raman and D. Krishnamurti

(From the Raman Research Institute, Bangalore)

Received November 27, 1952

1. Introduction

In a series of three recent papers in these *Proceedings*, we described and discussed the results of studies made with material selected from the rather extensive collection of iridescent crystals of potassium chlorate at our disposal. In particular, we dealt with the spectral character and polarisation of the iridescence of five selected crystals the optical behaviour of which indicated a high degree of regularity in their structure. Since then, we have made observations with a dozen other crystals of the same kind over a wider range of azimuths and obliquities of incidence than previously. A fairly complete picture of the phenomena has emerged from these studies. It is proposed in the present paper to describe our findings and to illustrate the same by a new set of spectrograms obtained with a typical specimen.

2. Some Theoretical Considerations

Potassium chlorate is a strongly birefringent crystal and the reflections which give rise to the iridescence owe their origin to the fact that the alternate layers of the polysynthetically twinned crystal are orientated differently from the rest. It might seem in these circumstances that a theoretical treatment of the problem would be very complicated. Fortunately, however, there are circumstances which considerably simplify the situation. In the first place, all the layers in the polysynthetic crystal have a common symmetry plane and a common axis perpendicular to it which coincides with the direction of maximum optical polarisability. Then again, while potassium chlorate is actually a biaxial crystal, its optical behaviour is not very different from that of an uniaxial crystal. In dealing with the problem, therefore, one can use the phraseology appropriate to an uniaxial crystal, and speak of an ordinary and an extraordinary beam, the directions of vibration in which are determined by the position of the optic axis (which is the direction of least polarisability) relatively to the direction of the wave-normal.

A beam of unpolarised light incident on the face of the crystal divides upon entry into two beams of light, *viz.*, the ordinary and the extraordinary

beams polarised in perpendicular planes. In the particular case when the directions in which these beams traverse the crystal lie in the symmetry plane, the ordinary and the extraordinary beams retain their character as such in their entire course through the crystal. In such a case, of course, there is no reflection at the twin-plane boundaries. So long as the directions of propagation do not deviate largely from the symmetry plane, we are justified as a first approximation in assuming a similar situation to subsist, *viz.*, that an ordinary beam remains an ordinary one and an extraordinary beam as extraordinary throughout. Similar assumptions may also be made in the same circumstances about the beams of light arising from the internal reflections. In other words, it will be assumed that light reflected as an ordinary or as an extraordinary beam retains this character until its final emergence from the crystal.

As has already been shown in the second of our earlier papers, the state of polarisation of a light beam traversing the crystal and reflected at a twin-plane boundary changes from the ordinary to the extraordinary and *vice versa* in the act of reflection, irrespectively of the angle of incidence, provided that the directions of the incident and reflected beams do not deviate greatly from the plane of symmetry, and the reflections are in consequence very weak. More generally, an ordinary beam is reflected both as an extraordinary and as an ordinary beam, while similarly an extraordinary beam is reflected both as ordinary and as extraordinary. The strength of the second component relatively to the first in each case would be determined jointly by the azimuth and by the obliquity of incidence, and may reach considerable values if the azimuthal angle as well as the angle of incidence are large.

3. SPECTRAL CHARACTER OF THE REFLECTIONS

Thus, in general, we have four sets of reflected beams generated at each of the twinning planes in the crystal and finally emerging from it. For convenience we can refer to them as the *o–o*, *o–e*, *e–o* and *e–e* reflections, the first letter indicating the state of polarisation in the incident light and the second in the reflected light. In general, also, the total optical path traversed in all these four cases would be different, and hence the wavelength for which the intensity of reflection is a maximum at any given angle of incidence, would be different for these four beams. Thus, in general, we should have four different reflection maxima in the spectrum; all the four would be plane-polarised, but in different ways. Since the ordinary index is substantially greater than the extraordinary index, it follows that the *o–o* reflection maximum would have the greatest wavelength of the four and that the *e–e* reflection maximum would have the smallest. Between them would lie the *o–e* and the *e–o* reflection maxima.

An explanation is necessary here to indicate why the positions of the *o–e* and the *e–o* reflection maxima in the spectrum would not in general be identical. The direction of minimum optical polarisability in potassium chlorate makes an angle of 38° with the normal to the surface of the plate. The refractive index of the ordinary ray is approximately independent of the directions of the incident and reflected beams within the crystal. But this is not the case in respect of the extraordinary index, which would be greater for the incident beam and less for the reflected beam or *vice versa* according as the light is incident on one side or the other of the normal to the plate. The position in this respect is reversed when we consider the alternate layers of the twinned crystal, since in the latter the direction of minimum polarisability is situated on the opposite side of the normal. There is thus a compensation which would be complete if the alternate layers in the polysynthetically twinned crystal are of equal thickness. In such a case the total optical paths for the *o–e* and the *e–o* reflected beams would be identical, and instead of a quartet of reflection maxima in the spectrum we would in general have only a triplet. There is no reason however for assuming that the periodic twinning of the crystal is always or even frequently of the special type referred to above. A regular periodic twinning is consistent with the alternate layers being of different thickness. In such a case it would follow that the total optical path for the *o–e* reflection is greater than the path for the *e–o* reflection, or *vice versa*.

4. Some Consequences of the Theory

The considerations set forth above have several verifiable consequences. In the first place, if the azimuth of incidence is 90°, *i.e.*, if the plane of incidence be normal to the plane of symmetry and the reflections are hence of maximum intensity, the incident and reflected beams lie symmetrically on either side of the normal, and hence the *o–e* and the *e–o* paths are necessarily identical irrespective of the angle of incidence and the nature of the twinning. Hence it follows that in this particular azimuth and irrespective of the angle of incidence, the *o–e* and the *e–o* reflections would overlap and the quartet of reflection maxima would be reduced to a triplet.

A second verifiable consequence of the theory is the effect of rotating the crystal in its own plane through two right angles. As the result of such rotation, the directions of travel of the incident and reflected beams with reference to the orientations of the optic axis within each layer of the crystal would be reversed. Hence the *o–e* and the *e–o* reflection maxima should also reverse their positions in the spectrum and such reversal should take place in a continuous manner, the two reflections approaching each other and coinciding when the azimuthal angle is 90°, and thereafter separating

again when the crystal is rotated further. That an interchange between the *e–o* and the *o–e* reflections is thus brought about would be indicated by a corresponding interchange in the plane of polarisation of these reflection maxima in the spectrum.

Another verifiable consequence is that the separation of the *o–e* and the *e–o* reflections of the spectrum would vary from specimen to specimen and in particular cases actually vanish, whereas the *o–o* and the *e–e* reflections would be widely separated in the spectrum in all cases, and their planes of polarisation would not be reversed when the crystal is turned round through 180°.

It follows from what has been stated earlier that the *o–o* and *e–e* reflections would vanish completely if the azimuth of incidence is nearly coincident with the plane of symmetry, and this is irrespective of the angle of incidence. Thus, for such azimuths, the quartet of reflections would reduce to a doublet the components of which would be polarised in perpendicular planes, the separation of the components also varying from specimen to specimen. The separation of the doublets should also increase with the angle of incidence. But the simultaneous spectral widening of the reflection maxima would not be very conspicuous in view of the small reflecting power at such azimuths of incidence.

Observed at nearly normal incidence, the *o–o* and the *e–e* components would vanish in all cases. If in addition the azimuth of observation is 90°, the *o–e* and the *e–o* components would also coincide. Thus instead of a quartet of reflection maxima, we would obtain a single and fairly sharply defined maximum in the spectrum. At more oblique incidences, the *o–o* and the *e–e* components would make their appearance; for any given angle of incidence, their intensity would be greatest when the azimuth of observation is 90°, whereas they would vanish when the azimuthal angle is 0° as already remarked. At intermediate azimuths, they may be expected to be visible but less conspicuously. When the azimuth of incidence is 90°, the *o–e* and the *e–o* components would appear overlapping each other in the same position. Hence at this azimuth the single sharp maximum which is seen at nearly normal incidence alters into a triplet when the incidence is made more oblique.

From what has been stated above, it follows that neither at an azimuth 0° nor at an azimuth 90° would the quartet of reflection maxima indicated by the theory be observable. The most favourable case for viewing it is when the azimuth of incidence is neither too small nor too large, and the incidence should also be fairly oblique, as otherwise the separation of the *o–e* and the *e–o* components may be too small to be detectable.

5. Description of the Spectrograms

The various features set forth above are illustrated in the series of spectrograms reproduced as Figs. 1 to 4 in Plate XVII and as Figs. 1 to 4 in Plate XVIII. These were recorded with a crystal which at nearly normal incidence exhibited a highly monochromatic iridescence at λ 5665 with a spectral width of about 25 A.U. A reflection of higher order is recorded at the same incidence at λ 4280, while a reflection of lower order comes into view at the extreme red end of the spectrum at oblique incidences. From these facts it is readily deduced that the reflection at λ 5665 is of the third order. The actual values of the azimuthal angle of incidence (ϕ) measured from the plane of symmetry and of the obliquity of incidence (θ) measured from the normal to the surface are indicated against each of the spectrograms in the figures.

Fig. 1 in Plate XVII reproduces a series of seven spectrograms taken at an azimuthal angle of about 5°, the angle of incidence increasing in steps from 5° to 65°. It will be seen that the reflection maximum is recorded as a doublet the components of which drift apart from each other and also towards shorter wavelengths with increasing obliquity. If the increasing dispersion of the instrument in the region of shorter wavelengths is taken into account, it will be seen that there is hardly any increase in the spectral width of each component with increasing obliquity of incidence. Fairly large exposures of the order of half an hour had to be given to record the doublets. This exposure, though considerable, fails to bring out the true secondary spectrum. Fig. 2 in the same Plate exhibits the polarisation of the doublet. The two spectrograms in the figure were recorded with equal exposures, a nicol being placed in front of the slit of the spectrograph with its vibration directions respectively vertical and horizontal. It will be seen that in the one case the component on the longer wavelength side has been extinguished while in the other the component on the shorter wavelength side has disappeared. Fig. 3 in the same Plate exhibits the reversal in the position of the two components produced by rotating the crystal through 180° in its own plane, the arrangements being otherwise identical with those used for recording Fig. 2.

Fig. 4 in Plate XVII shows the typical quartet spectrum. It will be seen that the two central components are both much wider and much more intense than the two outer ones. The latter indeed remain quite sharp even at oblique incidences whereas the former have widened out notably. A whole series of subsidiary maxima can be distinctly seen in the spectrograms recorded at the more oblique incidences. In the same figure the central doublet of the reflection of the higher order has come out weakly in two of the

spectrograms, and it will be seen that they are much sharper and more clearly separated than in the lower order reflection.

The seven spectrograms reproduced as Fig. 1 in Plate XVIII were recorded at an azimuthal angle of 60°. It will be seen that the increased azimuthal angle has brought about a notable increase in the intensity of the outer components as well as a diminution in their sharpness. Likewise, the two central components have broadened out so much so that at moderate obliquities they are hardly separated from each other. The separation is however clearly seen in the second order reflection appearing near the violet end of the spectrum. At the more oblique incidences the two central components though greatly broadened, are clearly separated. They are however so broad that they have masked the outermost components. The secondary maxima are clearly seen in many of the spectrograms.

Fig. 4 in Plate XVIII shows the triplet spectrum recorded at an azimuthal angle of 90°. The appearance of the outer components and the increase in their intensity and width as well as of the central component at increasing obliquities of incidence are clearly shown. Fig. 2 in the same Plate exhibits the polarisation of the outer components of the triplet and the lack of polarisation in the central component. The spectrograms shown in that figure were recorded by placing a nicol in front of the slit of the spectrograph with its vibration directions respectively vertical and horizontal and giving equal exposures. Fig. 3 was recorded under identical conditions except that the crystal was turned round in its own plane through 180°. It will be noticed that the components have now *not* interchanged their positions.

6. SUMMARY

It is shown from theoretical considerations and confirmed by the spectrograms reproduced in the paper that the sharply defined monochromatic reflection observed at nearly normal incidences splits up into a quartet in the general case of any arbitrary azimuth and obliquity of incidence. The outer components disappear thereby reducing the quartet into a doublet when the azimuthal angle is small. But if the azimuthal angle be 90° the two central components merge and the quartet reduces to a triplet. When the crystal is rotated in its own plane the two central components of the quartet come together, overlap and move out again in the same direction, thereby giving rise to a reversal of their polarisation characters. They owe their origin to the alternate layers of the polysynthetically twinned crystal being of unequal thickness.

REFERENCES

Raman, C. V. and Krishnamurti, D. .. *Proc. Ind. Acad. Sci.*, 1952, **36**, 315, 321, 330.

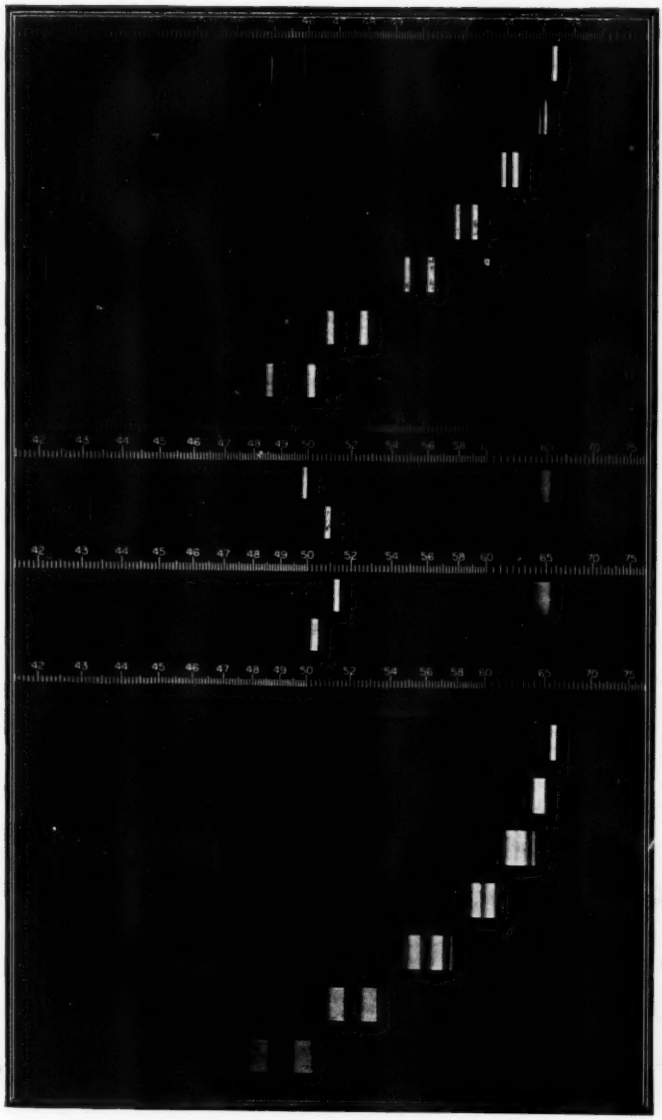

FIG. 1

FIG. 2

FIG. 3

FIG. 4

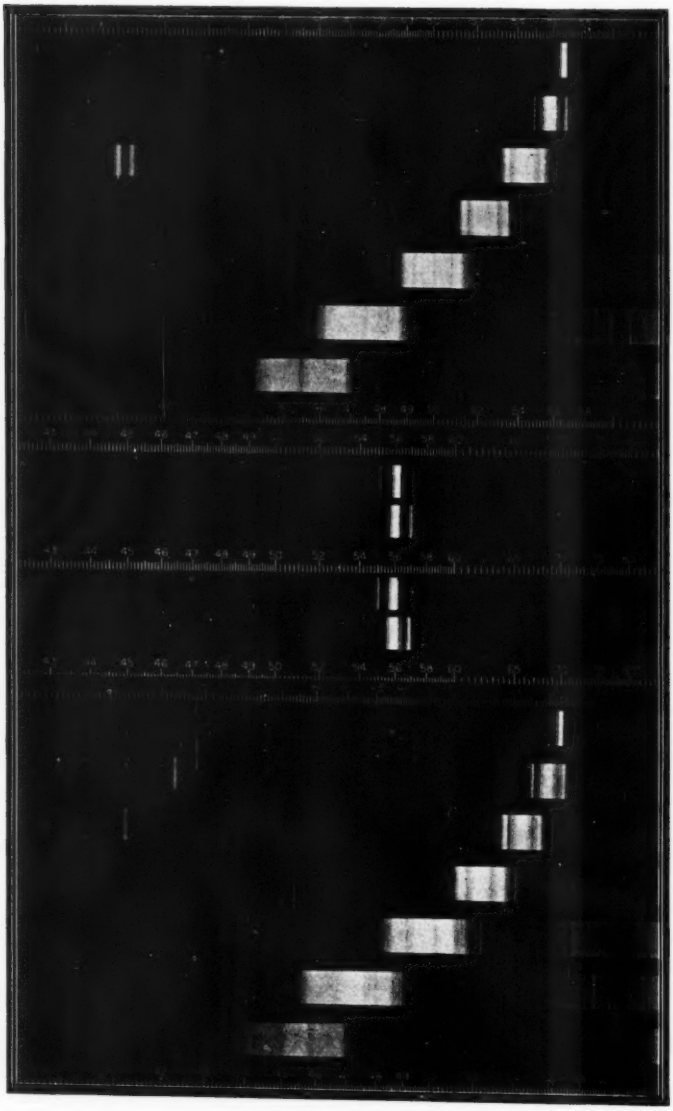

FIG. 1

FIG. 2

FIG. 3

FIG. 4

STUDIES IN THE CHEMICAL BEHAVIOUR OF SOME COMPOUNDS OF SULPHUR

Part II. Reaction Between Disulphur Monoxide and Hydrogen Iodide

By A. R. Vasudeva Murthy

(*Indian Institute of Science, Bangalore*)

Received July 23, 1952

(Communicated by Dr. B. Sanjiva Rao, F.A.SC.)

Introduction

B. S. Rao[1] obtained disulphur monoxide in the form of an orange-yellow solution in carbon tetrachloride and found that the oxide was stabilised by elemental sulphur. Stamm and Wiebusch[2] suggested that the orange-yellow solution consisted of "Polysulphur oxide". They studied the reaction between this liquid and a solution of hydrogen iodide in anhydrous formic acid and reported the reaction to be

$$S_xO + 2HI \rightarrow xS + H_2O + 2I.$$

Preliminary experiments by the present author, on the reaction between hydrogen iodide and the so-called "Polysulphur oxide" solution, showed that the reaction was far more complicated than had been realised by Stamm and his coworkers. For instance, it was found that hydrogen sulphide was one of the products of reaction. Its formation had not been reported by previous workers. A detailed study of the reaction was therefore undertaken.

Experimental

Carbon tetrachloride

Carbon tetrachloride (C.P. quality) was shaken with mercury for several hours to remove traces of sulphur. After filtration, the liquid was dried over phosphorus pentoxide and distilled in an all-glass apparatus, provided with a spray trap. The distillate was tested with mercury and found to be entirely free from sulphur. In storing, the dry tetrachloride was carefully protected from atmospheric moisture.

Anhydrous formic acid

Preparation of anhydrous formic acid presents certain difficulties. Methods for the preparation of the anhydrous acid have been reviewed by Weissberger and Proskauer.[3] The azeotropic process[4] has been successfully

employed for the commercial preparation of anhydrous formic acid, but cannot conveniently be used on the laboratory scale. Common desiccants like calcium chloride or phosphorus pentoxide are unsuitable, as they react with the acid. Boric anhydride however, is quite satisfactory.

Pellets of boric anhydride were prepared by carefully heating recrystallised boric acid in a stainless steel dish to 900° C. in an electric furnace and pouring the molten mass into carbon tetrachloride kept at — 16° C. The pellets were removed and kept in a vacuum desiccator and freed from carbon tetrachloride by evacuation.[5, 6, 7]

Formic acid (Merck, A. R.) containing about 1% water was freed from moisture by keeping in a flask in contact with pellets of boric oxide for about a week. It has to be pointed out that it is not desirable to store anhydrous formic acid in a stoppered flask for any length of time. There were three accidents in this laboratory owing to the bursting of stoppered flasks in which anhydrous formic acid had been stored. The cause of the accidents was found to be the development of pressure due to carbon monoxide, liberated by slow decomposition of formic acid (*cf.* Coolidge[8]). In storing the anhydrous acid, the stopper of the flask should be fitted with a safety U-tube filled with boric oxide pellets, and open to the atmosphere. Before use, the anhydrous acid was always freshly distilled under reduced pressure (12 to 18 mm. of Hg) at 22 to 25° C. in an all-glass apparatus. The acid was found to be free from water as determined by the critical solution temperature technique described by Ewins,[9] with benzene as solvent.

Anhydrous Hydrogen Iodide

Heisig and Lingane[10] have critically examined methods for the preparation of hydriodic acid and recommend the production of hydrogen iodide by the union between hydrogen and iodine vapour in presence of platinised asbestos as catalyst.

In the present investigation, the apparatus used by Heisig and Lingane was suitably modified to deliver pure dry hydrogen iodide. The hydrogen iodide was frozen in a tube cooled by liquid air and conveyed by sublimation to previously evacuated storage flasks one of which is shown in Fig. 1 giving a sketch of the apparatus employed.

To remove traces of oxygen in the electrolytic hydrogen, the gas was passed over platinized asbestos heated electrically to 450° C. and the moisture formed was absorbed by phosphorus pentoxide. The hydrogen picked up iodine from bulb A kept at 160° C. (in an oil bath) and when passed over platinised asbestos maintained at 600° C., produced hydrogen iodide. The

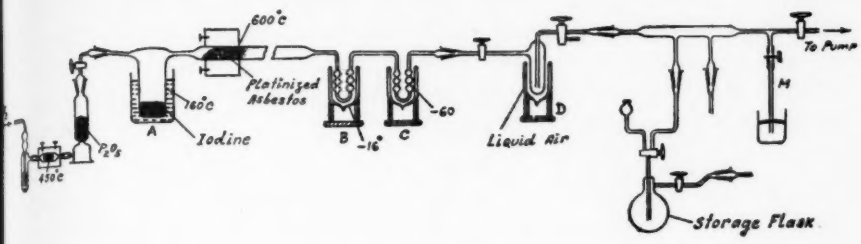

FIG. 1

uncombined iodine was frozen in B kept at −16° C. (freezing mixture) and the hydrogen iodide was completely stripped of iodine in C kept at −60° C. (alcohol cooled by solid carbon dioxide) and finally frozen in D, cooled by liquid air.

When sufficient hydrogen iodide had collected in D, the heating was stopped, but the stream of hydrogen was continued until the catalyst mass cooled down. After evacuation, the hydrogen iodide was allowed to evaporate into the storage flasks till the pressure rose to about 50 cm. of mercury as ascertained by momentary contact with the mercury manometer M.

The hydrogen iodide was quite free from iodine, there being no colouration when carbon tetrachloride was let into a storage flask.

Disulphur monoxide solution in carbon tetrachloride

The products of combustion of sulphur in oxygen at a pressure of 5–7 mm. of Hg were passed into an absorption vessel containing about 40 ml. of pure, dry carbon tetrachloride. The carbon tetrachloride was kept at − 16° C. (alcohol + carbon dioxide snow). An orange-yellow solution of disulphur oxide was obtained in about 30 minutes. To remove the sulphur dioxide present in the carbon tetrachloride, the combustion of sulphur was stopped and the stream of oxygen continued for 20 minutes. It was found that in this way, the sulphur dioxide could be completely removed. It was unnecessary to employ an inert gas to sweep off the sulphur dioxide (*cf.* B. S. Rao[1]). On removal of the sulphur dioxide, the carbon tetrachloride solution was transferred to a graduated weight-pipette of the Lung-Rey type containing an adequate amount of cooled carbon tetrachloride, to effect dilution.

Analysis of disulphur monoxide solution

The orange-yellow solution was analysed in the following way:—

(i) An aliquot was shaken up with mercury in an all-glass assembly, when the disulphur monoxide decomposed and formed sulphide of mercury,

liberating sulphur dioxide. The mercury sulphide was estimated by the method of B. S. Rao and M. R. A. Rao.[11] The sulphur dioxide was swept away in a stream of hydrogen (or nitrogen) and absorbed in 2N caustic soda solution (holding some cadmium hydroxide in suspension) and the sulphite formed was determined iodometrically.

(ii) Another aliquot of the yellow solution was transferred to a storage flask containing hydrogen iodide under reduced pressure. The products of the reaction (which was rapid) were hydrogen sulphide, iodine and water. After 10 minutes, dry nitrogen (or hydrogen) was bubbled through the carbon tetrachloride for one hour and the liberated hydrogen sulphide was absorbed in alkali (holding cadmium hydroxide in suspension) and was estimated iodometrically. No sulphite could be detected in the alkali absorbent. Iodine present in the carbon tetrachloride solution was estimated, after shaking the solvent with a strong aqueous solution of potassium iodide and titrating the iodine in the aqueous phase with standard thiosulphate. The carbon tetrachloride was then tested for the presence of elemental sulphur. In general, no sulphur was present in the solvent.

The results which are given in Table I show that the sulphur oxide held in solution by the carbon tetrachloride is disulphur monoxide. The sulphur

TABLE I

Reactions of Disulphur Monoxide

Serial No. of S_2O soln.	Decomposition by mercury				Reduction with hydrogen iodide				
	SO_2 obtained*	Elemental sulphur	Ratio of elemental sulphur to SO_2 S:SO_2	$S+S_2O$ present	H_2S obtained	Iodine liberated in g. atoms $\times 10^6$	Ratio of iodine to sulphur as H_2S	Elemental sulphur	S_2O corresponding to H_2S
1	14·95	45·4	3·01	60·35	60·86	183·3	3·01	..	60·86
2	6·01	17·83	2·96	23·83	23·75	72·85	3·06	..	23·75
3	27·68	82·15	2·97	109·83	109·05	329·86	3·02	1·08	109·05
4	23·10	68·20	2·96	91·30	89·85	270·4	3·00	1·21	89·85
5	10·86	33·50	3·08	44·36	44·50	132·4	2·98	..	44·5
6	18·96	56·85	3·07	75·81	75·05	225·1	3·00	1·15	75·05
	Average 3·01				Average 3·01				

* The quantities of disulphur monoxide taken and of the products of its reaction have been expressed in g. atoms of sulphur per g. of the original solution and have been multiplied by 10^6.

in combination with oxygen is quantitatively converted into hydrogen sulphide, and for every gram molecule of hydrogen sulphide formed, 3 gram atoms of iodine are liberated, the reaction being:

$$S_2O + 6HI \rightarrow 2H_2S + H_2O + 6I.$$

The experiments in which the carbon tetrachloride solution is treated with mercury also show that the sulphur oxide in solution is disulphur monoxide, for we get 3 gram moles of mercuric sulphide for every gram mole of sulphur dioxide, in terms of the equation

$$2S_2O + 3\,Hg \rightarrow 3\,HgS + SO_2.$$

Non-reducibility of elemental sulphur by hydrogen iodide at laboratory temperatures

For the purposes of the present investigation it was of importance to know if hydrogen iodide had any reducing action on sulphur at laboratory temperatures. A solution of known concentration of elemental sulphur in carbon tetrachloride was brought in contact with hydrogen iodide, air being carefully excluded. No iodine was liberated and quantitative estimations showed that the sulphur was entirely in the elemental state at the end of the experiment. Similar experiments were also carried out with elemental sulphur formed on keeping for a long time carbon tetrachloride solutions of disulphur monoxide, the sulphur dioxide formed during the decomposition of the lower oxide, being completely removed. No iodine was at all liberated.

Reaction between sulphur dioxide and hydrogen iodide

It is known that hydrogen iodide reduces sulphur dioxide to hydrogen sulphide. In the present investigation, it was necessary to examine the quantitative aspects of the reaction. A carbon tetrachloride solution of pure sulphur dioxide was standardised iodometrically. Aliquots were introduced into bulbs containing hydrogen iodide. The quantity of hydrogen iodide employed in each case was of the order of 600 to 650×10^{-6} g. mole per g. of the carbon tetrachloride solution. There was immediate reaction and the solvent turned yellowish violet. On keeping however, the normal colour of iodine in carbon tetrachloride solution was obtained. This suggested the possibility of the intermediate formation of the iodide or oxyiodide of sulphur.

This aspect of the reaction has been studied in detail and will be dealt with in a separate paper.

When the decomposition of the intermediate compound was complete, dry nitrogen (or hydrogen) was bubbled through the bulb and the

gaseous products were observed in 2N alkali holding some cadmium hydroxide in suspension. The sulphide and sulphite formed, were determined iodometrically. Iodine and free sulphur present in solution in carbon tetrachloride were also estimated by methods described earlier. The results are given in Table II.

TABLE II

Reaction between Sulphur Dioxide and Hydrogen Iodide

Expt. No.	SO_2 taken*	H_2S obtained	SO_2 unreacted	Free sulphur liberated	Iodine liberated (in g. atoms × 10^6 per g.)	Ratio of Iodine to Sulphur I : S	% SO_2 reduced to H_2S	% SO_2 reduced to S	% SO_2 unreacted	% SO_2 accounted for
1	10·30	10·25	..	..	62·10	6·05	99·5	..	..	99·5
2	3·27	3·25	..	..	20·10	6·19	99·4	..	..	99·4
3	6·95	6·90	..	..	41·13	5·98	99·3	..	..	99·3
4	85·70	41·20	25·40	19·30	290·6	7·05	48·7	22·5	29·6	100·8
5	64·6	30·80	18·36	15·60	225·4	7·30	47·7	24·1	28·5	100·3
6	352·0	3·5	256·0	93·60	452·0	129·0	1·0	26·6	72·7	100·3

* Quantities of sulphur and its compounds have been expressed in g. atoms of S × 10^6 per g. of solution.

The results given in the table show that under favourable conditions, hydrogen iodide reduces sulphur dioxide quantitatively to hydrogen sulphide in terms of the equation:

$$SO_2 + 6HI \rightarrow H_2S + 2H_2O + 6I.$$

For the above reaction to be quantitative, two conditions however, have to be fulfilled: (*a*) The sulphur dioxide concentration in carbon tetrachloride should be low (of the order of 10×10^{-6} g. mole per g. of solvent); (*b*) A large excess of hydrogen iodide should be present. The iodide employed should be at least ten times the amount required to react with the sulphur dioxide.

In experiments 4 to 6, Table II, the concentration of hydrogen iodide remained the same as in the earlier experiments while that of sulphur dioxide increased. As a result, the reduction of sulphur dioxide was incomplete, about 25% of the oxide being left unreacted in experiments 4 and 5 and about 70% in experiment 6. When the initial concentration of sulphur dioxide was of the order of 75 g. atoms $\times 10^{-6}$ per gram of the solution only 50% of the sulphur dioxide that had reacted, was converted into hydrogen

sulphide (the final product of reduction). In the last experiment where the concentration of sulphur dioxide was about 350×10^{-6} g. atom per g. of solution, only 1 to 2% of the sulphur dioxide was reduced to hydrogen sulphide.

As will be shown in a subsequent paper, the reaction between sulphur dioxide and hydrogen iodide takes place in several stages. The intermediate products are thionyl iodide and sulphur iodide, while the final product of reduction is hydrogen sulphide. The intermediate compounds are highly unstable and if the concentration of hydrogen iodide is inadequate to bring about rapidly, further reduction, these intermediate compounds suffer decomposition and yield elemental sulphur.

Reaction of disulphur monoxide solution in carbon tetrachloride with hydrogen iodide solution in formic acid

As already indicated, Stamm and Wiebusch[2] thought that " polysulphur oxide " was formed when the products of combustion of sulphur under low pressure of oxygen were passed through cold carbon tetrachloride. For analysis of the oxide, they employed formic acid solutions of hydrogen iodide or of potassium iodide and added water before estimating the iodine liberated. They calculated the oxygen in combination with sulphur on the assumption that each atom of oxygen corresponded to 2 atoms of iodine. The present author has found that hydrogen sulphide is formed when the orange yellow solution in carbon tetrachloride is treated with hydrogen iodide. Failure on the part of Stamm, *et al.*, to detect the hydrogen sulphide was due to the fact that on liberation of iodine, they added water to the reaction mixture. In presence of water, the iodine reacted with hydrogen sulphide, and also with sulphur dioxide, if any was present. Another unsuspected complication has been the catalytic decomposition of the lower oxides of sulphur by the formic acid employed as a solvent for hydrogen iodide by Stamm, *et al.* Such decomposition would materially reduce the production of hydrogen sulphide. Analytical determinations by the present author, employing hydrogen iodide without any formic acid have shown that the " poly-sulphur oxide " reported by the previous workers is practically pure disulphur monoxide. A detailed study was made of the influence of anhydrous formic acid on the reduction of the oxides of sulphur by hydrogen iodide.

Whether iodine (in carbon tetrachloride solution) had any action on sulphur dioxide or on hydrogen sulphide, in presence of anhydrous formic acid was first determined. To aliquots of iodine solution ($134 \cdot 8 \times 10^{-6}$ g. atoms per g. of carbon tetrachloride) in an all-glass apparatus out of contact with air, were added sulphur dioxide solutions ($66 \cdot 6 \times 10^{-6}$ g. atom of S per g.)

in carbon tetrachloride and 50 ml. of anhydrous formic acid. After various intervals ranging from 1 to 24 hours the contents were analysed for sulphur dioxide and iodine. It was observed that no iodine was consumed by the sulphur dioxide. Similar results were obtained when hydrogen sulphide was used instead of sulphur dioxide.

Aliquots of the orange-yellow solution (of disulphur oxide in carbon tetrachloride) were introduced into each of three bulbs A, B and C. A contained hydrogen iodide, B had the same quantity of the halide but dissolved in anhydrous formic acid (50 ml.) and C contained 50 ml. of the formic acid and about 0·5 g. of powdered potassium iodide that had been previously dried. Air in the bulb C had been removed before the introduction of the orange-yellow solution.

Iodine was liberated in all the three bulbs. After ten minutes, the contents of the bulbs were carefully analysed, using dry nitrogen to sweep away hydrogen sulphide and sulphur dioxide and to absorb them in alkali, in presence of cadmium hydroxide. The sulphide and sulphite formed were determined. No thiosulphate was found. The iodine and sulphur present in the carbon tetrachloride were also estimated. The data thus obtained were employed in calculating the extent of each of the reactions that took place.

The reactions were:

$$S_2O + 6HI \rightarrow 2H_2S + H_2O + 6I \qquad (A)$$

$$2S_2O \rightarrow SO_2 + 3S \qquad (B)$$

$$SO_2 + 6HI \rightarrow H_2S + 2H_2O + 6I \qquad (C)$$

If $0{\cdot}5\,a$ g. mole of S_2O undergoes Reaction A, and $0{\cdot}25\,b$ g. mole of S_2O takes part in Reaction B and c g. mole of the oxide undergoes Reaction C, it can be shown that quantities of the final products formed will be as follows:

$$\text{Sulphide} = a + c; \quad \text{Sulphite} = 0{\cdot}25\,b - c.$$

$$\text{Sulphur} = 0{\cdot}75\,b; \quad \text{Iodine} = 3a + 6c.$$

From the above, the extent of each of the Reactions A, B and C can be calculated. The results are given in Table III.

Two other reactions are possible:

(1) The hydrogen sulphide formed may, in presence of formic acid, react with sulphur dioxide to form sulphur and water, and (2) the sulphur dioxide may be reduced by the hydrogen iodide to sulphur:

$$2H_2S + SO_2 \rightarrow 3S + 2H_2O \qquad (D)$$

$$SO_2 + 4HI \rightarrow S + 2H_2O + 4I \qquad (E)$$

TABLE III

Influence of Formic Acid on the Reaction between Hydrogen Iodide and Disulphur Monoxide

Reaction between HI and S_2O	Experiment 1			Experiment 2		
	*a**	*b**	*c**	*a*	*b*	*c*
Sulphide** (H_2S) ..	54·8	46·45	10·95	18·30	5·60	3·60
Sulphite (SO_2) ..	..	5·77	8·00	..	1·93	2·60
Free Sulp ur (S) ..	..	32·48	35·95	..	10·80	12·15
Iodine (g. atom $\times 10^6$ per g.) ..	164·6	64·82	45·05	55·05	22·05	15·25
Iodine (calc.) ..	164·4	64·53	44·79	54·90	21·81	15·09
Disulphur monoxide used ..	54·80	54·70	54·90	18·30	18·33	18·35
%S_2O reduced to H_2S ..	100·0	20·5	12·7	100·0	21·4	11·8
%S_2O catalytically decomposed ..	..	78·8	87·3	..	78·7	88·1
%Conversion to H_2S of SO_2 produced in reaction B ..	..	46·8	33·5	..	46·4	35·4
%S_2O accounted for ..	100·0	99·3	100·0	100·0	100·1	99·9

** Quantities of sulphur and its compounds have been expressed in g. atoms of S $\times 10^6$ per g. of solution.

*a** had S_2O in CCl_4 and HI in CCl_4; *b** had S_2O in CCl_4 and HI in anhydrous formic acid; *c** had S_2O in CCl_4 and KI in formic acid.

As shown later in this paper, the reaction between hydrogen sulphide and sulphur dioxide is rather slow. It may, therefore, be ignored. The concentration of sulphur dioxide which is produced by the decomposition of disulphur monoxide is rather small, and to simplify the calculations it may be assumed, that the sulphur dioxide which has undergone reduction has produced only hydrogen sulphide and no sulphur.

From the above results, it may be concluded that in presence of an excess of hydrogen iodide, disulphur monoxide is completely reduced to hydrogen sulphide and water (Reaction A). In presence of anhydrous formic acid however, owing to the catalytic influence of the acid, only a part of the oxide is reduced by hydrogen iodide, while the major portion undergoes decomposition to sulphur dioxide and sulphur (Reaction B). Part of the sulphur dioxide produced during the Reaction B, is reduced by the hydrogen iodide to form hydrogen sulphide (Reaction C.) The reducing capacity of a formic acid solution of potassium iodide is far less than that of a solution

of hydrogen iodide in formic acid. Relatively less hydrogen sulphide is therefore formed in potassium iodide solutions.

The effect of anhydrous formic acid on the reduction of sulphur dioxide by hydrogen iodide was also studied following the same technique as had been employed for disulphur monoxide. The results are given in Table IV.

TABLE IV

Influence of Formic Acid on the Reaction between Hydrogen Iodide and Sulphur Dioxide

Reaction of HI and SO_2	Experiment 1			Experiment 2		
	*a**	*b**	*c**	*a*	*b*	*c*
SO_2** used ..	7·83	7·83	7·83	12·76	12·76	12·76
SO_2 unreacted ..	..	1·30	2·25	..	2·05	3·15
H_2S formed ..	7·78	2·76	1·85	12·68	3·80	3·10
Sulphur liberated ..	..	3·65	3·65	..	6·85	6·51
Iodine liberated ..	48·05	32·20	25·90	77·85	50·65	45·00
Iodine calculated ..	46·98	31·20	25·74	76·56	49·96	44·64
% SO_2 reduced to H_2S ..	99·4	66·4	54·8	99·4	65·5	58·2
% SO_2 converted to free S ..	..	15·6	15·6	..	16·1	24·6
% SO_2 unreacted ..	..	16·6	28·7	..	17·9	17·1
% SO_2 accounted for ..	99·4	98·6	99·1	99·4	99·5	99·9

** Quantities of sulphur and its compounds have been expressed in g. atoms of S $\times 10^6$ per g. of solution.

*a** had SO_2 in CCl_4 and HI in CCl_4; *b** had SO_2 in CCl_4 and HI in anhydrous formic acid and *c** had SO_2 in CCl_4 and KI in anhydrons formic acid.

The data presented show that in presence of anhydrous formic acid, the reduction of sulphur dioxide to hydrogen sulphide by hydrogen iodide, is incomplete. Only two-thirds of the sulphur dioxide is reduced to hydrogen sulphide, 12 to 18% of the dioxide does not at all react, while 16 to 19% of the oxide is reduced to elemental sulphur. The percentage of unreacted sulphur dioxide is much higher when the reductant is potassium iodide.

Reaction between sulphur dioxide and hydrogen sulphide in presence of anhydrous formic acid

The reaction between sulphur dioxide and hydrogen sulphide in presence of anhydrous formic acid was studied, employing dilute solutions of

sulphur dioxide and of hydrogen sulphide in carbon tetrachloride. It was found that the two gases did react to give sulphur and water. The reaction was rather slow.

At the end of the experiment (6 hours) dry nitrogen was bubbled through the reaction vessel to sweep away the unreacted gases which were absorbed by 2N sodium hydroxide having some cadmium hydroxide suspension. The sulphide and sulphite formed in the absorption vessel and elemental sulphur present in carbon tetrachloride were estimated in the usual way. No thiosulphate was found. The results are given in Table V.

TABLE V

Reaction between Sulphur Dioxide and Hydrogen Sulphide in Presence of Formic Acid

Reaction between SO_2 and H_2S	Experiment			
	1	2	3	4
SO_2* taken	26·38	18·97	38·72	16·23
H_2S taken	28·80	33·63	78·60	35·50
SO_2 unreacted	13·89	4·55	5·85	2·50
H_2S unreacted	4·50	4·85	12·46	6·86
S produced	36·90	43·25	98·74	41·65
% SO_2 unreacted	52·60	24·00	15·10	15·40
% SO_2 reacting with H_2S	46·60	76·02	85·00	85·10
% SO_2 accounted	99·20	100·02	100·10	100·50
Ratio of H_2S to SO_2	1·08	1·77	2·02	2·19

* Quantities of sulphur and its compounds have been expressed in g. atoms of S $\times 10^6$ per g. of solution.

It is well known that the union of hydrogen sulphide and sulphur dioxide is catalysed by moisture. As formic acid is also a highly polar liquid, it may be expected to catalyse the reaction. Formic acid does catalyse the reaction but the effect is comparatively small. It has been shown that in formic acid solutions, iodine oxidises neither hydrogen sulphide nor sulphur dioxide. In presence of water however, both the gases are oxidised by iodine. Thus, though water and formic acid are both highly polar, there is a marked difference in their influence on the chemical reactivity of hydrogen sulphide and sulphur dioxide.

Reaction between hydrogen sulphide and sulphur dioxide in presence of potassium iodide in formic acid

The reaction between hydrogen sulphide and sulphur dioxide was also studied in presence of potassium iodide in anhydrous formic acid. The

experimental technique was the same as already described. The following three reactions are possible:

$$(1)\quad SO_2 + 6HI \rightarrow H_2S + H_2O + 6I \qquad (C)$$

$$(2)\quad SO_2 + 4HI \rightarrow S + 2H_2O + 4I \qquad (E)$$

$$(3)\quad 2H_2S + SO_2 \rightarrow 3S + 2H_2O \qquad (D)$$

Interaction between hydrogen sulphide and sulphur dioxide, though catalysed by formic acid, is slow. The formation of sulphur by this reaction may therefore be ignored and it may be assumed that the sulphur produced is entirely got by the reduction of sulphur dioxide by hydrogen iodide. When this simplifying assumption is made, it is possible to calculate the extent of each of the two Reactions C and E. The results are presented in Table VI.

TABLE VI

Reaction between Sulphur Dioxide and Hydrogen Sulphide in Presence of Potassium Iodide in Formic Acid

Reaction between SO_2 and H_2S	Experiment		
	1	2	3
SO_2* taken	12·96	9·95	12·46
SO_2 unreacted	4·05	3·06	4·08
H_2S taken	10·80	12·56	14·83
Ratio of H_2S: SO_2	0·83	1·26	1·19
H_2S at end of reaction	15·15	15·56	18·25
H_2S surplus	4·35	3·00	3·42
Sulphur produced	4·53	3·89	4·87
% SO_2 reduced to H_2S (Reaction C)	33·5	30·1	27·4
% SO_2 reduced to sulphur (Reaction E)	35·0	39·1	39·0
% SO_2 unreacted	31·20	30·5	32·7
% sulphur accounted for	99·7	99·7	99·1
Free iodine found	45·14	33·87	40·46
Free iodine (calc.)	44·58	33·56	40·00

* Quantities of sulphur and its compounds have been expressed in g. atoms of S $\times 10^6$ per g. of solution.

The data show that when the reductant is potassium iodide dissolved in formic acid, the sulphur dioxide is reduced to hydrogen sulphide to an extent of 25 to 30% while with hydrogen iodide in absence of formic acid, the reduction of sulphur dioxide to hydrogen sulphide was practically complete (Table II).

Stability of disulphur monoxide

It was reported in Part I[12] of this series that when the products of combustion of sulphur in oxygen at a pressure of 5 to 7 mm. of mercury were condensed at $-70°$ C. all the sulphur dioxide present volatalised, leaving practically pure disulphur monoxide as an orange-yellow solid. The disulphur monoxide thus obtained, when warmed to $-16°$ C. appeared to be insoluble in carbon tetrachloride (also at $-16°$ C.) though solutions containing the pure oxide could be obtained by passing the products of combustion directly into carbon tetrachloride at $-16°$ C. and removing the sulphur dioxide present in solution. It was therefore of interest to investigate the reaction of the solid towards hydrogen iodide in presence of carbon tetrachloride.

The reaction was studied by the technique described earlier. The results are presented in Table VII.

TABLE VII

Reaction between Orange-Yellow Residue and Hydrogen Iodide in Presence of Carbon Tetrachloride

Reaction between S_2O and HI	Experiment		
	1	2	3
H_2S* evolved	12·36	8·96	20·77
Elemental sulphur	21·05	14·28	41·67
Iodine (g. atoms $\times 10^6$)	58·55	41·45	104·5
% S_2O undecomposed	15·9	18·0	11·0
% S_2O decomposed	84·0	81·8	88·9

* Sulphur and its compounds have been expressed in terms of g. atoms of S $\times 10^6$ per g. of solvent.

From the above experiments it was concluded that disulphur monoxide in absence of its solvent (carbon tetrachloride) decomposed rapidly. Only 11 to 18% of the oxide was left undecomposed when the oxide at $-70°$ C. was warmed to $-16°$ C. The apparent insolubility of the solid when brought in contact with carbon tetrachloride at $-16°$ C. was due to the fact that much of the disulphur monoxide had already decomposed to sulphur (and sulphur dioxide). The solubility of sulphur in carbon tetrachloride being small, the solid did not dissolve.

To show that carbon tetrachloride as solvent had stabilising action on disulphur monoxide, an aliquot of the solution of the oxide (obtained by passing the products of combustion into carbon tetrachloride at — 16° C. and freed from sulphur dioxide) was frozen at — 30° C., at which temperature there was no liquid solvent to keep the oxide in solution. The frozen mass was thawed and treated with hydrogen iodide in carbon tetrachloride at — 16° C., and the products of reaction analysed. The results are given in Table VIII.

TABLE VIII

Decomposition of Disulphur Monoxide in Carbon Tetrachloride Solutions, on Freezing

Decomposition of S_2O	Experiment		
	1	2	3
S_2O* taken	25·43	44·75	55·56
H_2S produced	16·72	15·4	14·30
Elemental sulphur	8·64	29·25	41·20
Iodine liberated	58·85	75·56	84·5
% S_2O undecomposed	54·3	12·6	1·0
% S_2O decomposed	45·3	87·2	98·86

* Quantities of sulphur and its compounds are expressed in terms of g. atoms of S $\times 10^4$ per g. of solution.

It was concluded from the above results that when disulphur monoxide solutions in carbon tetrachloride were kept frozen for different periods, the oxide decomposed to the extent of 45 to 98%. It was noticed that the intensity of orange-yellow colour of the carbon tetrachloride solution depended on the disulphur monoxide left undecomposed. When the decomposition of the oxide was almost complete, the solution was practically colourless. Solid disulphur monoxide is markedly less stable than a solution of the oxide in carbon tetrachloride.

SUMMARY

1. The orange-yellow liquid obtained when the products of combustion of sulphur in oxygen at low pressure are passed into cooled carbon tetrachloride (at — 16° C.) and the sulphur dioxide is removed, is a solution of almost pure disulphur monoxide.

2. Anhydrous hydrogen iodide quantitatively reduces disulphur monoxide into hydrogen sulphide. A corresponding amount of iodine is liberated.

3. Sulphur dioxide is also quantitatively reduced to hydrogen sulphide by hydrogen iodide, provided the concentration of sulphur dioxide is small and that of hydrogen iodide is relatively large. When hydrogen iodide is present in moderate excess, only a part of the sulphur dioxide is reduced to hydrogen sulphide, the rest being reduced to sulphur.

4. In presence of anhydrous formic acid, owing to the catalytic influence of the acid, only a part of the disulphur oxide is reduced by hydrogen iodide, while the major portion undergoes decomposition to sulphur dioxide and sulphur. The reducing capacity of a formic acid solution of potassium iodide is far less than that of a solution of hydrogen iodide in formic acid.

5. Anhydrous formic acid also affects the reduction of sulphur dioxide by hydrogen iodide. In presence of the acid, the reduction of the oxide to hydrogen sulphide, is incomplete. The percentage of unreacted sulphur dioxide is much higher when the reductant is potassium iodide in formic acid.

6. The union of hydrogen sulphide and sulphur dioxide is slowly catalysed by anhydrous formic acid.

7. When the products of combustion of sulphur (in oxygen under reduced pressure) are cooled to $-70°$ C., disulphur monoxide is obtained as an orange yellow solid. The solid is far less stable than a solution of the oxide in carbon tetrachloride.

Acknowledgment

The author wishes to acknowledge his grateful thanks to Dr. B. Sanjiva Rao for his keen interest in the work and for his valuable criticism. He is also thankful to Dr. M. R. A. Rao for his helpful suggestions.

References

1. Sanjiva Rao, B. .. *Proc. Ind. Acad. Sci.*, 1939, **10**, 491.
2. Stamm and Wiebusch .. *Naturwisenschaften*, 1944, **32**, 42.
3. Weissberger and Proskauer .. *Organic Solvents*, " Physical Constants and Methods of Preparation," Oxford University Press, 1935, p. 145.
4. British Celanese Ltd. .. British Patent 597,078, *January* 16, 1948, cited from *C. A.* 1948, 4603.
5. Schlesinger and Martin .. *Jour. Am. Chem. Soc.*, 1914, **36**, 1589.
6. Walton and Rosenbaum .. *Ibid.*, 1928, **50**, 1648.
7. Morton .. *Laboratory Technique in Organic Chemistry*. McGraw-Hill Book Co., 1938, p. 7.
8. Coolidge .. *Jour. Am. Chem. Soc.*, 1928, **50**, 2166.
9. Ewins .. *Jour. Chem. Soc.*, 1914, **105**, 354.
10. Heisig and Lingane .. *Inorganic Synthesis*, McGraw-Hill, 1939, **1**, 159.
11. Sanjiva Rao, B. and Rao, M. R. A. 10*th International Congress of Chemistry*, 1938, **3**, **4**, 62.
12. Vasudeva Murthy .. *Proc. Ind. Acad. Sci.*, 1952, **36**, 388.

STUDIES ON THE NATURE OF THE RACEMIC MODIFICATIONS OF OPTICALLY ACTIVE COMPOUNDS IN THE SOLID STATE

Part IX. Camphor-β-Sulphonamides, Camphor-β-Sulphonanhydramides, Camphor-β-Sulphon-phenyl, *o*-tolyl-, *m*-tolyl-, *p*-tolyl-, α-naphthyl-, and β-naphthyl-amides (*d* and *dl*)

BY BAWA KARTAR SINGH, F.A.SC., A. R. PANICKER AND M. K. RANGANATHAN

(From the Organic Chemistry Research Section, Banaras Hindu University)

Received May 27, 1952

THE enantiomorphic modifications may occur in equimolecular proportions to constitute what is known as a racemic form. Three cases are possible:

(1) *A racemic* '*conglomerate*' or a *mixture* of the two optically active and opposite forms (*d*- and *l*-) in equal proportions. There are, therefore, two solid phases, which can be separated, under suitable conditions, by the mechanical process of picking apart the two kinds of crystals. The classical example of this type is the racemic form of sodium ammonium tartrate. Examples of this type are not common. One of the writers in the course of his extensive investigations in this subject, has come across only two such cases: the first example is that of *p*-phenylenebisimino-*dl*-camphor.[1] Henderson and Rule[2] knowing that this racemic substance is a mixture or 'conglomerate', later achieved its complete resolution by repeated adsorption on *d*-lactose under chromatographic conditions. The second example is that of 3-nitro-*p*-toluidinomethylene-*dl*-camphor.[3]

(2) A *racemic compound* (*dl*) is composed of one molecule of each optical isomer (*d*- and *l*-). The molecule of such a compound is, therefore, dimeric. There is only one solid phase and separation by mechanical means is impossible. In general, racemic compounds appear to be more common than either 'conglomerates' (mixtures) or solid solutions.

(3) A *racemic solid solution* or '*mixed crystals*': a solid solution of the active and opposite forms (*d* and *l*) due to the enantiomorphs being isomorphous. There is only one phase, unlike the first case of a 'conglomerate'. The composition of the phase is not constant. Separation by mechanical means is impossible.

There are three methods of distinguishing racemic forms. Two of them, due to Roozeboom,[4] are physical: Freezing point or melting point method and solubility method. The third method—Biochemical—is due to Singh.[5]

Solubility-Composition Diagrams.—Roozeboom[4] and Bruni[6] have theoretically discussed, from the standpoint of Phase Rule, the solubility relationships of optical isomers and their racemic mixtures, compounds and solid solutions. Hitherto solubility—composition isotherms, which they had deduced theoretically, had not been verified experimentally until Singh and Perti[7] in the case of camphor-β-sulphonic acids and Singh and Nayar[8] in that of camphoric acids supplied these curves, including the triangular diagram prepared on the basis of Phase Rule studies. Later Singh and Nayar[9] investigated camphorcarboxylic acids and obtained solubility—composition and melting point—composition diagrams. In the case of each of the three acids above mentioned, 3 curves were obtained which conclusively proved that the racemic acids were true *dl*-compounds.

The Biochemical method, above referred to, is based on the following principle: The optically active and opposite forms (*d*- and *l*-) have different biological actions on micro- and higher-organisms, as found by Pasteur,[10] Piutty,[11] Cushny,[12] Singh[5] and others. The action of the racemic form will be generally different from those of the optically active forms: if it is a mixture, the properties of the racemic form will be the mean of those of the active forms ($d > dl > l$ or *vice versa*), whereas if it is a compound, its properties may be entirely different from those of the enantiomorphic forms. Thus if the biological effect of the racemic form is the *highest* or the *lowest* of the three forms, it is a compound. But if the effect is intermediate, then the problem is indeterminate, as the racemic compound may also show this effect. One of us,[5] applying this biological method has shown that the *dl*-form of camphor-β-sulphonic acid and some of its salts with organic bases are true *dl*-compounds—a result which is in agreement with the deductions made from the melting point and solubility methods of Roozeboom.

The melting point method of Roozeboom.—We have employed the melting point method as it is very convenient and requires very small amounts of the dextro, lævo and racemic forms. It consists in preparing the melting point—composition diagram. On the axis of composition are given the percentage composition of the mixtures of *d*-form with racemic form, and *l*-form with racemic form. In the case of a racemic mixture, the melting point of each optical isomer will be lowered by the addition of increasing amounts of the racemic form (mixture) till the eutectic point (the melting

point of the pure racemic form) is reached. Thus there will be two symmetrical curves (Type I) formed by joining the melting points of each of the optical isomers and the racemic form (eutectic mixture).

In the case of a racemic compound (racemate), three curves will be obtained with two symmetrical eutectic points and a maximum point (Type II, Figs. 1 to 8). The maximum point is the melting point of the racemic compound.

The mixed crystal or solid solution type of racemic substance (Type III) will give a single continuous curve formed by joining the melting points of the optically active and opposite forms and the racemic modification.

In our previous work,[13] we have employed the three modifications, *d*-, *l*- and *dl*-, in preparing the melting point-composition diagrams. The curves are exactly symmetrical about the middle point representing the melting point of the pure racemic form. This also follows from theoretical considerations based on Pasteur's principle of molecular dissymmetry, according to which the dextro and lævo forms of a compound are identical in the magnitude of their properties (except in direction in the case of vectorial properties). It is, therefore, sufficient to determine the melting point-composition diagram of mixtures of one of the optical isomers and the racemic form. We have accordingly employed the dextro and racemic forms and reproduced the other half of the diagram as true mirror image of the experimentally determined half portion of the diagram. This is represented by broken curves in Figs. 1 to 8.

DISCUSSION OF RESULTS

(Figs. 1 to 8)

All the substances described in this paper give three curves with a central maximum in the melting point-composition diagram (Type II) which established the nature of the racemic forms as *dl*-compounds. If the central portion of the curve is steep, the racemic compound is stable; if it is flattened, the racemic compound is unstable and is dissociated into its active components at its melting point. The area occupied by the central portion or branch of the diagram gives the range of stability of the racemic compound. If the minima or eutectic points are sharp and well defined, the racemic compound and the active isomers do not form solid solutions, whereas if the eutectic points are not sharp and well defined and the curves are continuous in the region near the eutectic points, it indicates the formation of mixed crystals between the active and racemic compound. We have applied these principles in the following *qualitative* discussion of the Roozeboom diagrams.

Singh and Nayar[14] in an earlier communication determined *quantitatively* the degree of dissociation of *dl*-camphor-carboxylic acid by applying Raoult's law of lowering of melting point of a substance in presence of a second substance and the law of mass action. In this way it was shown that the *dl*-acid was dissociated to the extent of about 27 per cent. at its melting point.

dl-*Camphor-β-Sulphonphenylamide* (Fig. 1 and Table I).—The melting point—composition diagram consists of three curves which shows that this

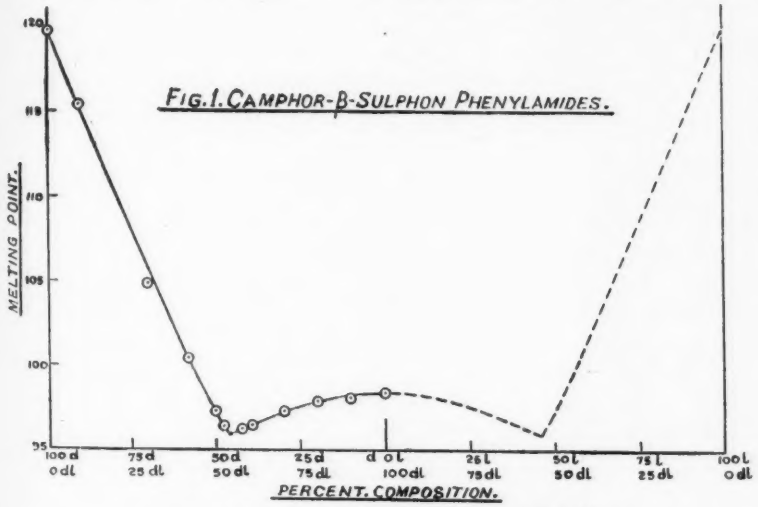

TABLE I. *Camphor-β-sulphonylphenylamides*

Mixed melting points of the racemic modification with *d*-isomer (Type II, compound)

Wt. % of the *d*-component	Wt. % of the racemic form	Melting point of the mixture
		°C.
100	0	119·8
90	10	115·4
70	30	104·8
60	40	100·4
50	50	97·2
48	52	96·4
45	55	95·8
42	58	96·2
40	60	96·4
30	70	97·3
20	80	97·8
10	90	98·0
0	100	98·4

racemic substance is a true *dl*-compound. The central portion is very much flattened indicating that the racemic compound is very unstable and is considerably dissociated at its melting point.

dl-*Camphor-β-Sulphon*-o-*tolylamide* (Fig. 2 and Table II).—It is also a racemic compound as the diagram consists of three curves. The central

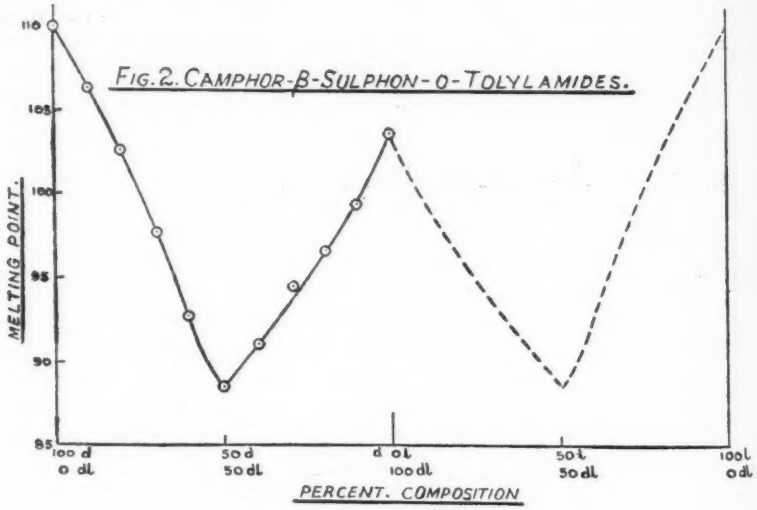

TABLE II. *Camphor-β-sulphonyl*-o-*tolyamides*

Mixed melting points of the racemic modification with *d*-form (Type II, compound)

Wt. % of the *d*-component	Wt. % of the racemic form	Melting point of the mixture
		°C.
100	0	110·0
90	10	106·3
80	20	102·5
70	30	97·6
60	40	92·7
50	50	88·5
40	60	91·0
30	70	94·6
20	80	96·6
10	90	99·4
0	100	103·6

portion is well marked and the curves rise and fall steeply indicating the stable nature of the *dl*-compound.

dl-*Camphor-β-Sulphon*-m-*tolylamide* (Fig. 3 and Table III).—The racemic form in this case also is a *dl*-compound. The central portion is somewhat flattened indicating some dissociation of the racemic compound at its melting point. The eutectic points are however sharp, and well defined.

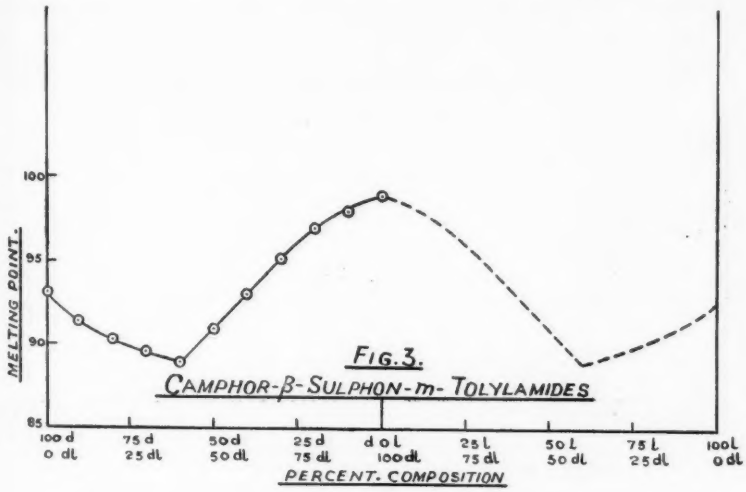

FIG. 3.
CAMPHOR-β-SULPHON-m-TOLYLAMIDES

TABLE III. *Camphor-β-sulphonyl*-m-*tolylamides*

Mixed melting points of the racemic modification with *d*-form (Type II, compound)

Wt. % of the *d*-component	Wt. % of the racemic form	Melting point of the mixture
		°C.
100	0	93·0
90	10	91·4
80	20	90·3
70	30	89·7
60	40	89·0
50	50	91·0
40	60	93·0
30	70	95·1
20	80	97·0
10	90	98·1
0	100	99·0

dl-*Camphor-β-Sulphon*-p-*tolylamide* (Fig. 4 and Table IV).—The melting point-composition diagram consists of three curves which shows that the racemic form is a compound. The central portion is well defined, rising and falling abruptly which indicates that the racemic compound is fairly stable. The eutectic points are sharp.

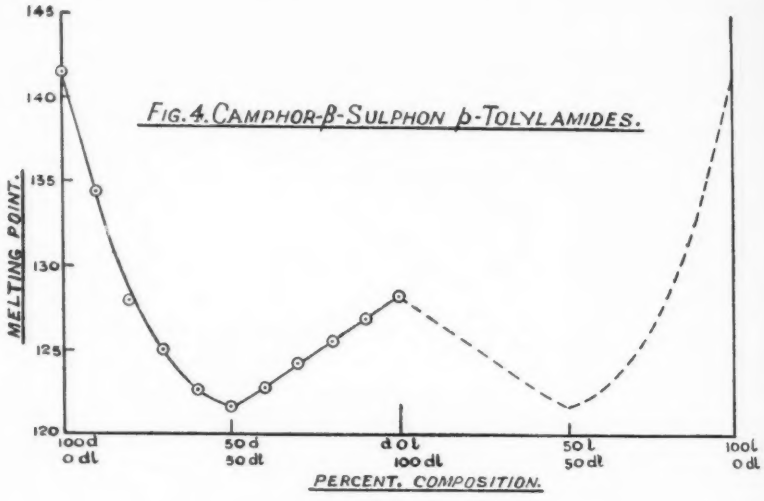

TABLE IV. *Camphor-β-sulphonyl*-p-*tolylamides*

Mixed melting points of the racemic modification with *d*-form (Type II, compound)

Wt. % of the *d*-component	Wt. % of the racemic form	Melting point of the mixture
		°C.
100	0	141·4
90	10	134·4
80	20	128·0
70	30	125·0
60	40	122·6
50	50	121·6
40	60	122·7
30	70	123·7
20	80	125·5
10	90	126·8
0	100	128·1

dl-*Camphor-β-Sulphonanhydramide* (Fig. 5 and Table V).—The diagram consists of three curves indicating the racemic form to be a compound. The central portion is very much flattened and rises and falls slowly and gradually indicating that the racemic compound is considerably dissociated at its melting point. The eutectic points are not sharp and well defined: the *d-dl* and *l-dl* sections of the curves are continuous near the minima which seems to point to the formation of mixed crystals between the active and inactive forms. This behaviour has previously been observed in the case of racemic forms of camphorcarboxylic acid and oxymethylene-camphor.[15]

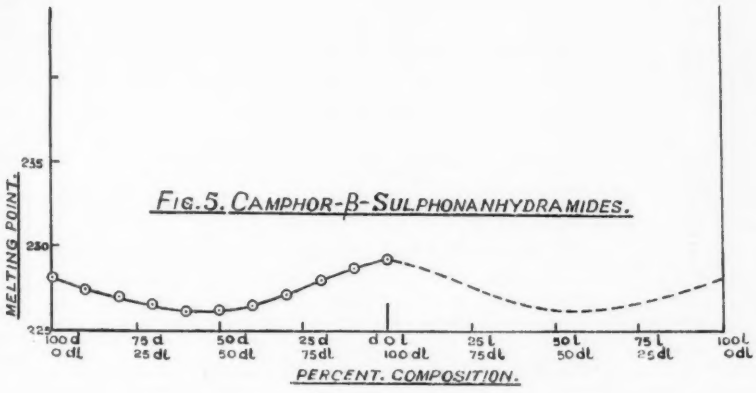

TABLE V. *Camphor-β-sulphonanhydramides*

Mixed melting points of the racemic modification with *d*-form (Type II, compound)

Wt. % of the *d*-component	Wt. % of the racemic form	Melting point of the mixture
		°C.
100	0	228·2
90	10	227·4
80	20	227·0
70	30	226·6
60	40	226·1
50	50	226·2
40	60	226·5
30	70	227·2
20	80	228·0
10	90	228·6
0	100	229·2

dl-*Camphor-β-Sulphonamide* (Fig. 6 and Table VI).—The melting point-composition diagram gives three curves. The central portion is well defined and rises and falls sharply, thus indicating that the racemic compound is stable and its range of stability is fairly large. Unlike the anhydramide, the eutectic points are sharp and there is no tendency to form mixed crystals between the racemic and the active forms.

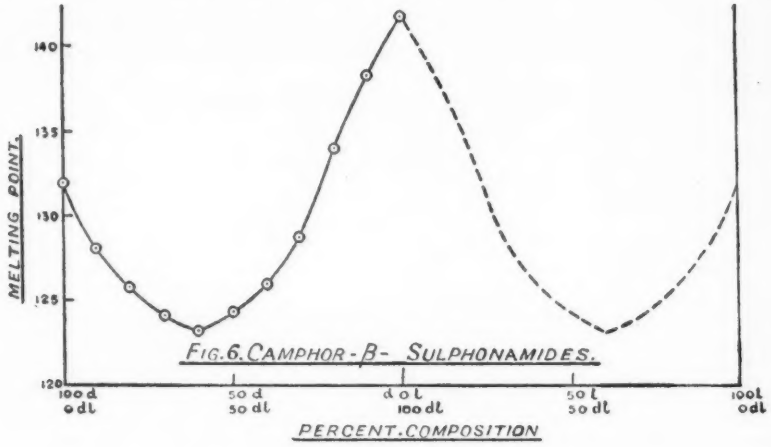

FIG. 6. CAMPHOR-β-SULPHONAMIDES.

TABLE VI. *Camphor-β-sulphonamides*

Mixed melting points of the racemic modification with *d*-form (Type II, compound)

Wt. % of the *d*-component	Wt. % of the racemic form	Melting point of the mixture
		°C.
100	0	132·0
90	10	128·0
80	20	125·9
70	30	124·0
60	40	123·1
50	50	124·2
40	60	126·0
30	70	128·6
20	80	134·0
10	90	138·2
0	100	141·8

dl-*Camphor-β-Sulphon-α-naphthylamide* (Fig. 7 and Table VII).—The three portions into which the diagram is divided show that the racemic form

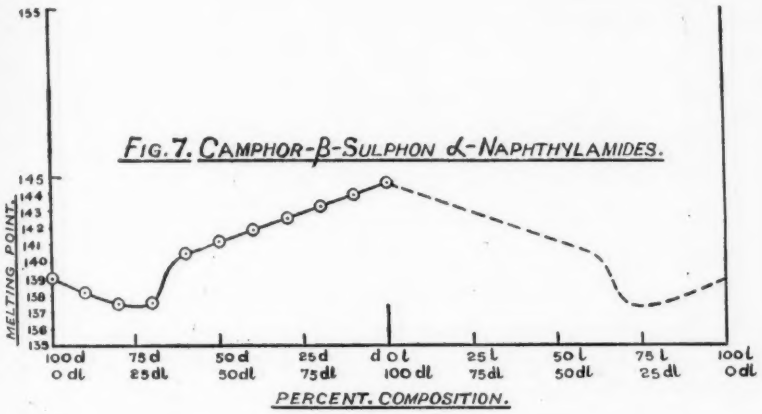

TABLE VII. *Camphor-β-sulphonyl-α-naphthylamides*

Mixed melting points of the racemic modification with *d*-isomer (Type II, compound)

Wt. % of the *d*-form	Wt. % of the racemic form	Melting point of the mixture
		°C.
100	0	139·0
90	10	138·2
80	20	137·5
70	30	137·6
60	40	140·5
50	50	141·2
40	60	141·8
30	70	142·6
20	80	143·2
10	90	144·0
0	100	144·6

is a compound. The central portion occupies a large part of the diagram and the *dl-d* and *dl-l* sections rise and fall fairly steeply, thus indicating that the racemic form is fairly stable and its range of stability is large. The somewhat continuous nature of the curves near the minima or eutectic points indicates tendency to the formation of mixed crystals between the racemic and the active forms in this region.

dl-*Camphor-β-Sulphon-β-naphthylamide* (Fig. 8 and Table VIII).—The diagram is divided into three well defined curves, which rise and fall steeply.

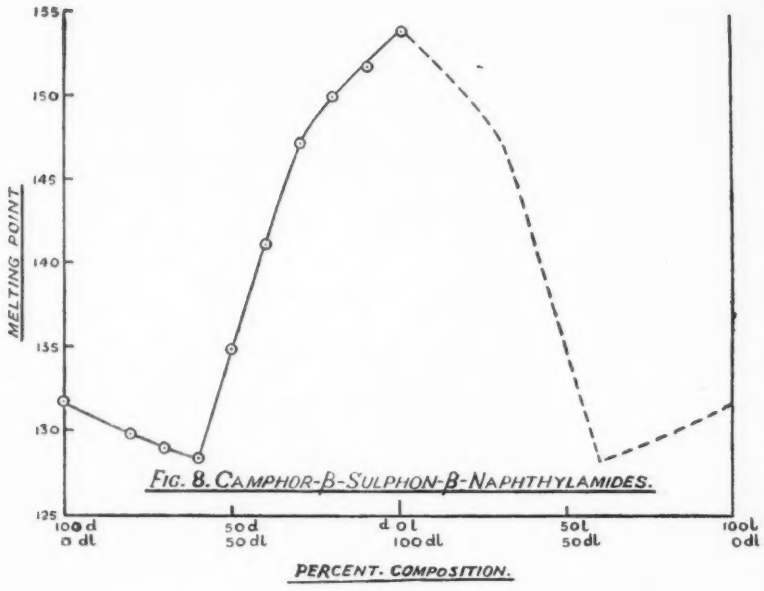

FIG. 8. CAMPHOR-β-SULPHON-β-NAPHTHYLAMIDES.

TABLE VIII. *Camphor-β-sulphonyl-β-naphthylamides*

Mixed melting points of the racemic modification with *d*-form (Type II, compound)

Wt. % of the *d*-component	Wt. % of the racemic form	Melting point of the mixture
		°C.
100	0	131·8
90	10	131·6
80	20	129·9
70	30	129·0
60	40	128·4
50	50	135·0
40	60	141·2
30	70	147·1
20	80	150·0
10	90	151·8
0	100	154·0

The central portion occupies a greater part of the whole diagram. The eutectic points are well defined and sharp. It may be, therefore, inferred that the racemic compound is stable and the range of its stability large.

Further there does not appear to be any tendency to form mixed crystals between the racemic compound and the optically active isomers in the region near the minima or the eutectic points.

EXPERIMENTAL

d-*Camphor-β-Sulphonamide*

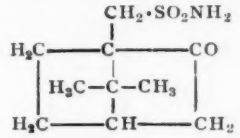

A stream of dry ammonia gas was passed for two hours through a solution of *d*-camphor-β-sulphonyl chloride in dry benzene till it was saturated. On filtering the solution, the residue consisted of *d*-camphor-β-sulphonamide and ammonium chloride. It was washed with water to remove ammonium chloride, when the residue consisted only of the amide. The amide was recrystallised from hot water as colourless needles, melting at 132° C. It is easily soluble in methyl alcohol and chloroform, less so in acetone and ethyl alcohol, sparingly soluble in benzene and ether and very sparingly soluble in cold water. The amide is converted into anhydramide when boiled with water for a long time.

It was originally prepared by Reychler,[16] using strong aqueous solution of ammonia, but was contaminated with camphor-β-sulphonanhydramide. Later Armstrong and Lowry[17] obtained the substance in the same way.

dl-*Camphor-β-Sulphonamide* was prepared in the same way as the dextro form as colourless plates, melting at 148·8°. It had similar solubility as the *d*-isomer.

S (Found) = 13·65 per cent.

S (Calc. for $C_{10}H_{17}O_3NS$) = 13·56 per cent.

d-*Camphor-β-Sulphonanhydramide*

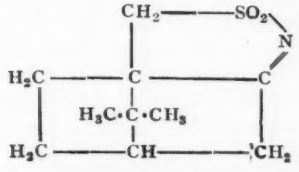

On mixing *d*-camphor-β-sulphonylchloride and ammonia liquor, a vigorous reaction took place. The reaction mixture was kept overnight in a closed tube. The solid was filtered off next day. The residue was boiled

with a small quantity of water to remove any amide. *d*-Camphor-β-sulphonanhydramide was recrystallised from a large quantity of alcohol (animal charcoal) as colourless plates melting at 228·2° C. It is soluble in acetone, chloroform and methyl alcohol, sparingly soluble in ethyl alcohol, benzene and ether and insoluble in water.

This compound was first prepared by Reychler,[16] who quotes its melting point as 223°, and later by Armstrong and Lowry[17] who give the same melting point. Both products were evidently contaminated with camphor-β-sulphonamide.

S (Found) = 14·9 per cent.

dl-*Camphor-β-Sulphonanhydramide* was prepared in the same way as the *d*- isomer as colourless plates melting at 229·2° C. It had similar solubility in different solvents as the *d*-isomeride.

S (Found) = 14·92 per cent.

S (Calc. for $C_{10}H_{15}SO_2N$) = 15·01 per cent.

d-*Camphor-β-Sulphonylphenylamide*

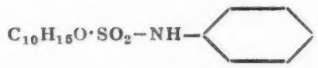

Molecular proportions of *d*-camphor-β-sulphonyl chloride, aniline (freshly distilled) and dry pyridine were heated together at 100° in a water-bath using an air condenser for about 12 hours. On cooling water was added when a semi-solid mass came down. It was dissolved in alcohol and again precipitated by cold water. It was recrystallised from 75 per cent. aqueous ethyl alcohol (animal charcoal) as colourless needles, melting at 120° C. It is easily soluble in chloroform, benzene and ethyl acetate, less so in methyl alcohol and ethyl alcohol, and insoluble in petroleum ether and water.

S (Found) = 10·3 per cent.

This substance was first prepared by Reychler[16] and later by Armstrong and Lowry[17] who also record its melting point as 119°.

dl-*Camphor-β-Sulphonylphenylamide* was prepared as its dextro isomeride and had similar structure and solubility. It melted at 98·4° C.

S (Found) = 10·2 per cent.

$C_{16}H_{21}O_3NS$ requires S = 10·4 per cent.

d-*Camphor-β-Sulphonyl*-o-*tolylamide*

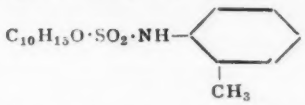

Molecular proportions of *d*-camphor-β-sulphonyl chloride, *o*-toluidine and pyridine were heated together and worked up as in the case of the last compound. It was obtained as colourless needles melting at 110° C. It is soluble in acetone, chloroform, benzene and ethyl acetate, less so in ethyl alcohol and insoluble in petroleum ether and water.

S (Found) = 9·90 per cent.

The *dl*-isomer was prepared by using *dl*-camphor-β-sulphonylchloride in the same way as the *d*-form, melting at 103·6° C. It had similar structure and solubility in different solvents.

S (Found) = 10·4 per cent.

$C_{17}H_{23}O_3NS$ requires S = 10·0 per cent.

d-*Camphor-β-Sulphonyl*-m-*tolylamide*

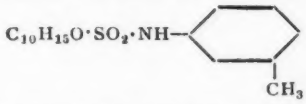

Molecular proportions of *d*-camphor-β-sulphonyl chloride, *m*- toluidine and pyridine, on being treated in the same way gave on crystallisation colourless long needles melting at 93° C. It is easily soluble in benzene, chloroform, ethyl acetate and ether, less so in ethyl alcohol and methyl alcohol and insoluble in petroleum ether and water.

S (Found) = 9·86 per cent.

The *dl*-isomer was obtained as colourless long needles melting at 99° C. It had similar solubility as the dextro form.

S (Found) = 10·2 per cent.

$C_{17}H_{23}O_3NS$ requires S = 10·0 per cent.

d-*Camphor-β-Sulphonyl* p-*tolylamide*

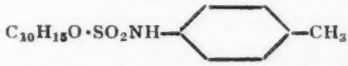

Molecular proportions of *d*-camphor-β-sulphonyl chloride, *p*-toluidine and pyridine, on being condensed and treated in the same way as in the

previous cases, gave colourless needles melting at 141·4° C. The compound is fairly soluble in acetone, chloroform, ethyl acetate and benzene, less so in ethyl alcohol and methyl alcohol and insoluble in water.

S (Found) = 10·0 per cent.

The *dl*-form was prepared, in the same way, as the *d*-form, using *dl*-camphor-β-sulphonyl chloride, as colourless needles melting at 128° C.

S (Found) = 10·01 per cent.

$C_{17}H_{23}O_3NS$ requires S = 10·0 per cent.

d-*Camphor-β-Sulphonyl-β-naphthylamide*

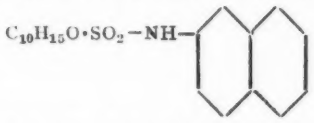

d-Camphor-β-sulphonyl chloride, β-naphthylamine and pyridine were taken and mixed in molecular proportions, when the mixture acquired a deep red colour with evolution of heat. It was heated (air condenser) for 12 hours in water-bath at 100° C. On cooling cold water was added, when a solid mass separated, containing some unreacted amine. It was re-crystallised (animal charcoal) from dilute aqueous alcohol as colourless needles, melting at 131·8° C.

It is easily soluble in ether, benzene, ethyl alcohol, methyl alcohol and chloroform, less so in acetone and insoluble in water.

S (Found) = 9·01 per cent.

dl-Camphor-β-sulphonyl-β-naphthylamide (m.p. 154° C.) was prepared in the same way and had similar structure and solubility as its dextro isomeride.

S (Found) = 8·87 per cent.

$C_{20}H_{23}O_3NS$ requires S = 8·96 per cent.

d-*Camphor-β-Sulphonyl-α-naphthylamide*

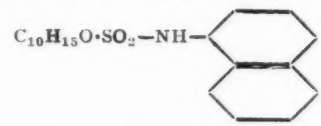

Molecular proportions of *d*-camphor-β-sulphonylchloride, α-naphthylamine and pyridine were heated in the same way as in the preparation of the

β-naphthylamide, except that the time of heating was longer (18 hours), probably on account of steric hindrance. It was crystallised from aqueous alcohol as colourless prismatic needles melting at 139° C. It is easily soluble in ether, benzene, ethyl alcohol, methyl alcohol, and chloroform, and insoluble in water.

S (Found) = 9·07 per cent.

The *dl*-isomer (m.p. 144·6° C.), prepared in the same way as the dextro compound, had similar structure and properties.

S (Found) = 9·09 per cent.

$C_{20}H_{23}O_3NS$ requires S = 8·96 per cent.

dl-*Camphor-β-Sulphonylchloride*

$C_{10}H_{15}O \cdot SO_2Cl$

Singh and Manhas[18] record the melting point of racemic camphor-β-sulphonylchloride as 72°–74°, which is incorrect; it should be 84° C.

S (Found) = 12·78 per cent.

$C_{10}H_{15}O_3SCl$ requires S = 12·62 per cent.

The melting point-composition diagrams were prepared as follows: an intimate mixture of the racemic form and the dextro isomeride was prepared by taking exact weights of the components in different proportions in an agate mortar and thorough mixing and grinding. Six determinations of the melting point (capillary tube method) of each mixture were made with Siebert and Kuhn thermometers graduated to 0·2° C. and the mean value was taken as the melting point of the mixture. The results are recorded in Tables I to VIII and the corresponding melting point-composition diagrams in Figs. 1 to 8.

The rotatory and refractive dispersion studies of these and allied sulphonamides are in progress.

Summary

The dextro and racemic camphor-β-sulphonamides and their aryl derivatives have been prepared. By studying Roozeboom's melting point-composition diagrams, it was shown that all the eight racemic forms were true *dl*-compounds. The stability relationships of the different sulphonamides have been qualitatively discussed with the aid of these diagrams.

ACKNOWLEDGEMENTS

We wish to make grateful acknowledgements to the Banaras Hindu University and the U.P. Government Scientific Research Committee for the provision of research facilities and the award of research assistantships to two of us (A.R.P. and M.K.R.).

REFERENCES

1. Singh, B. K. and Bhadhuri, B. N. .. *Jour. Ind. Chem. Soc.*, 1930, **7**, 545.
2. Henderson and Rule .. *Jour. Chem. Soc.*, 1939, 1568.
3. Singh, B. K. and Tewari, R. K. *Proc. Ind. Acad. Sci.*, 1947, **25 A**, 389.
4. Roozeboom, B. .. *Ber.*, 1899, **32**, 537; *Zeit. Physik. Chem.*, 1899, **28**, 494.
5. Singh, B. K. *et al.* .. *Proc. Nat. Acad. Sci. India*, 1944, **14**, 171.
6. Bruni .. *Gezetta*, 1900, **30**, 35.
7. Singh, B. K. and Perti, O. N. *Proc. Ind. Acad. Sci.*, 1945, **22 A**, 170.
8. Singh, B. K. and Nayar, B. K. K. .. *Ibid.*, 1945, **22**, 46; 1947, **25**, 368.
9. „ „ .. *Ibid.*, 1947, **26**, 271.
10. Pasteur, L. .. *C. R. Acad. Sci.*, 1886, **103**, 138.
11. Piutti .. *C. R. Soc. Biol.*, 1886, **103**, 137.
12. Cushny .. *Biological Relations of Optically Isomeric Substances* (London: Bailliére, Tindall and Cox, 1926).
13. Singh, B. K., *et al.* .. *Proc. Nat. Acad. Sci., India*, 1943, **13**, 59; 1944, **14**, 79; *Proc. Ind. Acad. Sci.*, 1947, **25 A**, 389; 1947, **26 A**, 271.
14. Singh, B. K. and Nayar, B. K. K. .. *Proc. Ind. Acad. Sci.*, 1949, **29 A**, 162.
15. Singh, B. K. *et al.* .. *Ibid.*, 1947, **25**, 389; 1947, **26**, 271.
16. Reychler .. *Bull. Soc. Chem.*, 1898 (iii), **19**, 120.
17. Armstrong, *et al.* .. *Jour. Chem. Soc.*, 1902, **81**, 1448; 1906, **89**, 1046.
18. Singh, B. K. and Manhas, K. M. S. .. *Proc. Ind. Acad. Sci.*, 1949, **30 A**, 87.

ON THE PENETRATING COMPONENT IN AIR SHOWERS

By B. Chowdhuri, R. C. Saxena and A. Subramanian
(*Tata Institute of Fundamental Research, Bombay*)

Received September 10, 1952
(Communicated by Prof. H. J. Bhabha, F.A.SC., F.R.S.)

Introduction

In recent years, the penetrating component of air showers which can traverse more than 10 cm. of lead has become a subject of much interest.

The relative abundance of these penetrating particles in air showers has been found by several investigators to be of the order of 2%.

Experiments carried out during the last two years give us information regarding the nature of the penetrating particles and the type of interaction which gives rise to these particles in air showers.

The results obtained by Cocconi, Tongiorgi and Greisen (1949) established that these particles are μ-mesons not produced locally in the absorber surrounding the detecting apparatus. On the other hand, evidence for the presence of particles which can produce showers with two or more secondaries under 15 cm. of lead, was found by one of the present workers (1950) by a counter hodoscope arrangement. Brown and McKay (1949) and Fretter (1949) were also able to observe the presence of interacting particles in air showers by cloud chamber studies.

Greisen, *et al.* (1950) and Sitte (1950), working at 4,300 m. and 3,240 m. respectively, found the relative intensity, in air showers, of the component showing no interaction with nuclei and that showing such interaction. From the Cascade Theory, it follows that the primary energy required to produce an air shower recorded at a given altitude in the atmosphere is a function of that altitude. At a given altitude, the probability of recording low energy showers which have gone beyond the cascade maximum is much less than for those which are close to the maximum. Thus, in effect, the altitude at which one works always introduces a bias in favour of showers in the neighbourhood of the cascade maximum. Therefore, at mountain altitudes, investigators will generally select showers of initial energies ranging from 10^{12} ev. to 10^{14} ev., but at sea level one selects showers of higher energies, from 10^{15} ev. to 10^{16} ev., which are in the neighbourhood of the cascade maximum at sea level.

It is important to know how the relative intensities of the different components in air showers vary with the initial energy and with distance from the shower axis. The way in which the production of the various shower secondaries depends on the initial energy may give some information regarding the mechanism of energy transfer among the various components in the initial act of interaction. By conducting an experiment at sea level we are able to study the effect of the high energy part of the energy spectrum on the composition of the different components in air showers. In order to get more information regarding the nature and the composition of the penetrating particles in extensive showers by a cloud chamber study, we carried out the present experiment at Bombay.

§2. EXPERIMENTAL ARRANGEMENT

The experimental arrangement shown in plan consisted of a threefold counter coincidence array for selecting samples of extensive air showers. Each of the counter trays A, B and C had three counters covering a total area of 360 cm.^{2} They were placed at the vertices of a triangle of side 3-metres on a horizontal plane. A cloud chamber, shielded by 10·5 cm.

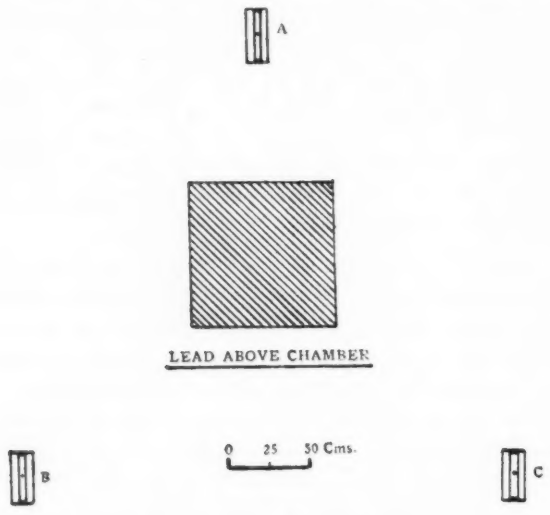

FIG. 1. Plan of the Experimental Arrangement

of lead absorber on the top and 10 cm. of lead on the sides, was placed at the centre of the arrangement in a plane about 120 cm. lower. In part of the experiment, an additional layer of 7 cm. of lead was placed above the

chamber. The chamber contained four lead plates of 0·5 cm. thickness each. At a later stage of the experiment, these were replaced by seven such plates. The cloud chamber was triggered by the threefold coincidence pulse, caused by air showers. The resolving time of the system was of the order of 25 μ secs. For illumination, Sieflash tubes were used. The photographs were taken on Kodak R 55 film.

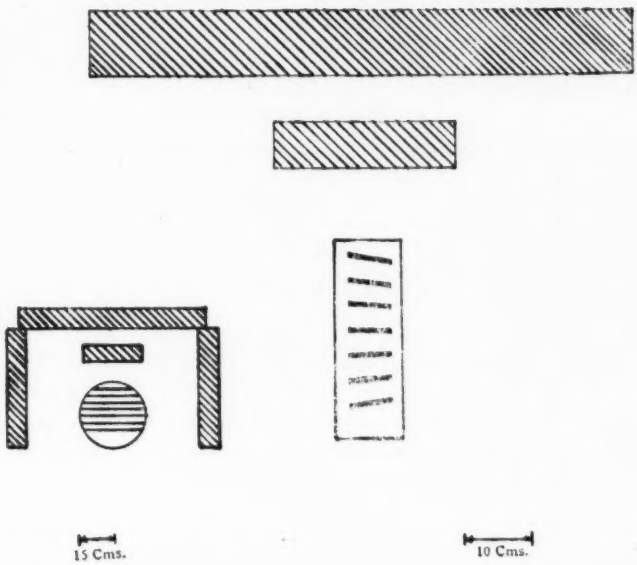

FIG. 2. Front and Side Views of the Cloud Chamber and the Lead Absorbers

§3. RESULTS AND ANALYSIS OF DATA

The threefold coincidence arrangement alone, without the cloud chamber, gave a counting rate for air showers of $4 \cdot 2 \pm 0 \cdot 1$ per hour.

The total number of shower photographs taken with this threefold coincidence arrangement was 4,463. 168 of these photographs show three main kinds of event.

(*a*) Photographs showing only single tracks traversing at least one lead plate in the chamber without any cascade multiplication.

(*b*) Photographs showing multiple tracks of the same age which do not meet at any point in the lead absorber.

(*c*) Photographs showing tracks of two or more locally produced particles. The particles are considered to be locally produced, if the planes of their tracks meet at some point in the absorbers above or in the cloud chamber.

Table I gives all the data collected for groups (*a*) and (*b*).

TABLE I

	Single Tracks	Double Tracks	Triple Tracks
Observed No. of Photographs ..	143	5	1

Events under group (*c*) were found to be of three types.

1. *Showers Produced above the Chamber.*—Showers produced in the lead absorber above the chamber are those which emerged with at least two penetrating secondaries from the bottom of the absorber. The secondaries penetrated all the lead plates in the cloud chamber without any cascade multiplication.

2. Showers or starts produced inside the chamber in one of the lead plates, unaccompanied by any other particles under the lead absorber.

3. *Large Showers.*—These were mostly mixed showers having one or more parallel penetrating particles accompanied by a local penetrating shower or a soft cascade shower.

TABLE II

No. of Pb Plates	Showers produced above		Showers produced inside		Large Showers	Time hr.
	Obs. No.	Multiplicity	Obs. No.	Multiplicity		
Events under 10·5 cm. Pb Absorber						
4	1 2	2 3	2	2	1	689
7	0		1	3	1	
Events under 17 cm. Pb Absorber						
4	2	2	2	3	4	789
7	0		1	3	0	

Multiplicity is here defined as the total number of tracks which emerge from the bottom of the respective absorber.

A total number of 20 penetrating tracks, not meeting in the lead absorber, were found in these large showers.

Showers in the Cloud Chamber (Column 3, Table II).—It was observed that most of the secondaries of showers produced in the cloud chamber (Column 3), did not penetrate even a single lead plate. These must therefore be very low energy events. Further, it is to be noted that all such events, except one, were initiated by neutral primaries.

Scattering Angle Measurements.—The scattering of particles by the lead plates in the chamber was measured for all the particles which did not meet locally. A total number of 174 tracks were measured. The angles were obtained by reprojecting the photographs on a screen. Since the accuracy of measurements was of the order of 2°, we grouped the tracks within 2° intervals of angle. Most of the particles were found to scatter within the angular range of 0–2°. Five cases of scattering $\gtrsim$ 15° were observed. Table III shows the statistics of tracks scattered within different angular intervals.

TABLE III

Angles ..	0–2°	2–4°	4–6°	6–8°	8–10°	10–12°	12–14°	$\gtrsim$ 15°
No. of tracks ..	147	13	5	3	0	0	1	4

§4. DISCUSSION

The results given in the previous section permit us to distinguish between different types of penetrating particles in air showers.

(i) *Particles Not-interacting with Nuclei.*—These are particles which do not produce any secondary nuclear interaction in the lead plates in the chamber, and are not generated locally.

(ii) *Particles Interacting with Nuclei.*—These are particles which either give rise to showers in the surrounding absorbers or undergo nuclear scattering in the lead plates. They cannot be interpreted as electrons since they pass through the other lead plates in the chamber without any cascade multiplication.

Table I gives the statistics of all ionising penetrating particles recorded in the cloud chamber after traversing the lead absorber above. The majority of these did not produce or undergo any nuclear interaction in the lead plates in the chamber. One notices from Table III that a small number of particles

suffered large angle scattering in passing through the lead plates. These may be due to ionising penetrating particles other than μ-mesons. The more detailed analysis given below tends to confirm this.

§4 (*a*) *Large Angle Scattering :*

One finds from Table III that most of the particles are scattered within the angular range 0–2° and that in the distribution a cut-off is noticeable after 8°. William's theory (1939) predicts a cut-off for the distribution of multiple scattering for sea level mesons at about 7°, which is in agreement with our distribution.

Further, it is also possible to calculate the mean angle of scattering expected from William's formulæ, if one knows the energy of the particles.

Knock-on Electrons.—Assuming that the majority of the single particles are μ-mesons, it is possible to calculate the average energy of these singly ionising particles knowing the percentage of electrons which are in equilibrium with the penetrating particles. Bhabha's theory (1938) predicts that the proportion of electrons in equilibrium with μ-mesons of energy 5×10^8 ev. is of the order of 1% in lead, while for 1 Bev. μ-mesons, it increases to 6%. From our measurements, we find that about 2% knock-on electrons accompany the penetrating particles. Considering the energy loss in traversing 10 cm. of lead absorber, we estimate that most of the single penetrating particles arrive on the top of the absorber above the chamber, with energies of the order of 10^9 ev. This may be a slight under-estimate, if the group of penetrating particles includes also a certain number of interacting particles of heavier mass.

Assuming that the average energy of the particles recorded is of the order of 1 Bev., one finds that the mean angle due to multiple scattering is 1° 40′ for 2 cm. thickness of lead. Thus one can safely attribute the cases of scattering angle $\gtrsim 15°$ to nuclear interactions.

Five cases of nuclear scattering were recorded in 174 tracks in a total traversal of 3,515 gm./cm.^{2} lead, which gives an interaction length of 703 gm./cm.^{2} or 64 cm. Pb. The cross-section for nuclear scattering for μ-mesons was found to be of the order of $\sim 10^{-28}$ cm.^{2} per nucleon by Wilson (1939) and Sahiar (1951). Amaldi's experiment gave a still lower value of the order of 10^{-29} cm.^{2} corresponding to an interaction mean free path in lead of 40 m. Even taking the larger cross-section obtained by Wilson and Sahiar, one finds that the number of nuclear scatterings to be expected in 3,515 gm./cm.^{2} traversal is less than one, if all the particles are μ-mesons whereas the observed number is five. Further, one finds from

Table II, Column 3, a few cases of shower production in the lead plates inside the chamber. All these events were most probably produced by the single interacting particles which were present below the top lead absorber. These interacting particles were either those which failed to generate showers in the absorber above or the secondaries of showers produced in the top absorber with all other secondaries absorbed.

§4 (*b*) *Evaluation of the Flux of Single Ionising Interacting Particles Present below the top Absorber*

One can calculate the flux of ionising interacting particles incident on the cloud chamber below the lead absorber, considering the 4 cases of large-angle scattering (two under 10·5 cm. Pb and two under 17 cm. Pb), together with one shower produced by an ionising particle, traversing 26 gm./cm.^{2} material on an average, corresponding to the thickness of the lead plates in the chamber, neglecting the first plate. The fiux I_ρ is found to be 32 for an interaction mean free path of 160 gm./cm.^{2} for the interacting particles. Therefore, 32 out of 143 single track photographs were due to single ionising interacting particles. A further correction has to be made for the presence of-random μ-mesons of the same counter age incident on the same effective solid angle of the apparatus. In order to estimate the background of these random penetrating particles, we took 1970 random photographs. The proportion of photographs showing single penetrating tracks was found to be $(1{\cdot}5 \pm 0{\cdot}3)\%$. We therefore deduct the corresponding number from the single tracks namely $4463 \times {\cdot}015 = 66{\cdot}9$ to get finally the correct number of photographs showing tracks of μ-mesons associated with air showers namely 44.

The corrected number of events showing single μ-mesons and their rates relative to the number of shower events are given in the following table.

TABLE IV

No. of Air Shower Photographs = R	No. of Photographs showing single μ-meson tracks = $R_{\mu 1}$	$\frac{R_{\mu 1}}{R}$
4463	44	·0098 ± ·0020

This ratio $R_{\mu 1}/R$ can be used for determining $\beta = \mu/e$, the ratio of μ-mesons to electrons in air showers.

Assuming a uniform shower density of Δ particles/m^2 over the experimental arrangement, the probability that n counters of area s will be set off is

$$P^n(\Delta s) = (1 - e^{-s\Delta})^n$$

If $f(\Delta)\,d\Delta$ is the number of showers per unit time with densities between Δ and $\Delta + d\Delta$ at the place of observation, then the threefold coincidence rate is given as

$$c_{s_1} = \int_0^\infty (1 - e^{-s\Delta})^3 f(\Delta)\, d\Delta.$$

The differential density spectrum of air showers was studied by Clay (1943), Daudin (1943), Cocconi, Loverdo and Tongiorgi (1946). It is well represented by a power law of the form

$$f(\Delta)\, d\Delta = \mathrm{A}\, \Delta^{-\gamma}\, d\Delta \tag{1}$$

where r, which is $\approx 2{\cdot}5$, varies slightly with both density and altitude. Thus the total number of threefold coincidences, which is the same as the total number of shower photographs is

$$\mathrm{R} = \mathrm{A}' \int_0^\infty (1 - e^{-s\Delta})^3\, \Delta^{-\gamma}\, d\Delta \tag{2}$$

The expression (2) can be extended to find the rate of photographs showing 'n' tracks of μ-mesons accompanied by air showers of average density of Δ particles/m^2. Assuming a Poisson distribution of μ-mesons, the probability of observing 'n' μ-mesons traversing a cloud chamber of effective area S_1 is

$$e^{-\beta\Delta S_1} \frac{(\beta\Delta \mathrm{S}_1)^n}{n!}$$

Thus the expected total number of photographs showing 'n' μ-mesons is

$$\mathrm{R}_{\mu(n)} = \mathrm{A}' \int_0^\infty (1 - e^{-s\Delta})^3\, e^{-\beta\Delta S_1}\, \frac{(\beta\Delta \mathrm{S}_1)^n}{n!}\, \Delta^{-\gamma}\, d\Delta.$$

Mathematical justification for these procedures is given by Broadbent and Janossy (1948).

Considering only the events showing single μ-mesons, we get the ratio

$$\frac{\mathrm{R}_{\mu 1}}{\mathrm{R}} = \frac{\int_0^\infty (1 - e^{-s\Delta})^3\, e^{-\beta\Delta S_1}\, \beta\Delta \mathrm{S}_1 \cdot \Delta^{-\gamma}\, d\Delta}{\int_0^\infty (1 - e^{-s\Delta})^3 \cdot \Delta^{-\gamma}\, d\Delta}.$$

The above expression, for a fixed value of 'γ', is a function of $\beta = \mu/e$ which is the ratio of the number of μ-mesons relative to the total number of charged shower particles. The value of $\beta = 0{\cdot}0070$ gives the best fit for the observed ratio of $\frac{\mathrm{R}_{\mu 1}}{\mathrm{R}}$. Thus the intensity of μ-mesons relative to electrons in air showers is $0{\cdot}70\%$. In order to check this value, we have calculated the

expected number of events showing two simultaneous μ-mesons in the cloud chamber relative to the total number of shower photographs, $\frac{R_{\mu 2}}{R}$, assuming $\beta = 0{\cdot}70\%$. The calculated value is $0{\cdot}42 \times 10^{-3}$, whereas the observed value is $1{\cdot}1 \times 10^{-3}$. The agreement is not bad considering the large statistical uncertainty in the values.

In order to compare our results with those of other workers, it is necessary to know the primary energy and the average density and thus the average distance of our experimental arrangement from the cores of the showers recorded.

§4 (*c*) *Average Density of Air Showers Recorded by Our Arrangement*

With a shower selecting arrangement consisting of three or more counters in coincidence, one expects to detect showers with a very wide range of density. It has been shown by Fretter (1949) and Singer (1951) that even such a general type of shower selecting arrangement, with not a very large separation between the counter trays, can be used to select showers of a particular average density with the cores striking not very far away from the arrangement. This is clear from the behaviour of the function given in the R.H.S. of (2) which gives the probability of detecting a shower by a threefold coincidence. The function $P(S\Delta)$, for a fixed value of S, rises from zero to unity over a narrow range of Δ, while $f(\Delta)$ is a rapidly decreasing function of Δ. Thus the integrand of (2) shows a pronounced maximum for a particular value of the density Δ, depending on the size of the counters. Curve (1) shows the relative counting rates for various densi-

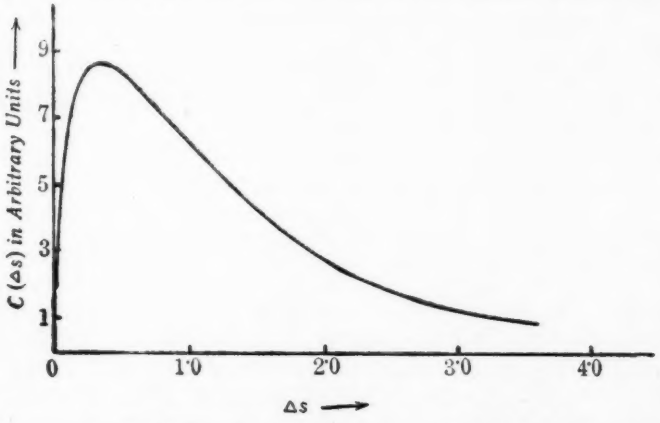

FIG. 3. *Curve I.* Probability of recording a shower with the three-fold coincidence arrangement as a function of shower density

ties of Δ as a function of '$S\Delta$' for our arrangement. We find that our arrangement was most sensitive to showers having a density of 10 particles/m^2.

Primary Energy of the Showers.—The choice of the primary energy at a given altitude depends on the density of showers and hence on the effective area of the counters. Thus every shower selecting arrangement consisting of *n*-fold coincidence counters at a given altitude always favours showers initiated by a particular energy.

In order to determine the probability of detection of extensive showers at a given depth 'z' in the atmosphere, it is necessary to know the density Δ_r of a shower with its core striking at a distance 'r' from the detecting apparatus. $\Delta_r = N_z\, \phi\,(r/r_1)$, N_z is the total number of shower particles at a depth 'z'. $\phi\,(r/r_1)$ is the Moliere function for the lateral distribution of shower particles at the plane where the cascade has its maximum and r_1 is the characteristic scattering length. At sea level $r_1 = 60$ m.

We use Bethe's approximation to the Moliere function which is

$$\phi\,(r/r_1) = [\cdot 454/r/r_1]\,(1 + 4\,r/r_1)\; e^{-4\cdot 4(r/r_1)^{2/3}}.$$

The probability of detecting a shower by a threefold coincidence arrangement at a distance r from the shower axis is

$$P^3\,(s\Delta_r) = (1 - e^{-s\Delta_r})^3 = [1 - e^{-sN\phi(r/r_1)}]^3.$$

S is the area of each counter tray. The number of showers containing a total number of particles between N and N + ΔN can be expressed as a function of the total number of particles N as

$$F\,(N)\,dN = K \cdot N^{-\gamma}\,dN.$$

The contribution to the total counting rate from showers of various total number of shower particles striking at all distances from the experimental arrangement can be given by

$$R\,(N, S) = N^{-\gamma} \int_0^\infty [1 - e^{-sN\phi(r/r_1)}]^3 \cdot 2\pi r dr.$$

Curve (2) gives the function R (N, S) against the logarithm of NS. [Procedure is given by Fretter (1949)].

We find that the maximum contribution to the total counting rate comes from showers with a total number of particles $N = 2\cdot 8 \times 10^4$. According to the Cascade theory, the initial energies of showers of a total number of particles $2\cdot 8 \times 10^4$ at sea level are of the order of 10^{15} ev. if the showers are originated by a single photon or electron. Since it is now believed that the showers are initiated by photons which are the decay products of neutral

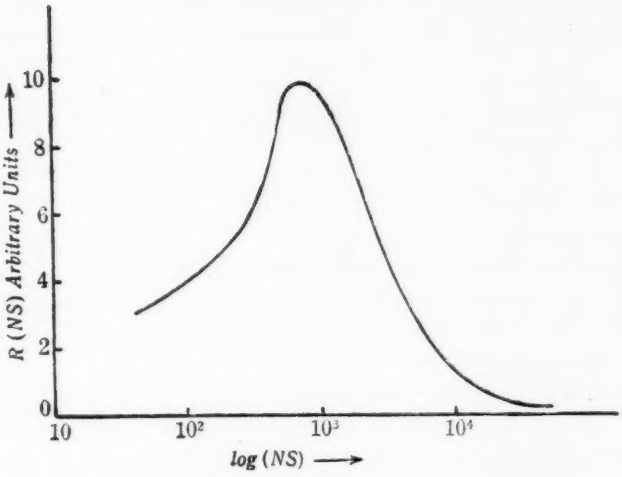

FIG. 4. *Curve II.* Relative contribution of showers of various size (N) against the logarithm of *NS*

mesons, produced in the interactions of the primaries with the nuclei of air, the question of the multiplicity of production of neutral π-mesons will arise.

The total number of shower particles could for instance also be produced by 7 π° mesons with an energy of 2×10^{14} ev. each. This corresponds to an initial energy $\sim1\cdot4\times10^{15}$ ev. for the shower. The discrepancy between this value and that calculated neglecting the multiplicity is not large. Even for the higher multiplicities, the discrepancy may not be very serious. For instance, in an extreme case, when the initial energy of each π°-meson $\sim5\times10^{13}$ ev., the corresponding multiplicity will be ~50 and the energy of the shower will be $\sim2\cdot5\times10^{15}$ ev.

Since the average density of the showers detected was 10 particles/m.^{2}, one finds that most of the showers of $\sim10^{15}$ ev. initial energies strike with their cores within 10 m. from the experimental arrangement.

We conclude that our experimental arrangement measured the relative abundance of the μ-meson component in extensive showers of primary energy of the order of 10^{15} ev. with their cores striking within 10 m. from the arrangement.

Greisen, *et al.*, measured the ratio of μ-mesons to electrons as 0·8% at 5 m. from the cores of the showers at 4300 m. elevation, while Sitte*

* We are indebted to Professor K. Sitte for kindly communicating these results.

obtained 0·78% and 0·74% for showers of 10^{13} ev. and 10^{14} ev. initial energy at 4300 m. and 3240 m. respectively. Thus we find that our value of 0·70% for μ/e ratio is in very good agreement with those reported by previous workers. We conclude that the relative proportion of μ-mesons to electrons probably does not vary greatly in showers of primary energy ranging from 10^{13} ev. to 10^{15} ev.

§5. Nuclear Interacting Component in Air Showers

We have already noticed in §4 (*b*) that a nuclear interacting component is present in air showers, which following Rossi, we shall call the N-component. The flux of these particles, both ionising and non-ionising, incident on the top of the cloud chamber below the lead absorber may be calculated from the number of events showing nuclear interaction in the cloud chamber, using the following expression.

$$N_s = I\,(1 - e^{-x_1/\lambda \text{coll}}).$$

N_s = the total number of nuclear interactions produced by both neutral and ionising N-particles traversing x_1 gm./cm.^{2} of material in the cloud chamber (events given in Column 3, Table II, together with those showing large angle scattering), where $x_1 = 26$ gm./cm.^{2} λ coll, the collision mean free path, is 160 gm./cm.^{2} I is the flux of the N-component incident on the chamber below the lead absorber. We find the N-component flux to be *66*. In order to know the relative proportion of N-component to μ-mesons, it is necessary to know the total number of μ-mesons recorded during the same interval of time in the same effective solid angle. The total number of tracks due to the penetrating particles is found to be 174, considering all single and multiple tracks which did not meet in the surrounding absorbers. With all corrections applied as pointed out earlier in Section 4 (*b*), the flux μ of-mesons is found to be 75 and the ratio of the N-component to the μ-meson component in air showers is thus

$$I/\mu = 0{\cdot}88.$$

Since the flux I has been calculated considering events in the cloud chamber produced by single ionising and non-ionising particles incident on it and since only a few events contain more than one particle originating in the lead absorber above, I must approximately correspond to the number of N-particles incident on the top absorber with energy sufficient to penetrate 10 to 17 cm. of lead or sufficient to produce secondaries at least one of which is capable of penetrating to the cloud chamber.

Therefore this result shows that the N-particles in air showers are nearly as abundant as μ-mesons.

Comparison with the Results of Other Workers.—Several investigators working at mountain altitudes obtained the ratio of the N-component to μ-mesons in air showers. Greisen, working at 4300 m., obtained $0{\cdot}60 \pm {\cdot}15$ for this ratio, while a much lower value of $0{\cdot}26 \pm {\cdot}03$ was reported by Sitte at 3240 m.

Recently repeating the measurements at both elevations Sitte has reported a slightly higher value of $(38 \pm 5)\%$ at 3240 m. and $(62 \pm 7)\%$ at the higher altitude in agreement with Greisen. Our value for the ratio of the N-component to μ-mesons given in the previous section is considerably higher, but it includes particles of comparatively lower energy. Both the previous workers considered the flux of the N-component which can produce meson showers of two or more secondaries in lead absorber of thickness 12 cm. or more (with total kinetic energy of charged secondaries at least 1·5 to 2·5 Bev.).

These nuclear interacting particles must be very energetic. Therefore in order to compare our result with those obtained by Sitte and Greisen, we must estimate the flux of the N-component capable of producing showers of two or more penetrating secondaries, considering only the events produced in the lead absorber above the chamber (Table II, Column 2).

It has been found that the interaction length for shower production changes with the primary energy. Froelich, *et al.*, observed that the mean free path varies from 190 gm./cm.^{2} to 160 gm./cm.^{2} over the energy range 1 to 10 Bev. Walker (1950) also reported a decrease of the mean free path with increasing shower size. The mean free path for shower production changes from 200 gm./cm.^{2} to 140 gm./cm.^{2} when the number of shower particles increases from 3 to 7.

The minimum energy of the primaries of these showers can be obtained if one knows the total kinetic energy of the secondary particles. We find that the minimum number of penetrating particles in the showers produced in the absorber above the chamber is two. For the cases of mixed showers, the multiplicity is of course found to be higher. In all these events, we measured the multiple scattering suffered by the secondaries in the total 2 cm. thickness of the lead plates. It was observed that most of the particles were scattered within 0–2° except two cases, which were found to scatter by 3°. Thus the minimum limit for the kinetic energy of these secondaries can be determined from the theory of multiple scattering. William's formula gives $8{\cdot}7 \times 10^8$ ev. energy corresponding to 2° mean angle of multiple scattering in a lead plate of 2 cm. thickness, and for 3° the energy is of the order of $3{\cdot}5 \times 10^8$ ev. Thus the minimum total kinetic energy of

charged secondaries even in showers of two penetrating particles is of the order of 1·7 Bev. These showers are of energies comparable to those recorded by other workers.

In our experiment the flux of the N-component capable of generating meson showers of at least two particles which penetrate all the lead plates in the chamber, is found to be 22 for a mean free path of 200 gm./cm.^{2} Thus the intensity of the energetic N-component relative to the μ-meson component in air shower is

$$N/\mu = 0{\cdot}29 \pm 0{\cdot}08.$$

The sea level ratio of nuclear interacting particles to μ-mesons $\sim 29\%$ in showers of initial energy $\sim 10^{15}$ ev., is consistent with McCusker's (1950) result, who working at sea level obtained about 30% N-particles in the penetrating radiation of air showers. Other workers reported 62% and 38% recording showers of 10^{13} ev. and 10^{14} ev. initial energies between the atmospheric depths of 600 gm./cm.^{2} and 700 gm./cm.^{2} This decrease of N-component with increasing atmospheric depth is much smaller than the decrease expected from simple absorption.

One may therefore conclude that in showers of initial energy $\sim 10^{15}$ ev. the multiplication of nuclear interacting particles continues throughout the atmosphere. A fraction of secondaries produced in these N-component cascades are still energetic enough to come down to sea level to reproduce near the local absorber.

SUMMARY

Results of the present experiment on the penetrating component of extensive showers lead to the following conclusions. The penetrating particles in extensive showers are of two types. A large proportion of the particles show no interaction with nuclei. The relative abundance of the non-interacting component in air showers is found to $\sim 0{\cdot}7\%$ for showers of primary energy $\sim 10^{15}$ ev. at about 10 m. from the cores of the showers at sea level.

There is also evidence for the presence of an appreciable percentage of the particles showing interaction with nuclei even at sea level. This indicates the occurrence of cascades of nuclear collisions in these showers.

The N-component capable of producing penetrating showers of at least two ionising secondaries (with minimum total kinetic energy of the secondaries $\sim 1{\cdot}7$ Bev.) is found to be 29% as great as that of the non-interacting penetrating particles. Whereas the ratio of the N-component μ-mesons, considering all low energy events (energy ~ 1 Bev.) is found to be of the order of 0·88. This shows that large number of N-particles of

low energy exists in air showers at sea level. On comparing our results with those of other workers recording showers of lower initial energies at mountain altitudes, we find that the ratio of μ-mesons to electrons is practically identical for all these showers while the ratio of the N-component to μ-mesons decreases from 62% to 29% over an energy range 10^{13} ev. to 10^{15} ev. between the atmospheric depths of 600 gm./cm.^{2} and sea level. This decrease of the N-component with increasing atmospheric depth is much smaller than that expected due to simple attenuation of the N-component in the atmospheric length traversed between these two levels.

Acknowledgments

We wish to record here our sincere thanks to Professor H. J. Bhabha for all encouragements and facilities he has given us for conducting this experiment.

We are also greatly indebted to Professor B. Peters for helpful criticism.

References

Amaldi, E. and Fidecaro, G. .. *Nuovo Cimento*, 1950, 7.

Bhabha, H. J. .. *Proc. Roy. Soc.*, 1938, **164**, 257.

Broadbent, D. and Janossy, L. .. *Ibid.*, 1948, **192**, 364.

Brown, W. W. and McKay, A. S. .. *Phys. Rev.*, 1949, **76**. 1035.

Chowdhuri, B. .. *Proc. Phys. Soc.*, 1950, **63**, 165.

Clay, J. .. *Physica*, 1943, **9**, 897.

Cocconi, G., Loverdo, A. and Tongiorgi, V. *Phys. Rev.*, 1946, **70**, 841.

——, Tongiorgi, V. and Greisen, K. *Ibid.*, 1949, **75**, 1063.

Daudin, J. .. *Ann. de Phys.*, 1943, 18.

Froehlich, F. E., Harth, E. M. and Sitte, K. Private Communication.

Greisen, K., Walker, W. D. and Walker, S. P. *Phys. Rev.*, 1950, **80**, 535.

John Ise Jr. and Fretter, W. S. .. *Ibid.*. 1949, **76**, 933.

McCusker, C. B. A. .. *Proc. Phys. Soc.* 1950, **63 A**, 1240.

Sahiar. A. B. .. *Proc. Ind. Acad. Sci.* 1951, **34**, 201.

Singer, S. F. .. *Phys. Rev.* 1951, **81**, 579.

Sitte, K. .. *Ibid.*, 1950, **78**, 721.

Walker, W. D. .. *Ibid.*, 1950, **77**, 686.

Williams, E. J. .. *Proc. Roy. Soc.*, 1939, **169**, 531.

Wilson, J. G. .. *Ibid.*, 1940, **174**, 73.

ON THE FORMATION OF ALPHA-PARTICLES IN RADIOACTIVE NUCLEI

By S. Jha

(*Tata Institute of Fundamental Research, Bombay*)

Received September 19, 1952

(Communicated by Prof. H. J. Bhabha, F.R.S., F.A.SC.)

Abstract

The factors by which the claculated half-lives of the alpha-disintegration of odd-even, even-odd and odd-odd nuclei deviate from the observed ones cannot all be explained by the alpha-particles carrying away a large angular momentum or by the unusual contraction in the nuclear radius due to structural peculiarities. The departure is attributed to the probability of the formation of alpha-particles before emission. In this paper, an estimate of the relative probability of the formation has been made on the shell-model and on the assumption that an alpha-particle is formed out of two neutrons and the two protons when they all have the same angular momentum. The alpha decay of Po^{212}, Po^{210} and Bi^{211} and that of the two long-lived states of Po^{211} has been discussed.

§1

With a large addition, in recent years, in the list of the alpha-emitting isotopes, the total being now over a hundred, it has been found that there is a significant regularity if one plots the logarithm of the alpha-decay half-life against the alpha disintegration-energy separately for even-even, even-odd, odd-even and odd-odd nuclei [Perlman, Ghiorso and Seaborg (1950)]. Assuming the nuclear radius $r = 1{\cdot}48 \times 10^{-13}\, A^{-1/3}$ these authors calculated, with the Gamow formula

$$\log_{10}\lambda = 21{\cdot}843 + \tfrac{1}{2}(\log_{10}E) - \log_{10}r + 0{\cdot}217\,(4/A - 4) - 1{\cdot}104\,(Z-2)/\{E\,[1 + (4/A - 4]\}^{\frac{1}{2}}\alpha_0 + 1{\cdot}104\,(Z-2)/\{E\,[1 + (4/A - 4]\}^{\frac{1}{2}} \cdot \sin\alpha_0 \cos\alpha_0, \qquad (2)$$

with $\cos\alpha_0 = 0{\cdot}5893\ [Er/(Z-2)]^{\frac{1}{2}}$,

the decay half-life for different energies for each value of Z from $Z = 83$ to $Z = 93$. For the even nuclei, the observed points fall very nearly on the calculated curve [Perlman and Ypsilantis (1950), Kaplan (1951), and Rasmussen (1952)]. If any of these even-even isotopes emits more than one energy-group of alpha-particles, the point for each group falls on the

calculated curve. On the other hand, in the case of even-odd, odd-even and odd-odd isotopes, the points representing the observed values of the decay-energy and the half-life fall well above the calculated curve, implying that the actual half-life is more than what would be expected in the simple Gamow picture of the alpha-particle emission. Whenever there are more than one alpha-group being emitted from an even-odd, or odd-even or odd-odd isotope, the one with the maximum energy, presumably the one leading to the ground-state of the daughter product, shows the maximum departure from the calculated curve, and the one with the minimum energy shows the least departure.

Basing the consideration of the alpha-particle emission process on the Gamow picture, wherein it is assumed that the alpha-particle exists as an entity with a certain kinetic energy held within the potential barrier of the daughter nucleus, one can attribute these departures either to the contraction of the nuclear radius due to some structural peculiarity, for instance the closing of the neutron or proton shell, or to the alpha-particle carrying away a large angular momentum, which in effect reduces the nuclear radius and increases the half-life of decay. The analysis of the data by Perlman, Ghiorso, Seaborg (1950) shows clearly that one cannot attribute all the departure to one or both of these causes. Preston (1951) has sought to explain these departures on the hypothesis of a non-central interaction of the alpha-particles outside the nucleus with the unsymmetrically distributed protons in the product nucleus. He has tried to show that by means of this coupling, an alpha-particle can take energy from the daughter nucleus or give energy to it, and thus alter its own ability to penetrate the barrier. As is stated by Preston, this interaction may at best account for a part of the departure. The predominant cause of the departure seems to be that alpha-particles may not exist as such inside heavy nuclei, but that they are formed out of two neutrons and two protons before emission. In the case of the even-even nuclei, the time of formation presumably is very small; but in other cases it is relatively large. The magnitude of the probability of formation perhaps depends on the nuclear configuration of the initial and the final state. This possibility has been discussed by Perlman, Ghiorso and Seaborg (1950), Feather (1951, 1952), Preston (1951), Nordstrom (1951) and Asaro, *et al.* (1952).

§2

We propose here to suggest a mechanism of the formation of alpha-particles inside atomic nuclei on the nuclear shell model; and, on this basis, we shall attempt a qualitative explanation of the relative prohibition of the

alpha-particle formation in different classes of nuclei. If two neutrons and two protons are to fuse together to form an alpha-particle, they must be in a situation where they would interact strongly. It is a well-established fact that the force operating between the nucleons is a short range one. It has long been suggested, in order to account for the instability of the systems with an odd number of neutrons and an odd number of protons in contrast with the stability of the systems with an even number of neutrons and an even number of protons, that the neutrons and protons interact strongly only when they are approximately in the same quantum state; that is how the stability of systems like ${}_3Li_3^6$, ${}_5B_5^{10}$ and ${}_7N_7^{14}$ comes about. It is an observed fact that only *s*-wave slow neutrons are captured by protons and deuteron targets, the fast ones are not. One could thus suggest that in order that an alpha-particle may be formed out of two neutrons and two protons, it is necessary that they should be close together, and that they should have the same angular momentum. In this connection, it may be stated that if B (n_1) and B (n_2) be the binding-energies of the last two neutrons [*i.e.*, the binding energy of the Nth and the (N − 1)th neutrons in ${}_ZM_N^A$], and B (p_1) and B (p_2) the binding-energies of the last two protons [*i.e.*, the binding-energy of the Zth and the (Z − 1)th proton in ${}_ZM_N^A$) in an isotope, the energy of the alpha-particle emitted from it is given by

$$E_\alpha = D_\alpha - [B(n_1) + B(n_2) + B(p_1) + B(p_2)], \qquad (1)$$

where D_α is the binding energy of an alpha-particle [Jha (1950), Jha and Dube (1952)]. In other words, the energy of an alpha-particle emitted from the nuclei of an isotope is the difference of the energy required to pull out two neutron and two protons, and the energy liberated when they fuse to form an alpha-particle. In the shell model, the neutrons and protons are supposed to be packed in different *l* and J states in accordance with the Pauli principle. In heavy nuclei, on this model, the neutrons being much larger in number than the protons, are filled up to much higher levels than the protons, and the last few neutrons and protons have usually very different *l* and J values. In view of the condition, described above as most favourable for the formation of an alpha-particle out of two neutrons and protons, we suggest that in alpha-active isotopes, the two uppermost protons make a transition to the J-state of the two uppermost neutrons, and in that state serving as an intermediate or virtual state, they, having the same angular momentum, coalesce to form an alpha-particle with an energy given by (1). In the Gamow and Condon-Gurney theory of alpha decay, the disintegration constant λ is given by

$$\lambda = Ce^{-F(V, Z, r)}$$

where v, Z and r are the alpha-particle velocity, the atomic number and the effective nuclear radius respectively, and C is a constant interpreted as the frequency with which the alpha-particle in the potential barrier of the daughter nucleus encounters the potential barrier, and the exponential part represents the penetrability of the potential barrier. The non-zero time of formation of alpha-particles prior to their leakage through the potential barrier will make this factor C different for different nuclear species. The coefficient C can be expressed as the product of two factors.

$$C = D \times G,$$

where D is the probability of the formation of an alpha-particle and G the frequency with which the alpha-particle strikes the potential barrier, D, being a function of the state of the parent nucleus in which the disintegration takes place, of the state of the daughter product which the disintegration leads to, and perhaps also of the disintegration energy. In the cases of the even-even alpha-emitters, where, according to Perlman, Ghiorso and Seaborg (1950) the observed half-life is very nearly that given by the Gamow formula, this factor would be unity; but in the cases of the even-odd, odd-even, and odd-odd isotopes where there are large deviations from the Gamow formula, this factor should be a small fraction, thus making the decay half-life larger. In the mechanism of the formation of the alpha-particle suggested here, this factor D would correspond to the probability of the transition of the two low-lying protons to the state of the two uppermost neutrons.

§3

It has not been possible so far to calculate the probability of the proton transitions suggested here; but if one assumes that it is of the same type as the isomeric transitions, *i.e.*, the probability of transition is small if the change of angular momentum is large, and the energy change is small, and that it is large if the change of angular momentum is small and the energy change is large [Weisskoff (1951), Goldhaber and Sunyar (1951)], one has then a basis for making some estimates.

In order to be able to proceed further, one needs to know the nuclear configuration of the alpha-active isotopes. Unfortunately the data available to us are not sufficient to enable us to write the nuclear configurations with any confidence. Even then it is possible to describe our point of view more definitely and give qualitative explanations. We propose to discuss the case of Po^{212}, Po^{211}, Po^{210} and Bi^{211}. From the fact that the spin of ${}_{83}Bi^{209}_{126}$ is 9/2 [Mack (1950)], on Mayer's model and Mayer's hypothesis about the spins of the even-odd and odd-even nuclei [Mayer (1950)] the 83rd proton

occupies the level $1h_{9/2}$. According to Mayer, the odd nucleon usually occupies a low J level, but in heavy nuclei, the protons have a tendency, perhaps because of the Coulomb repulsion, to occupy a state of high angular momentum. Since in the neighbourhood of the level $1\,h_{9/2}$ this level has the highest J value, it is natural to assume that in ${}_{84}$Po, both the protons outside of the shell will occupy $1\,h_{9/2}$. According to Feather and Richardson (1948) and Perlman, Ghiorso and Seaborg (1950), the 127th neutron in ${}_{82}Pb^{209}_{127}$ is in the level $1\,i_{11/2}$ but, according to Mayer and Moszkowski and Nordheim (1951), and Nordheim (1951), the 127th neutron in ${}_{82}Pb^{209}_{127}$ and in ${}_{81}Tl^{208}_{127}$ goes to the level $2\,g_{9/2}$ but in ${}_{83}Bi^{210}_{127}$ it goes to $3\,d_{5/2}$. It may not be out of place to state here that these assignments are in keeping with Nordheim's rule about the spin of odd-odd nuclei [Nordheim (1950)] but the validity of this rule is being questioned. [A. Mukerji and P. Preiswerk (1952)]. These irregularities may occur for the single 127th neutron, but perhaps one could take that the pair of neutrons, the 127th and the 128th in ${}_{84}Po^{212}_{128}$ are $1i_{11/2}$. We can write tentatively for the configuration of ${}_{84}Po^{212}_{128}$.

Protons	.. ..	$1\,h_{9/2}{}^2$
Neutrons	.. ..	$1\,i_{11/2}{}^2$

Perhaps the heavier even-even nuclei of polonium and the even-even nuclei of Emanation (Z = 86), Radium (Z = 88), and Thorium (Z = 90) with the neutron number between 128 and 138 will have the same configuration for the last two protons and the last two neutrons.

The probability of the formation of an alpha-particle in ${}_{14}Po^{212}_{128}$ is of the order of the probability of the transition of the two protons in the level $1\,h_{9/2}$ to the level $1\,i_{11/2}$. The energy difference between these two levels would be approximately equal to the difference of the decay-energy of Ra E and the decay-energy of a neutron (*i.e.*, about 0·4 MeV). If we denote by P the probability of the transition of a nucleon from one state to the other, the transition probability of the two protons in Po^{212} is of the order of

$$\underset{\Delta E \sim 0{\cdot}4\ \text{MeV}}{P\,(h_{9/2} \rightarrow i_{11/2},\ \text{yes})} \times \underset{\Delta E \sim 0{\cdot}4\ \text{MeV}}{P\,(h_{9/2} \rightarrow i_{11/2},\ \text{yes})}$$

(yes meaning the change of parity).

The probability of the formation of an alpha-particle in this isotope is, on our picture, of the order of

$$\underset{\Delta E \sim 0{\cdot}4\ \text{MeV}}{P\,(\Delta J = 1,\ \text{yes})} \times \underset{\Delta E \sim 0{\cdot}4\ \text{MeV}}{P\,(\Delta J = 1,\ \text{yes})}$$

$_{84}Po^{210}_{126}$.—According to Mayer and Moszkowski and Nordheim (1951), the 81st proton occupies the level $3\,s_{\frac{1}{2}}$ and the 125th neutron the level $3\,p_{\frac{1}{2}}$. We are interested in the level occupied by the 126th neutron and the 82nd proton. One could perhaps think of the β^--decay in a rather schematic way that the topmost neutron gives off a β^--particle and becomes converted into a proton and then makes transition to the lower proton states. On this picture, the fact that the 125th neutron in $_{81}Tl^{206}_{125}$ makes a direct transition by β^--decay to the ground state of the 82nd proton in $_{82}Pb^{206}_{124}$ leads us to think that the paired 82nd proton does not occupy a level of high angular momentum. Perhaps the 82nd proton and the 126th neutron occupy the $3\,s_{\frac{1}{2}}$ and $3\,p_{\frac{1}{2}}$ levels respectively.

For the configuration of $_{84}Po^{210}_{126}$, we write

Protons	.. ..	$3\,s^2_{1/2}\;1\,h^2_{9/2}$
Neutron	.. ..	$3\,p^2_{1/2}$

In order to estimate the transition probability of two protons in the state $1\,h_{9/2}$ to the state $3\,p_{1/2}$, we need to know the energy difference between these levels; from the absence of gamma-rays in the β^--decay of Ra E, one could perhaps guess that excited states of Po^{210} would be more than about 0·4 MeV above its ground state. The probability of the formation of alpha-particles in Po^{210} would be of the order of

$$P\,(h_{9/2} \rightarrow p_{1/2}\ \text{no}) \times P\,(h_{9/2} \rightarrow p_{1/2},\ \text{no})$$
$$\Delta E > 0{\cdot}4\ \text{MeV} \qquad E > 0{\cdot}4\ \text{MeV}$$

Or

$$P\,(\Delta J = -4,\ \text{no}) \times P\,(\Delta J = -4,\ \text{no})$$
$$E > 0{\cdot}4\ \text{MeV} \qquad E > 0{\cdot}4\ \text{MeV}$$

For Po^{210}, Perlman, Ghiorso and Seaborg (1950) report a departure factor of 30. The position is not unsatisfactory in that if the height of the virtual level $3\,p_{1/2}$ in Po^{210} were the same as that of $g_{9/2}$ in Po^{212}, the departure factor would have been enormous; it is perhaps the larger energy difference that has made the departure factor as small as 30.

$_{83}Bi^{211}_{128}$.—We write for the configuration of this isotope [according to Feather (1952), the 83rd proton should be $2\,f_{5/2}$].

Proton ..	.. ..	$3\,s^2_{1/2}\;1\,h_{9/2}$
Neutrons	.. ..	$3\,p^2_{1/2}\;1\,i^2_{11/2}$

In this case, the height of the proton level $1\,i_{11/2}$ above the $1\,h_{9/2}$ would be of the order of 0·4 MeV but its height above the level $3\,s^2_{1/2}$ may well be

2 MeV or more. The probability of the alpha-particle formation is of the order of

$$P(h_{9/2} \rightarrow i_{11/2}, \text{ yes}) \times P(s_{1/2} \rightarrow i_{11/2}, \text{ no})$$
$$\Delta E \sim 0{\cdot}4 \text{ MeV} \qquad \Delta E \sim 2 \text{ MeV}$$

Or

$$P(\Delta J = 1, \text{ yes}) \times P(\Delta J = 5, \text{ no})$$
$$\Delta E \sim 0{\cdot}4 \text{ MeV} \qquad \Delta E \sim 2 \text{ MeV}$$

The departure factor in the alpha decay of this isotope, according to Perlman, Ghiorso and Seaborg (1950), for the two groups of alphas is 150 and 750.

Lastly we discuss the case of $_{84}Po^{211}$. This isotope decays with the emission of alpha-particles of energy 7·28 MeV from its ground state, but from its isomeric state, which has an energy of excitation of about 0·3 MeV, with the emission of alpha-particles of energies 7·58, 7·03, 6·7 and 6·46 MeV [Neumann and Perlman (1951), Spiess (1951)]. According to Feather (1952), the departure factor is much larger for the alpha-disintegration $_{84}Po^{211}$ (isomeric state) $\rightarrow$ $_{82}Pb^{207}$ than for the disintegration from the ground state of Po^{211}. We write for the configuration of this isotope in the ground state,

Proton	.. ..	$1\, h_{9/2}^2$
Neutrons	.. ..	$3\, p_{1/2}^2\, 1\, i_{11/2}$

and, since the difference of spins between the ground and the isomeric state is required to be 5 units, it is not unreasonable, although it involves a crossing of levels, to write for the configuration of the isomeric state

Protons	.. ..	$1\, h_{9/2}^2$
Neutrons	.. ..	$3\, p_{1/2}^2\, 4\, s_{1/2}$

The probability of the formation of an alpha-particle from the ground state of $_{84}Po^{211}$, on our picture, is of the order of

$$P(h_{9/2} \rightarrow i_{11/2}, \text{ yes}) \times P(h_{9/2} \rightarrow i_{11/2}, \text{ yes}) \times P(p_{1/2} \rightarrow i_{11/2}, \text{ yes})$$

Or

$$P(\Delta J = 1, \text{ yes}) \times P(\Delta J = 1, \text{ yes}) \times P(\Delta J = 5, \text{ yes})$$

and that from the isomeric state of $_{84}Po^{211}$ is of the order of

$$P(h_{9/2} \rightarrow s_{1/2}, \text{ yes}) \times P(h_{9/2} \rightarrow s_{1/2}, \text{ yes}) \times P(p_{1/2} \rightarrow s_{1/2}, \text{ yes})$$

Or

$$P(\Delta J = 4, \text{ yes}) \times P(\Delta J = 4, \text{ yes}) \times P(\Delta J = 0, \text{ yes}).$$

The energy change in the transitions in the isomeric state is in each case larger by 0·3 MeV. It can be seen that the probability of the alpha-particle formation from the isomeric state is much smaller. If we take the spin of $_{83}Ac\ C^{211}$ to be 5/2 [Feather (1952)] and the same for $_{85}At^{211}$, thus having the

83rd and the 85th proton in these isotopes in the state $2f_{5/2}$ we have a basis for understanding the disparity in the k-capture and β^--decay probabilities to the ground and the isomeric state of $_{84}Po^{211}$.

§4

We have shown, on the basis of our mechanism of the formation of an alpha-particle, how the departure factor in the alpha-disintegration of the even-odd and odd-even isotopes can be much larger than compared to the alpha-disintegration of the even-even nuclei. On this view, there should be some prohibition in the alpha-disintegration of the even-even nuclei also; perhaps a more accurate determination of the alpha-decay half-life and the alpha-decay energy may reveal some deviation. It must be emphasised that the probability of the alpha-particle formation depends, in the view presented in this paper, very much on the configurations of the parent and daughter nuclei. In this paper, an almost mechanical use of the Mayer level scheme has been made. For instance, although there are instances that the spin values of two isotopes (masses differing by two units) are different, and the spin values of two isotones are different, the 83rd proton in $_{83}Bi^{211}$ has been assumed to be in $h_{9/2}$ level on the basis of spin of $_{83}Bi^{209}$. It is worthwhile mentioning here that although on Mayer's scheme the order of levels for protons below 82 is $\ldots.2\,d_{5/2},\ _{3/2},\ 3\,s_{1/2}$ and $1\,h_{11/2}$, and for the neutrons below 126 $\ldots.2f_{7/2},\ _{5/2},\ 3\,p_{3/2},\ _{1/2}$ and $1\,i_{13/2}$, the observed order for the protons appears to be $\ldots.1\,h_{11/2},\ 2\,d\ _{3/2}$ and $3\,s_{1/2}$ and for the neutrons $2\,d_{5/2},\ _{3/2},\ 1\,i_{13/2}$ and $3\,p_{1/2}$ [Klinkenberg (1952)]. For reasons discussed before, it seems that the 82nd proton occupies the level $3\,s_{1/2}$ when there are 82 protons only, and the 126th neutron occupies the level $3\,p_{1/2}$ when there are 126 neutrons only. In dealing with the phenomenon of alpha-decay on the shell model, one is interested not only in the levels occupied by the last proton and the last neutron but the last three or four neutrons and protons. It seems that there is a rearrangement of the shell, being completed at $Z = 82$, when more protons are added, and that there is a rearrangement of the shell at $N = 126$ when more neutrons are added. One is led to think like this to explain, on the shell model, the occurrence of many alpha groups from the isotopes of $_{83}Bi$ and $_{84}Po$. No attempt was made to estimate the relative probabilities of the formation of alpha-particle of different groups either in the even-even or other classes of nuclei, but the method is exactly similar. One can guess however that when there are many groups of alpha-particles being emitted, there is, in our picture of the alpha-particle formation, a definite relationship between the transition-probability-ratio of the emitted gamma rays and the ratio of the departure factors. It

must be pointed out that an equal probability of the formation for each of the many groups of the alpha-particles emitted from even-even nuclei is difficult to understand.

The case of ${}_{84}Po^{211}_{127}$ requires some comments. The assignment of the spin 11/2 for ${}_{84}Po^{211}_{127}$ and 5/2 for ${}_{83}Bi^{211}_{128}$ is based on the assumptions that one can separate out the J-dependent departure factor in the alpha-disintegrations, and that the departure factors in the alpha-disintegration of the odd A isotopes of Polonium are the same as in the even A isotopes [Feather (1952)]. This seems to be true of the odd A isotopes of Polonium ($Po^{213, 215}$) [Perlman, Ghiorso and Seaborg (1950)]; and this is understandable from our point of view; it happens to be so because of the 129th and the 131st neutron occupying the large J levels, and the small angular momentum difference in the neutron and the proton ground states. Since in the alpha-disintegration of Po^{211} the 126 neutron in $p_{1/2}$ state is involved, it is reasonable to think that the departure factor here must be larger than in the heavier isotopes of polonium, the spin values 11/2 and 5/2 are, therefore, an overestimate. It does not affect our argument for showing a larger prohibition of the formation of the alpha-particles in the isomeric state of Po^{211}.

ACKNOWLEDGEMENTS

My sincere thanks are due to Professor H. J. Bhabha for his kind interest in this work. I have profited greatly from discussions with Dr. A. K. Saha of the Institute of Nuclear Physics, Calcutta, Professor B. Peters and Drs. A. Mukerji and B. V. Thosar of this Institute. I owe a deep debt of gratitude to the Maharajadhiraj of Darbhanga, whose kind financial assistance enabled me to prolong my stay abroad when the beginning of this work was made. I wish to express my gratefulness to Miss Grizel Blair of Oslo for her hospitality.

REFERENCES

Asaro, F., Reynolds, F. L. and Perlman, I. .. *Phys. Rev.*, 1952, **87**, 277.

Feather, N. .. *Phil. Mag.*, 1951, **42**, 568.

———— .. *Ibid.*, 1952, **43**, 476.

—— and Richardson, H. O. W. .. *Proc. Phys. Soc.*, 1948, **61**, 452.

Goldhaber, M. and Sunyar, A. W. .. *Phys. Rev.*, 1951, **83**, 906.

Jha, S. .. *Thesis*, Edinburgh University, 1950

—— and Dube, G. P. .. *Ind. Journ. Physics*, 1952, **26**, 15.

Kaplan, I. .. *Phys. Rev.*, 1951, **81**, 962.

Klinkenberg, P. F. A. .. *Rev. Mod. Phys.*, 1952, **24**, 63.

Mack, J. E. .. *Ibid.*, 1950, **22**, 64.

Mayer, M. G. .. *Phys. Rev.*, 1950, **78**, 16.

Mayer, M. G., Moszkowski, S. A. and Nordheim, L. W.		*Rev. Mod. Phys.*, 1951, **23**, 315.
Mukerji, A. and Preiswerk, P.	..	*Helv. Acta. Phys.*, 1952, **25**, 387.
Neumann, H. M. and Perlman, I.	..	*Phys. Rev.*, 1951, **81**, 958.
Nordheim, L. W.	..	*Ibid.*, 1950, **78**, 294.
————	..	*Rev. Mod. Phys.*, 1951, **23**, 322.
Perlman, I., Ghiorso, A. and Seaborg, G. T.		*Phys. Rev.*, 1950, **77**, 26.
—— and Ypsilantis, T. J	..	*Ibid.*, 1950, **79**, 30.
Preston, M. A.	..	*Ibid.*, 1951, **82**, 515.
Rasmussen, J. O.	..	*Nuclear Science Abstract*, 1952, **6**, 46.
Spiess, F. N.	..	*American Report*, UCRL, 1951, 1494
Weisskopf, V F	..	*Phys. Rev.*, 1951, **83**, 1073.

RELATIVISTIC FIELD QUANTIZATION

By B. M. Udgaonkar

(*Tata Institute of Fundamental Research, Bombay*)

Received September 2, 1952

(Communicated by Prof. H. J. Bhabha, F.R.S., F.A.SC.)

§1. Introduction

The purpose of this paper is to show how any equation belonging to the entire scheme of relativistic field equations proposed by Bhabha (1949), describing a particle having one or more finite and non-zero values of the rest-mass and any arbitrary spin can be quantized. A particular equation in the scheme, so quantized, can, of course, be physically interpreted only if either the free charge density or the free energy density is positive definite. Incidentally, the method also yields a necessary and sufficient condition for the free charge density or energy density to be non-zero.

§2. General Theory*

Bhabha (*loc. cit.*) has shown that on the basis of the very general assumptions underlying the present relativistic quantum mechanics, the most general expression in the Lagrange function, quadratic in the components of the wave function ψ, can always be written in the canonical form

$$(\psi a^{\dagger}\, \mathrm{D}^{k} p_{k} + \beta\chi)\,\psi, \tag{1}$$

where† $p_k = -i\partial/\partial x^k$; χ is an arbitrary constant of the same dimensions as p_k; D, $\mathrm{D}a^k$, and $\mathrm{D}\beta$ are six hermitian matrices of which D is non-singular. The wave equation arising from this Lagrangian is

$$(\mathrm{P} + \beta\chi)\,\psi \equiv (a^k p_k + \beta\chi)\,\psi = 0. \tag{2}$$

The wave-function ψ transforms according to a representation $\mathcal{R}$ of the Lorentz group, so that a transformation t of the co-ordinates,

$$x'^k = t_l^k x^l, \tag{3}$$

causes a transformation of the wave-function ψ, given by

$$\psi'(x') = \mathrm{T}\psi(x), \tag{4 a}$$

---

* For a detailed account of the general theory, reference may be made to Bhabha (1949), referred to in this paper as A.

† x^0, x^1, x^2, x^3 are the four co-ordinates of a point in space-time, and the metric tensor is taken in the usual form : $g_{00} = -g_{11} = -g_{22} = -g_{33} = 1$; $g_{kl} = 0$, if $k \neq l$; also, the units are so chosen that $\hbar = c = 1$.

where T is the matrix representing t in $\mathcal{R}$. The invariance of the expression (1) under transformations of the Lorentz group then requires the six matrices D, α^k, β to transform according to

$$\mathrm{T}^\dagger \mathrm{D} \mathrm{T} = \mathrm{D}, \tag{4 b}$$

$$\mathrm{T}^{-1} \alpha^k \mathrm{T} = t_l{}^k \alpha^l, \tag{4 c}$$

$$\mathrm{T}^{-1} \beta \mathrm{T} = \beta. \tag{4 d}$$

We shall only consider the case where β is non-singular, so that the particle has no state of rest-mass zero. In this case β can always be taken as the unit matrix, without loss of generality.

It can be readily shown from (4) that the quantities

$$\psi^\dagger \mathrm{D} \psi, \ \psi^\dagger \mathrm{D} \alpha^k \psi, \ \psi^\dagger \mathrm{D} \alpha^l p^k \psi \tag{5}$$

are respectively an invariant, a vector, and a tensor of second rank. The last two can be shown to satisfy the continuity equation in virtue of (2), and can therefore be interpreted as respectively the charge-current density vector and the energy-momentum density tensor of the field. The charge density, therefore, is

$$\psi^\dagger \mathrm{D} \alpha^0 \psi, \tag{6}$$

and the energy density is,

$$\psi^\dagger \mathrm{D} \alpha^0 p_0 \psi. \tag{7}$$

An important conclusion from the general theory is that the matrix

$$\mathrm{P} \equiv \alpha^k p_k \tag{8}$$

has the transformation property [following from (4 *c*)]

$$\mathrm{P}' = \alpha^k p_k{}' = \mathrm{T} \alpha^k p_k \mathrm{T}^{-1},$$

i.e., it is an " invariant " matrix, and further it satisfies an equation of the type (*cf.*, Bhabha, 1949)

$$\mathrm{P}^m (\mathrm{P}^2 - a_1{}^2 p^2)(\mathrm{P}^2 - a_2{}^2 p^2) \cdots (\mathrm{P}^2 - a_n{}^2 p^2) = 0, \tag{9}$$

where $p^2 = p_k p^k$, m is an integer, and $a_1, a_2, \ldots, a_n$ are the non-zero eigen-values of α^0, the corresponding minimal equation of α^0 being

$$(\alpha^0)^m \{(\alpha^0)^2 - a_1{}^2\} \cdots \{(\alpha^0)^2 - a_n{}^2\} = 0. \tag{10}$$

The equation (2) (with $\beta = 1$) has plane wave solutions of the type

$$\psi = \exp\ (i p_k x^k)\, \phi, \tag{11}$$

where ϕ is a column vector whose elements depend on p_k but not on x^k, only if p^2 has one of the values $\chi^2/a_1{}^2$, $\chi^2/a_2{}^2, \ldots \chi^2/a_n{}^2$. The rest-masses of the particle are defined as the positive square-roots of the eigen-values of

the operator p^2. Putting $p^2 = \chi^2/a_\rho^2$ in (9), it follows that, corresponding to a rest-mass χ/a_ρ (*cf.*, Bhabha, 1949),

$$\mathrm{P}^m (\mathrm{P}^2 - \chi^2) \prod_{\substack{i=1 \\ i \neq \rho}}^{n} (\mathrm{P}^2 - a_i^2 \chi^2/a_\rho^2) = 0, \tag{12}$$

so that

$$\mathrm{P}^m (\mathrm{P} - \chi) \prod_{\substack{i=1 \\ i \neq \rho}}^{n} (\mathrm{P}^2 - a_i^2 \chi^2/a_\rho^2) \tag{12a}$$

is a matrix whose columns give the solutions of (2) corresponding to a momentum $\vec{p}$ and energy $(\vec{p}^2 + \chi^2/a_\rho^2)^{\frac{1}{2}}$.

§3. QUANTIZATION

In order to quantize the wave field, we expand an arbitrary state-vector ψ as a Fourier series in the plane wave solutions

$$\psi(x) = \sum_{\vec{p}, r, \lambda} a(\vec{p}, r, \lambda)\, \phi(\vec{p}, r, \lambda)\, e^{ip_k x^k}, \tag{13}$$

where

$$\phi(\vec{p}, r, \lambda)\, e^{ip_k x^k} \tag{14}$$

is a plane wave solution of the equation (2), characterized by a certain value of the rest-mass x/a_ρ, the momentum $\vec{p}$, and energy $p_0(r) = \pm\, \omega_\rho(\vec{p}) = \pm\, (\vec{p}^2 + \chi^2/a_\rho^2)^{\frac{1}{2}}$, where $r = \rho p_0/|\, p_0\,|$, and by a parameter λ labelling the different spin-states corresponding to given values of p and r. λ takes the values 1, 2, ..., $2s + 1$, if the state belongs to a spin s. Σ stands for a summation over all values of r, and λ, and an integration over all values of $\vec{p}$.

The ϕ's corresponding to a given value of $\vec{p}$ but different values of r satisfy the orthogonality condition

$$\phi^\dagger (\vec{p}, r', \lambda')\, \mathrm{D}\alpha^0\, \phi(\vec{p}, r, \lambda) = 0, \text{ if } r \neq r'. \tag{15}$$

This is seen as follows. Making the substitution (14) for ψ in the wave equation (2), and multiplying from the left with D, one gets (for $\beta = 1$),

$$\mathrm{D}(p_0 \alpha^0 + p_k \alpha^k + \chi)\, \phi(\vec{p}, r, \lambda) = 0, \; k = 1, 2, 3, \tag{16}$$

where now the p's are numbers. The hermitian conjugate of (16), for a different value r' is

$$\phi^\dagger (\vec{p}, r', \lambda')\, \mathrm{D}(\vec{p}_0 \alpha^0 + p_k \alpha^k + \chi) = 0. \tag{17}$$

Multiplying (16) on the left by $\phi^\dagger(\vec{p}, r', \lambda')$, (17) on the right by $\phi(\vec{p}, r, \lambda)$, and subtracting, one then gets

$$(p_0 - p_0')\,\phi^\dagger(\vec{p}, r', \lambda')\,D\alpha^0\phi(\vec{p}, r, \lambda) = 0,$$

thus proving (15), since $p_0 \neq p_0'$ if $r \neq r'$.

Further, the ϕ's corresponding to the same values of $\vec{p}$ and r can always be chosen so as to satisfy

$$\phi^\dagger(\vec{p}, r, \lambda)\,D\alpha^0\phi(\vec{p}, r, \lambda') = 0, \text{ if } \lambda \neq \lambda'.$$

This may be done, for example, by following the Schmidt orthogonalization process. If $\phi^\dagger D\alpha^0\phi$ is not zero, we can normalize it to ± 1, and we therefore have

$$\phi^\dagger(\vec{p}, r, \lambda)\,D\alpha^0\phi(\vec{p}, r', \lambda') = \epsilon(\vec{p}, r, \lambda)\,\delta_{rr'}\delta_{\lambda\lambda'}, \tag{18}$$

where $\epsilon = \pm 1$ or 0, depending on whether the charge density for the state $(\vec{p}, r, \lambda)$ is positive, negative or zero. Since, in order to have a physically sensible theory, either ϵ or ϵp_0 has to be positive in all the states, ϵ may, in the following, be regarded as a function of r alone and written as $\epsilon(r)$.

Now on substituting (13) into the expressions (6) and (7), and integrating over the whole space, we get for the total charge Q and the total energy H:

$$\begin{aligned} \mathrm{Q} &= \sum_{\vec{p}, r, \lambda} a^*(\vec{p}, r, \lambda)\,a(\vec{p}, r, \lambda)\,\phi^\dagger(\vec{p}, r, \lambda)\,D\alpha^0\phi(\vec{p}, r, \lambda) \\ &= \sum_{\vec{p}, r, \lambda} \epsilon(\vec{p}, r, \lambda)\,a^*(\vec{p}, r, \lambda)\,a(\vec{p}, r, \lambda); \end{aligned} \tag{19}$$

and

$$\mathrm{H} = \sum_{\vec{p}, r, \lambda} p_0\epsilon(\vec{p}, r, \lambda)\,a^*(\vec{p}, r, \lambda)\,a(\vec{p}, r, \lambda). \tag{20}$$

If ϵ is $+1$ for every plane-wave solution, *i.e.*, if "the free charge density is positive definite" (*cf.*, Bhabha, 1951, §4), we can treat the a's and a^*'s as absorption and emission operators and quantize according to Fermi-Dirac statistics, the negative energy solutions (for $p_0 = -\omega$) being reinterpreted following Dirac's hole theory. If the free charge density is not positive definite, but the free energy density is, *i.e.*, if ϵp_0 is always positive, then the total energy (20) will be positive and we can quantize in the usual way following Bose-Einstein statistics. Correspondingly, the bracket [ ] in the following is to be understood as a commutator bracket if the free

energy density is positive definite and as an anti-commutator bracket if the free charge density is positive definite. If neither the free charge density nor the free energy density is positive definite, we cannot have a physically sensible theory. That there exists an equation in this scheme describing a particle with two different mass-states and with a positive definite free charge density has been demonstrated by Bhabha recently (1952).

Interpeted as emission and absorption operators, the a's and a^*'s are now subjected to the commutation relations

$$[a(\vec{p}, r, \lambda),\ a^*(\vec{p'}, r', \lambda')] = \epsilon(\vec{p}, r, \lambda)\,\delta(\vec{p} - \vec{p'})\,\delta_{rr'}\delta_{\lambda\lambda'}, \quad (21)$$

the bracket [ ] being understood as above. We then have

$$[\psi_i(x), (\psi^\dagger \mathrm{D})_j(x')] = \sum_{\vec{p}, r, \lambda} \sum_{\vec{p'}, r', \lambda'} [a(\vec{p}, r, \lambda), a^*(\vec{p'}, r', \lambda')]$$

$$\times \phi_i(\vec{p}, r, \lambda)\{\phi^\dagger(\vec{p'}, r', \lambda')\,\mathrm{D}\}_j e^{ip_0 t} - ip_0' t' - i\vec{p}\cdot\vec{x} + i\vec{p'}\cdot\vec{x'} \quad (22)$$

The purpose of multiplying $\psi^\dagger$ with D will be clear from what follows.

In virtue of (21), (22) becomes

$$[\psi_i(x), (\psi^\dagger \mathrm{D})_j(x')] = \sum_{\vec{p}, r, \lambda} \epsilon(\vec{p}, r, \lambda)$$

$$\times \{\phi(\vec{p}, r, \lambda)\,\phi^\dagger(\vec{p}, r, \lambda)\,\mathrm{D}\}_{ij} e^{ip_0(t - t') - i\vec{p}\cdot(\vec{x} - \vec{x'})} \quad (23)$$

For the evaluation of the commutation brackets of the ψ's we therefore have to evaluate the matrix sum $\sum_\lambda \phi\phi^\dagger \mathrm{D}(\vec{p}, r, \lambda)$, the sum being over the different values of λ for given values of $\vec{p}$ and r. For this we shall need the following result:

$$\phi^\dagger(\vec{p}, r, \lambda)\,\mathrm{D}\phi(\vec{p}, r, \lambda') = -\frac{\mathrm{M}^2}{p_0 \chi}\,\phi^\dagger(\vec{p}, r, \lambda)\,\mathrm{D}\alpha^0\phi(\vec{p}, r, \lambda') \quad (24)$$

$$= -\frac{\mathrm{M}^2}{p_0 \chi}\,\epsilon(\vec{p}, r, \lambda)\,\delta_{\lambda\lambda'}.$$

Here $|\mathrm{M}| = \chi/a_\rho$ is the rest-mass of the particle in the states considered. (24) can be proved as follows:

We have already noted that $\phi^\dagger \mathrm{D}\alpha^k\phi$ is a vector; we therefore have

$$\phi^\dagger(\vec{p}, r, \lambda)\,\mathrm{D}\alpha^0\phi(\vec{p}, r, \lambda') = t_k^{\,0}\,\phi^\dagger(0, r, \lambda)\,\mathrm{D}\alpha^k\,\phi(0, r, \lambda'),$$

where t_l^k is the Lorentz transformation from the reference system where the momentum of the particle is zero (rest-system) to that where it is $\vec{p}$. Now, from considerations of symmetry, the current must vanish in the rest-system, *i.e.*,

$$\phi^\dagger (0, r, \lambda)\, \mathrm{D}\alpha^k\, \phi (0, r, \lambda) = 0, \quad \text{for } k = 1, 2, 3.$$

We therefore have

$$\phi^\dagger (\vec{p}, r, \lambda)\, \mathrm{D}\alpha^0 \phi (\vec{p}, r, \lambda') = t_0{}^0 \phi^\dagger (0, r, \lambda)\, \mathrm{D}\alpha^0 \phi (0, r, \lambda')$$

$$= \frac{p_0}{\mathrm{M}}\, \phi^\dagger (0, r, \lambda)\, \mathrm{D}\alpha^0 \phi (0, r, \lambda') \qquad (25)$$

But when $\vec{p} = 0$, we get from (2),

$$\phi^\dagger (0, r, \lambda)\, \mathrm{D}\, (\mathrm{M}\alpha^0 + \chi)\, \phi (0, r, \lambda') = 0,$$

so that

$$\phi^\dagger (0, r, \lambda)\, \mathrm{D}\alpha^0 \phi (0, r, \lambda') = -\frac{\chi}{\mathrm{M}}\, \phi^\dagger (0, r, \lambda)\, \mathrm{D}\phi (0, r, \lambda')$$

$$= -\frac{\chi}{\mathrm{M}}\, \phi^\dagger (\vec{p}, r, \lambda)\, \mathrm{D}\phi (\vec{p}, r, \lambda')$$

since $\phi^\dagger \mathrm{D}\phi$, as noted already, is an invariant. Substituting this in (25) we finally get (24).

Consider now the matrix

$$\mathrm{A} = \sum_\lambda \phi (\vec{p}, r, \lambda)\, \phi^\dagger (\vec{p}, r, \lambda)\, \mathrm{D}, \qquad (26)$$

the sum being taken over the different spin states λ corresponding to the same values of $\vec{p}$, and r. Under a Lorentz transformation, which transforms ϕ into $\phi' = \mathrm{T}\phi$, we have

$$\mathrm{A}' = \sum_\lambda \phi (\vec{p}', r, \lambda)\, \phi^\dagger (\vec{p}', r, \lambda)\, \mathrm{D}$$

$$= \sum_\lambda \mathrm{T}\phi (\vec{p}, r, \lambda)\, \phi^\dagger (\vec{p}, r, \lambda)\, \mathrm{T}^\dagger \mathrm{D}$$

$$= \mathrm{T} \{\sum_\lambda \phi (\vec{p}, r, \lambda)\, \phi^\dagger (\vec{p}, r, \lambda)\, \mathrm{D}\}\, \mathrm{T}^{-1}$$

$$= \mathrm{TAT}^{-1}, \qquad (27)$$

where we have made use of (4 *b*). The matrix A is thus "an invariant matrix", in the sense that A′ is the same function of the numbers p_k' that A is of p_k. Now since the α's form an irreducible set, A must be expressible as a polynomial in the α's, with coefficients which are functions of the p's,

and since A is an invariant matrix, the α's and p's in this polynomial must occur in the invariant combination $\mathrm{P} \equiv p_k a^k$. In other words, A must be a polynomial in P, say $f(\mathrm{P})$. Further, since P satisfies the minimal equation (12) and since A has the property

$$(\mathrm{P} + \chi)\,\mathrm{A} = \sum_{\lambda} (\mathrm{P} + \chi)\,\phi\,(\vec{p}, r, \lambda)\,\phi^{\dagger}\,(\vec{p}, r, \lambda)\,\mathrm{D}$$
$$= 0, \tag{28}$$

this polynomial must be unique, apart from a numerical multiplier. For, firstly, the polynomial has to be of degree less than the degree of the minimal equation (12) of P: if it were of a higher degree, it could be reduced to such a one by using (12). Secondly, the degree must be only one less than the degree of the minimal equation, since, from (28)

$$(\mathrm{P} + \chi) f(\mathrm{P}) = 0$$

is an equation satisfied by P and this would otherwise be of degree less than its minimal equation, which is impossible. Finally, if $f'(\mathrm{P})$ were another polynomial satisfying the required conditions [and hence of the same degree as $f(\mathrm{P})$], and if it be written so that the coefficient of the highest power in P is the same in $f(\mathrm{P})$ and $f'(\mathrm{P})$,

$$(\mathrm{P} + \chi)\,\{f(\mathrm{P}) - f'(\mathrm{P})\} = 0$$

would be an equation satisfied by P which, again, would be of lower degree than (12). $f'(\mathrm{P})$ must, therefore, be identical with $f(\mathrm{P})$, or $f(\mathrm{P})$ is unique but for multiplication by an arbitrary number. From (28) and (12) we now conclude that

$$\mathrm{A} = k_r \mathrm{P}^m\,(\mathrm{P} - \chi) \prod_{\substack{i=1 \\ i \neq \rho}}^{n} (\mathrm{P}^2 - a_i^2 \chi^2 / a_\rho^2) \tag{29}$$

In order to calculate the constant k_r in (29), we first note that

$$\mathrm{A}\phi\,(\vec{p}, r, \lambda') = \sum_{\lambda} \phi\,(\vec{p}, r, \lambda)\,\phi^{\dagger}\,(\vec{p}, r, \lambda)\,\mathrm{D}\phi\,(\vec{p}, r, \lambda')$$
$$= \sum_{\lambda} \phi\,(\vec{p}, r, \lambda)\,(-\mathrm{M}^2/p_0\chi)\,\epsilon\,(\vec{p}, r, \lambda')\,\delta_{\lambda\lambda'}$$
$$= -\frac{\mathrm{M}^2}{p_0\chi}\,\epsilon\,(\vec{p}, r, \lambda')\,\phi\,(\vec{p}, r, \lambda') \tag{30}$$

Here use has been made of (24).

The charge density ϵ on the right-hand side of (30) may be ± 1 or 0. We now wish to exclude the non-physical case where the charge density (and hence the energy density too) is zero. A necessary and sufficient condition for this is immediately obtained from (29) and (30). If the factor $(\mathrm{P}^2 - a_\rho^2 p^2)$

occurs more than once in (9), *i.e.*, if the factor $\{(\alpha^0)^2 - a_\rho^2\}$ occurs more than once in the minimal equation (10) of α^0, a factor $(P^2 - \chi^2)$ will appear on the right-hand side of (29), and since

$$(P + \chi)\,\phi = 0,$$

we will have

$$A\phi\,(\vec{p}, r, \lambda) = 0,$$

or, from (30),

$$\epsilon\,(\vec{p}, r, \lambda) = 0,$$

i.e., the charge density, and hence also the energy-density (which is simply p_0 times the charge density), in the free-state of mass χ/a_ρ would vanish. Hence *a necessary condition in order that the free charge and energy densities be non-zero is that the minimal equation of α^0 must not contain a repeated factor, i.e.*, it must be of the form

$$(\alpha^0)^m\,\{(\alpha^0)^2 - a_1^2\}\,\{(\alpha^0)^2 - a_2^2\} \ldots \{(\alpha^0)^2 - a_n^2\} = 0, \quad (31)$$

with all the a_i different.* *This condition is also sufficient.* For, if it holds, then from (29) and (30),

$$\begin{aligned} -\frac{M^2}{p_0\chi}\,\epsilon\,(\vec{p}, r, \lambda')\,\phi\,(\vec{p}, r, \lambda') &= A\phi\,(\vec{p}, r, \lambda') \\ &= k_r P^m\,(P - \chi)\,(P^2 - a_1^2\chi^2/a_\rho^2) \ldots \\ &\qquad (P^2 - a_n^2\chi^2/a_\rho^2)\,\phi\,(\vec{p}, r, \lambda') \\ &= k_r\,(-\chi)^m\,(-\chi - \chi)\,(\chi^2 - a_1^2\chi^2/a_\rho^2) \ldots \\ &\qquad (\chi^2 - a_n^2\chi^2/a_\rho^2)\,\phi\,(\vec{p}, r, \lambda'), \end{aligned}$$

since $P\phi = -\chi\phi$. Here all brackets on the right-hand side are non-zero. Hence ϵ does not vanish unless k_r and hence $\sum_\lambda \phi\phi^\dagger D$ vanishes. But $\sum_\lambda \phi\phi^\dagger D$ is non-null, and this proves the sufficiency.

From the above equation, we now have, (on putting $M^2 = \frac{\chi^2}{a_\rho^2}$),

$$k_r = \frac{(-1)^m\,\epsilon\,(r)}{2p_0 a_\rho^{\,2}\chi^{m+2n-2}\prod_{i\,+\,\rho}\left(1 - \frac{a_i^2}{a_\rho^2}\right)} = \frac{k_r'\,\epsilon\,(r)}{2p_0}, \text{ say} \quad (32)$$

---

* The necessity of this condition has also been deduced by Fedorov [*Doklady Akad. Nauk. SSSR* (N.S.), 79, 787 (1951)]. It is also an immediate consequence of lemma 3 and equation (22) in Bhabha (1952).

which finally gives

$$\sum_{\lambda} \phi(\vec{p}, r, \lambda)\, \phi^{\dagger}(\vec{p}, r, \lambda)\, \mathrm{D}\epsilon(r) = \frac{k_r'}{2p_0}\, \mathrm{P}^m (\mathrm{P} - \chi) \prod_{\substack{i=1 \\ i \neq \rho}}^{n} (\mathrm{P}^2 - a_i^2 \chi^2 / a_\rho^2) \tag{33}$$

(since $\epsilon^2 = 1$) with k_r' given by (32). k_r' does not depend on the sign of p_0 and may therefore be written as k_ρ'. The right-hand side of (33) gives the value of the sum for either sign of p_0.

It may be remarked that the equation (33) is of interest in itself, apart from its use in finding the commutation relations, since it is needed in finding the matrix elements for any process.

The commutation rules can now be readily written down. In the sum occurring on the right-hand side of (23), let us pick out the contribution due to the states corresponding to a single mass (χ/a_ρ) and break this up further into the contributions corresponding to $r = +\rho$ and $r = -\rho$ respectively. This sum is

$$\begin{aligned}
&\sum_{\vec{p}} \{\sum_{\lambda} \phi(\vec{p}, \rho, \lambda)\, \phi^{\dagger}(\vec{p}, \rho, \lambda) \mathrm{D}\epsilon(\rho)\}_{ij}\, e^{i\omega_\rho (t - t') - i\vec{p}\cdot(\vec{x} - \vec{x}')} \\
&\quad + \sum_{\vec{p}} \{\sum_{\lambda} \phi(\vec{p}, -\rho, \lambda)\, \phi^{\dagger}(\vec{p}, -\rho, \lambda)\, \mathrm{D}\epsilon(-\rho)\}_{ij}\, e^{-i\omega_\rho (t-t') - i\vec{p}\cdot(\vec{x} - \vec{x}')} \\
&\quad = \sum_{\vec{p}} e^{-i\vec{p}\cdot(\vec{x} - \vec{x}')} \frac{k_\rho'}{2\omega_\rho} \Big\{ \mathrm{P}^m (\mathrm{P} - \chi) \prod_{\substack{i=1 \\ i \neq \rho}}^{n} (\mathrm{P}^2 - a_i^2 \chi^2 / a_\rho^2)\, e^{i\omega_\rho (t - t')} \\
&\quad - \text{same with } \rho \text{ replaced by } (-\rho) \Big\}_{ij} \\
&\quad = k_\rho' \{\mathrm{P}^m (\mathrm{P} - \chi) \prod_{\substack{i=1 \\ i \neq \rho}}^{n} (\mathrm{P}^2 - a_i^2 \chi^2 / a_\rho^2)\}_{ij} \sum_{\vec{p}} \frac{e^{-i\vec{p}\cdot(\vec{x} - \vec{x}')}}{2\omega_\rho(\vec{p})} \\
&\qquad \times \left\{ e^{i\omega_\rho (t-t')} - e^{-i\omega (t - t')} \right\},
\end{aligned}$$

where P is now to be interpreted as a differential operator: $\mathrm{P} \equiv -i\alpha^k \frac{\partial}{\partial x^k}$.

But $\sum_{\vec{p}} \frac{e^{-i\vec{p}\cdot(\vec{x} - \vec{x}')}}{2\omega_\rho(\vec{p})} \left\{ e^{i\omega_\rho (t - t')} - e^{-i\omega_\rho (t-t')} \right\} = -i\mathrm{D}_\rho(x - x')$,

where D_ρ is the invariant D-function corresponding to a mass χ/a_ρ. We therefore get as the contribution of all states corresponding to the single mass χ/a_ρ:

$$-ik_\rho' \{\mathrm{P}^m (\mathrm{P} - \chi) \prod_{\substack{i=1 \\ i \neq \rho}}^{n} (\mathrm{P}^2 - a_i^2 \chi^2 / a_\rho^2)\}_{ij}\, \mathrm{D}_\rho(x - x') \tag{34}$$

(23) therefore becomes

$$[\psi_i(x), (\psi^\dagger \mathrm{D})_j(x')] = \sum_{\rho=1}^{n} - ik_\rho' \{\mathrm{P}^m (\mathrm{P}-\chi) \prod_{\substack{i=1 \\ i\neq\rho}}^{n} (\mathrm{P}^2 - a_i^2\chi^2/a_\rho^2)\}_{ij} \mathrm{D}_\rho(x-x') \tag{35}$$

The other commutation brackets are zero.

A few particular cases may be noted.

(i) *Dirac equation for spin* $\frac{1}{2}$.—Here P satisfies $\mathrm{P}^2 - \chi^2 = 0$, hence $k' = 1$; $\mathrm{D} = a^0$; hence the commutation rule is

$$[\psi_i(x), \{\psi^\dagger(x')\, a^0\}_j]_+ = -i(\mathrm{P}-\chi)\,\mathrm{D}(x-x'). \tag{36}$$

(ii) *Duffin-Kemmer equation for a particle of spin* 0 *or* 1.—Here P satisfies $\mathrm{P}(\mathrm{P}^2 - \chi^2) = 0$; hence $k' = -\dfrac{1}{\chi}$ also $\mathrm{D} = \eta_0 = 2a_0^2 - 1$ and the commutation rule is

$$[\psi_i(x), \{\psi^\dagger(x')\,\eta_0\}_j]_- = \frac{i}{\chi}\{\mathrm{P}(\mathrm{P}-\chi)\}_{ij}\,\mathrm{D}(x-x') \tag{37}$$

(iii) *Dirac-Fierz-Pauli equation for spin* 3/2.—Here P satisfies $\mathrm{P}^2(\mathrm{P}^2 - \chi^2) = 0$; hence $k' = 1/\chi^2$ and commutation rule is

$$[\psi_i(x), \{\psi^\dagger(x')\,\mathrm{D}\}_j]_+ = -\frac{i}{\chi^2}\{\mathrm{P}^2(\mathrm{P}-\chi)\}_{ij}\,\mathrm{D}(x-x') \tag{38}$$

(iv) *Bhabha equation for a particle with two mass-states.**—Here, for the states of mass χ, P satisfies

$$\mathrm{P}^2(\mathrm{P}^2 - \chi^2)(\mathrm{P}^2 - \chi^2\lambda^2) = 0,$$

so that the corresponding $k_1' = 1/\chi^4(1-\lambda^2)$; for the states of mass χ/λ, P satisfies

$$\mathrm{P}^2(\mathrm{P}^2 - \chi^2)(\mathrm{P}^2 - \chi^2/\lambda^2) = 0,$$

so that the corresponding $k_2' = -1/\chi^4(1-\lambda^2)$. Hence the commutation rule is

$$[\psi_i(x), \{\psi^\dagger(x')\,\mathrm{D}\}_j]_+ = -\frac{i}{\chi^4(1-\lambda^2)}\{\mathrm{P}^2(\mathrm{P}-\chi)(\mathrm{P}^2-\chi^2\lambda^2)\mathrm{D}_1(x-x')$$
$$-\mathrm{P}^2(\mathrm{P}-\chi)(\mathrm{P}^2-\chi^2/\lambda^2)\,\mathrm{D}_2(x-x')\}_{ij}, \tag{39}$$

where D_1 and D_2 are the D-functions corresponding to the masses χ and χ/λ respectively.

In conclusion, I wish to express my gratefulness to Professor H. J. Bhabha for suggesting the problem and for helpful discussions.

* Bhabha, 1952,

SUMMARY

A method is given for quantizing any relativistic wave equation for a particle of arbitrary spin and non-zero finite values of the rest-mass, which can be written in the canonical form

$$(\alpha^{\dot{\kappa}} p_{\dot{\kappa}} + \chi)\, \psi = 0.$$

The general commutation rule of the ψ and $\psi^{\dagger}$ is given by (35) in every case.

A necessary and sufficient condition to be satisfied by the α's in order that the charge-density and the energy density be non-zero has been deduced and is that the minimal equation of α^0 should not have repeated factors other than α^0 itself.

REFERENCES

Bhabha, H. J. .. *Rev. Mod. Phys.*, 1949, **21**, 451.
——————— .. *Proc. Ind. Acad. Sci.*, 1951, **34A**, 335.
——————— .. *Phil. Mag.*, 1952, **43**, 33.

BEHAVIOUR OF SURFACE-ACTIVE SUBSTANCES AT THE DROPPING MERCURY ELECTRODE

By K. S. G. Doss, F.A.Sc. and S. L. Gupta

(Indian Institute of Sugar Technology, Kanpur)

Received July 7, 1952

Introduction

Surface-active substances are known to affect the capacity of mercury-aqueous solution interfaces. A quantitative study of the phenomenon has been started in this laboratory and a previous communication gives the effect of a number of organic substances like acetone, thymol blue, isobutyl alcohol and gelatin at different concentrations on the capacity of the dropping mercury electrode near the electro-capillary zero.[1] Further the effect of some sparingly soluble substances like benzene, toluene, xylene and amyl alcohol has also been reported. The present paper deals with the extension of the work to other cathodic potentials. A general theory has been formulated for accounting for the observed phenomenon.

Experimental

The apparatus employed in the present investigation is the same as what has been described before.[2] This consists in applying a constant a.c. pulse of $\pm$ 40 mv. r.m.s. over the d.c. potential and observing the a.c. component of the resulting pulsating current. The magnitude of the average a.c. current is nearly a measure of the average differential capacity of the dropping mercury electrode. The averaging is not only with reference to the area of the mercury drop which is changing all the time but also with reference to the applied cathodic potential which is oscillating all the time. One important improvement was that a regulated a.c. supply was employed thereby avoiding any fluctuations in current due to fluctuations in a.c. mains. This regulation was brought about by using a current regulator lamp (Barretter of G.E.C., England) so that the sine wave form of the original current supply was maintained in the regulated supply as well.

The constants of the dropping mercury electrode are as follows:—

$$'m' = 0{\cdot}00306 \text{ gm./sec.}$$

't' is given in the tables.

The effect of bromo cresol purple, thymol blue, bromo thymol blue and cetyl pyridinium bromide on the capacity of the dropping mercury electrode was investigated at different cathodic potentials applied through the pool

electrode. The potentials of the capillary electrode have been expressed with reference to the saturated calomel electrode. The indifferent electrolyte was 0·1 N—KCl which was shaken with a little mercury and calomel to avoid any time effects while in contact with the pool. Further, 0·5% of sodium sulphite was added to avoid any influence of dissolved oxygen.

All the above substances investigated showed similar behaviour. The results obtained with bromo cresol purple are given in detail in Table I and Fig. 1. The a.c. current observed is roughly a measure of the capacity. The exact values can be calculated if needed from the data given.

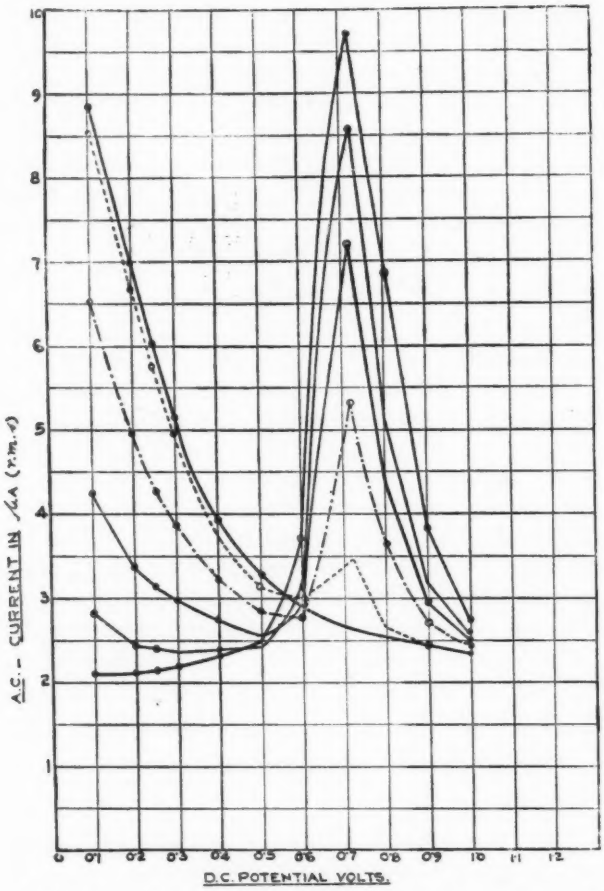

Fig. 1. Behaviour of Bromocresol Purple at the Dropping Mercury Electrode in Pulsating Fields.

TABLE I

Electrolyte: 0·1 N KCl + 0·5% Na_2SO_3

D.C. potential (volts)	Current μA (r.m.s.)	Time for 25 drops
0	71·6	17·4″
0·1	8·84	17·8″
0·2	6·95	18·8″
0·25	6·02	18·8″
0·3	5·16	18·8″
0·4	3·90	18·2″
0·5	3·25	18·0″
0·6	2·89	17·8″
0·7	2·65	17·6″
0·8	2·54	17·0″
0·9	2·43	16·0″
1·0	2·36	15·2″

Electrolyte: 0·1 N KCl + 0·5% Na_2SO_3 + 0·0002% bromocresol purple

D.C. potential (volts)	Current μA (r.m.s.)	Time for 25 drops
0	71·6	18·8″
0·1	8·55	19·4″
0·2	6·69	19·8″
0·25	5·77	19·8″
0·3	4·99	19·2″
0·4	3·70	18·4″
0·5	3·15	18·2″
0·6	3·00	18·0″
0·7	2·81	17·4″
0·72	3·46	17·2″
0·8	2·67	16·8″
0·9	2·45	16·0″
1·0	2·37	15·4″

Electrolyte: 0·1 N KCl + 0·5% Na_2SO_3 + 0·001% bromocresol purple

D.C. potential (volts)	Current μA (r.m.s.)	Time for 25 drops
0	63·6	19·4″
0·1	6·46	19·8″
0·2	4·94	20·2″
0·25	4·27	20·2″
0·3	3·87	19·6″
0·4	3·20	18·8″
0·5	2·86	18·6″
0·6	2·74	18·2″
0·7	3·98	17·8″
0·72	5·30	17·5″
0·8	3·56	17·0″
0·9	2·68	16·4″
1·0	2·45	15·6″

Electrolyte: 0·1 N KCl + 0·5% Na_2SO_3 + 0·002% bromocresol purple

D.C. potential (volts)	Current μA (r.m.s.)	Time for 25 drops
0	62·2	18·6″
0·1	4·25	19·4″
0·2	3·38	19·8″
0·25	3·14	20·0″
0·3	2·99	20·0″
0·4	2·74	19·4″
0·5	2·56	19·2″
0·6	2·84	18·8″
0·7	6·07	18·4″
0·72	7·22	18·0″
0·8	4·34	17·4″
0·9	2·92	16·6″
1·0	2·49	15·8″

Electrolyte: 0·1 N KCl + 0·5% Na_2SO_3 + 0·003% bromocresol purple

D.C. potential (volts)	Current μA (r.m.s.)	Time for 25 drops
0	57·3	17·6″
0·1	2·82	18·0″
0·2	2·47	18·2″
0·25	2·41	18·2″
0·3	2·39	18·2″
0·4	2·38	18·2″
0·5	2·41	18·4″
0·6	3·18	18·4″
0·7	7·46	18·2″
0·72	8·61	17·6″
0·8	5·19	17·5″
0·9	3·14	17·0″
1·0	2·54	16·0″

Electrolyte: 0·1 NKCl + 0·5% Na_2SO_3 + 0·006% bromocresol purple

D.C. potential (volts)	Current μA (r.m.s.)	Time for 25 drops
0	17·0	17·4″
0·1	2·12	17·8″
0·2	2·12	18·2″
0·25	2·14	18·2″
0·3	2·17	18·4″
0·4	2·32	18·4″
0·5	2·43	18·4″
0·6	3·78	18·2″
0·7	8·78	18·2″
0·72	9·70	18·2″
0·8	6·88	18·0″
0·9	3·82	17·4″
1·0	2·73	16·4″

Discussion

1. *The Effect of Bromocresol Purple on the Form of Capacity, Voltage Curve.*—Curve 1, Fig. 1 gives the a.c. current voltage curve for the indifferent electrolyte (N/10 KCl in 1% aqueous Na_2SO_3) in absence of any surface-active substance. The capacity of the dropping mercury electrode is high at low cathodic voltages and falls quickly up to about 0·5 volts and then much more slowly up to 1 volt. In presence of bromocresol purple, the capacity values at lower cathodic potentials get lowered. Higher concentrations produce progressively greater lowering. The percentage lowering of the capacity is maximum at a cathodic potential of 0·25 volt which is nearly the electro-capillary zero of the system; at still higher cathodic potentials the capacity lowering effect diminishes and at potentials higher than 0·5 to 0·6 volt there is actually an increase in the capacity with increase in voltage. The a.c. current voltage curve exhibits a maximum at a cathodic potential of 0·72 volt and then sharply falls off. The curve becomes steeper at the maximum as the concentration of bromocresol purple increases and the maximum rises to very high magnitudes at the higher concentrations. It is also of interest to note that all the maxima occur at the same cathodic potential within the limits of experimental error irrespective of the concentration of bromocresol purple.

2. *The Theory of the Capacity Phenomena at Mercury Capillary Electrodes.*—Whereas the lowering of the capacity brought about by surface-active substances was observed by many earlier workers, the enormous rise in the capacity has not been quantitatively studied earlier. A qualitative detection of large increase in the capacity has been reported by Heyrovsky and co-workers[3] who employed oscillographic potential-time curves. A theory has been put forth by these workers to explain the behaviour. Doss and Kalyanasundaram[4] proposed a different formulation to explain the data on pyridine. We shall attempt to give a more generalised theory with a view to interpret all the data available.

The changes in the capacity are caused essentially by adsorption of the surface-active substances at the mercury solution interfaces. The surface-active substances adsorbed may act in two ways. (1) They may alter the distribution of ions in the double layer on the aqueous side of the interfaces and (2) they may interfere with the interactions necessary between the two phases for the transmission of electric charge across the interface. Though by definition a surface-active substance is one which lowers the surface tension of water and should therefore, be expected to get adsorbed at the air-aqueous interface, it is found that these very substances also get adsorbed at

oil-aqueous solution interfaces as well as at mercury-aqueous solution interface. This appears to be due to the hydrophobic portion (which is invariably present in surface-active substances) trying to get out of water irrespective of what it finds outside water, be it air, oil, or mercury. Such adsorption would take place relatively unhindered at the electrocapillary zero. At potentials on either side of the electrocapillary zero the mercury drop would get charged positively or negatively which would result in the water dipoles being attracted to the charged interface. Consequently the adsorption of surface-active substances would fall off on either side of the electrocapillary zero.

The maximum adsorption may not however exactly coincide with the electrocapillary zero as one has to take into account the possible effects of the surface-active substances being ionized and having dipolar groups within their molecules. At potentials sufficiently removed from the electrocapillary zero on either side there would be the desorption of the surface-active substance leading to a rise in the capacity of the electric double layer. If this desorption takes place more or less sharply, the dropping mercury electrode would exhibit a high differential capacity at that stage and would lead to a high a.c. current maximum in pulsating fields.

Let us derive an expression for the variation of adsorption with the potential of the dropping mercury electrode. It is assumed that adsorption equilibrium is nearly, if not completely, attained. Following Glasstone, Laidler and Eyring[5] it is assumed that the heat of adsorption of the surface-active substance is lowered by k_2V at a potential of V volts with reference to electro-capillary zero. Further the heat of adsorption of bromo cresol purple which is negatively charged would get lowered due to mutual interaction of the molecules in the adsorbed layer by an amount equal to $K_3\theta$, where θ is the fraction of the total surface of the mercury drop covered by bromo-cresol purple. Thus the equation for adsorption becomes

$$\frac{\theta}{1-\theta} = k_1.ce^{\frac{\epsilon_0 - k_2V - k_3\theta}{kT}} \tag{1}$$

differentiating we get

$$\frac{d\theta}{dV} = -\frac{k_2}{\frac{kT}{\theta(1-\theta)} + k_3}. \tag{2}$$

In examination, equation (2) shows that $\frac{d\theta}{dV}$ becomes maximum when $\theta = 0{\cdot}5$. This would also be nearly the stage at which there would be a maximum change of capacity with voltage.

Let V* be the potential at which θ becomes 0·5, then, we get, from equation 1,

$$k_1 c = e^{-\frac{\epsilon_0 - k_2 V^* - 0{\cdot}5k_3}{kT}} \tag{3}$$

or

$$\frac{dV^*}{d\ln c} = \frac{kT}{k_2}. \tag{4}$$

From (4), it is clear that V* should be a rectilinear function of *ln* C.

3. *Application of the Above Theory to the Effect of Bromocresol Purple System.*—It is found (*vide* Fig. 1) that the bromocresol purple shows the maximum depressing effect upon the capacity at a cathodic potential of 0·25 volt. An examination of the time per drop (Table I) indicates that this potential is nearly the electrocapillary maximum, as required by the theory.

The steep maximum exhibited by the curves (Fig. 1) at a cathodic potential of 0·72 volt, is to be explained as due to a high value of $\frac{d\theta}{dV}$. The position of maximum should therefore, nearly correspond to V*. Equation (4) shows that V* should be a linear function of *ln* C which is found to hold as shown by Doss and Kalyanasundaram[4] in the case of data on pyridine obtained by Heyrovsky and co-workers. This also holds in the present case; but the slope of the curve of V* plotted against *ln* C is zero within the limits of experimental error. The low value of the slope is presumably due to a high value of k_2. The value of the constant k_2 is determined by the extent to which the voltage (with reference to electrocapillary zero) applied effects the selective adsorption of water dipoles, and thereby brings about the desorption of the surface-active substance. The factors which affect K_2 need further investigation.

Conclusion

It is clear from the observations recorded in this paper that many of the surface-active substances not only lower the differential capacity of the dropping mercury electrode due to the adsorption in the neighbourhood of electrocapillary zero, but also they produce a steep sharp local rise in differential capacity at higher cathodic potentials where desorption of the substance occurs. There would also be a similar steep rise at high anodic potentials but other complications may come up at these high potentials. These results point to the possibility of variations in behaviour which can be taken advantage of to some extent, to characterise the surface-active substances. For the quantitative determination, one can take advantage

of as much the rise in capacity at high cathodic potentials as the lowering of the capacity at the electrocapillary zero. The question as to which of these would give better results is a matter for further investigation.

SUMMARY

It is found that the differential capacity of the dropping mercury electrode is affected mainly in two ways by added surface-active substances. At about the electrocapillary zero there is a strong lowering of the capacity due to adsorption of surface-active substances. At some higher cathodic potential there is enormous increase in differential capacity leading to a maximum and is followed by a sharp fall in the capacity; the latter is due to the desorption taking place more or less sharply at the higher cathodic potentials. The theory of the phenomenon has been formulated.

ACKNOWLEDGEMENT

The authors wish to thank Professor J. M. Saha, Director, Indian Institute of Sugar Technology, for his kind interest in the work.

REFERENCES

1. Doss and Kalyanasundaram .. *Proc. Ind. Acad. Sci.*, 1952, **35**, 27.
2. ———— .. *Ibid.*, 1951, **33**, 298.
3. J. Heyrovsky, Sorm and Forejt *Czechoslovak Chem. Comm.*, 1947, Collection XII, 11.
4. Doss and Kalyanasundaram .. *Curr. Sci.*, 1951, **20**, 199.
5. Glasstone, Laidler and Eyring *Theory of Rate Processes*, McGraw-Hill, 1941.

STRUCTURE OF HALOGENATES OF THE TYPE A $(BO_3)_2 \cdot H_2O$.

I. Barium Chlorate Monohydrate. Ba $(ClO_3)_2 . H_2O$

BY GOPINATH KARTHA

(Department of Physics, Indian Institute of Science, Bangalore)

Received September 6, 1952

(Communicated by Prof. R. S. Krishnan, F.A.SC.)

1. INTRODUCTION

A SERIES of compounds of the general type A $(BO_3)_2$, where A is a divalent metal and B a halogen, has been known for a long time, but a complete structure analysis of this type has not yet been undertaken. An important class of this type is the series of hydrated salts A $(BO_3)_2 . H_2O$ (Groth, 1908) many of which have been reported to be isomorphous. To this isomorphous series belong the crystals of Sr $(BrO_3)_2 . H_2O$; Ba $(ClO_3)_2 \cdot H_2O$; Ba $(IO_3)_2 . H_2O$; Pb $(ClO_3)_2 . H_2O$ and Pb $(BrO_3)_2 . H_2O$. The most common among these being Ba $(ClO_3)_2 \cdot H_2O$, a complete structure analysis of this crystal was undertaken.

The crystal structure data for halogenates in general are remarkably scarce. The structures of some unhydrated salts of monovalent metals which have the general formula ABO_3 have been analysed. They are found to have varying types of symmetry, from cubic to monoclinic depending on the elements A and B. In all the cases of chlorates and bromates studied, the BO_3^- ion has the same low pyramidal structure even though appreciable variation of bond lengths and angles might occur. Some of the iodates thus far studied do not show the low pyramidal configuration for the iodate ion, presumably due to the large crystal radius of the I^{+5} ion, *e.g.*, lithium iodate (Zachariasen and Barta, 1931) does not show separate iodate ions in the solid state, but each iodine atom is surrounded by six oxygen atoms each of which is equidistant from two iodine atoms. Hence we see a wide range of variation in the arrangement of atoms and the resultant symmetry in this type of crystals; and additional information regarding the structure of these crystals and the configuration of the halogenate ions and their variation from crystal to crystal would be welcome. The results of the analysis undertaken for the first crystal, *viz.*, barium chlorate monohydrate are presented in this paper.

The paper is divided into two parts. The first part deals with examination of morphological data, determination of the geometry and symmetry of the unit cell, the experimental procedure and the steps necessary to obtain a set of values for the various structure amplitudes on which the structure analysis is based. The second part deals with the use of these observed structure amplitudes in the actual determination of atomic parameters by two-dimensional Patterson and Fourier methods. A discussion of the proposed structure and an examination of the optical properties of the crystal based on it are included in the same part.

PART I

Experimental Details and Evaluation of Structure Amplitudes

2. Morphological and Optical Data

Barium chlorate monohydrate crystallises from a saturated aqueous solution in the form of needles elongated along the *c*-axis. The morphological studies (Eakle, 1896) showed the crystal to belong to the monoclinic prismatic class with axial ratios, $a:b:c = 1{\cdot}1416:1:1{\cdot}1981$ and monoclinic angle $\beta = 86° 26'$. The *m* planes {110} are the most well developed. In most crystals neither {100} nor {010} faces were well developed. The optical data are:—strong positive birefringence, optic axial plane (010), acute bisectrix makes with the *c*-axis an angle $23\frac{1}{4}°$ in the acute angle, the refractive indices are $\alpha = 1{\cdot}5622$, $\beta = 1{\cdot}5777$ and $\gamma = 1{\cdot}635$, and $2V = 55° 30'$.

3. Unit Cell and Space Group

Using rotation and Weissenberg photographs, the unit cell dimensions and space group of the crystal have been determined (Kartha, 1951). The cell constants are: $a = 8{\cdot}86$ Å, $b = 7{\cdot}80$ Å, $c = 9{\cdot}35$ Å and $\beta = 93° 30'$ and these agree well with the morphological data. The density of the crystal was found to be 3·18 gm. per c.c. and this gives the number of molecules per unit cell to be four. For this unit cell, the systematic absent reflections were *hkl* for $h + k + l$ odd; *hk*0 for $h + k$ odd and *h*0*l* for either *h* or *l* odd. Since the crystal belongs to the monoclinic prismatic class, the space group is uniquely determined to be $C^6_{2h}-I2/c$. By a simple transformation of axes this can be brought to the orientation C2/*c* as given in the International Tables; but for the purpose of structure analysis the configuration I2/*c* which has unit cell constants nearest to that of a cube is preferred.

4. Experimental Details

Filtered copper radiation was used for the determination of cell constants and space group. But, due to the very large value (approximately

570 cm.$^{-1}$) of the linear absorption coefficient of the crystal for CuKα radiation it was not possible to use this radiation in obtaining photographs for the purpose of making intensity estimates. Further, the scattering factor for barium is still large at the largest value of (sin θ/λ) obtainable with CuKα radiation, so that sufficient observational data could be obtained only by using a radiation of considerably smaller wave-length. Because of these reasons Mo radiation filtered through zirconium filter was used throughout for recording the reflections. Even though the linear absorption coefficient was stil large, being about 70 cm.$^{-1}$ for Mo Kα radiation, the absorption errors could be reduced by using sufficiently small crystals and approximate absorption corrections.

The Weissenberg moving film method was used throughout for photographic recording, not only because indexing in that case would be easier, but especially due to the fact that the background intensity around the spots would be appreciably reduced. The spots were recorded by the multiple film method suggested by Robertson (1943) to increase the range of observed intensities. A batch of three films interleaved with silver foils of 0·001″ thickness was used. The absorption of the foil, film and two thicknesses of black paper together was found by microphotographic methods to reduce the intensity of spot from film to film by a factor of 2·5. Thus, assuming it to be possible to observe an intensity range of 1–100 in a single film, a range of intensities of 1–1600 could be thus obtained. The spots were indexed using the Buerger charts (Buerger, 1942) and the intensities were visually estimated by comparison with previously prepared standard set of intensity spots. Intensity estimates were obtained for each spot from all the three films and the mean, weighted in favour of the medium intensity spot was taken for further calculations.

The *c*-axis being the needle axis and the *m* planes being very well developed in most crystals the *hk*0 reflections were the easiest to obtain. For this, a crystal ground at the top to the form of a cylinder of radius 0·1 mm. leaving the crystallographic faces at the bottom clear was used. The crystal was set on an optical goniometer and the needle axis was made vertical, the reflections from the unground planes below being used to set the prism zones vertical. The crystal was then transferred to the Weissenberg camera without disturbing the setting and the zero level photograph was taken by the normal beam method. With the *a*- and *b*-axes, difficulties arose due to the fact that the crystal was rotated about an axis almost perpendicular to the needle axis. Here the heavy absorption by the crystal when either the incident or reflected beam is in the direction of the needle axis during rotation is liable to seriously affect the intensity values and accurate absorption

corrections will have to be applied if reliable data are to be expected. These corrections are tedious to calculate for a crystal whose section in the reflecting plane is not a circle. The inaccuracy due to neglecting a detailed absorption correction could be reduced by using the anti-equi-inclination method of recording the zero-layer with a large inclination angle. Then, in no position of the crystal during its rotation will the incident or the diffracted beam have to travel through the whole length of the needle axis. This technique was used for obtaining the $0kl$ and $h0l$ reflections.

5. CORRECTIONS FOR THE INTENSITIES

Once a set of relative intensities is obtained, the next step is to get a set of structure factors based on these assuming the intensities to obey the mosaic crystal formula. A number of corrections have to be made at this stage to the observed intensities, the nature of these corrections increasing in complexity and uncertainty when very accurate values are needed. But, for most purposes of structure analysis it is sufficient to make the most important corrections, *viz.*, Lorentz and polarisation corrections, as well as the absorption and temperature corrections.

The Lorentz and polarization corrections were made using the tabulated values of Buerger and Klein (1945) for the c-axis normal beam photograph and using the charts prepared by the author (Kartha, 1952) for the other two anti-equi-inclination photographs. In the case of the c-axis photograph, for which the crystal was ground in the form of a cylinder, the absorption correction was made following the method suggested by Bradley (1935) for cylindrical powder specimens. In the case of a- and b-axis photographs no absorption correction was made, but the errors arising from absorption were reduced by using a crystal of about 0·3 mm. cross-section and an anti-equi-inclination angle of 30°. The effect of neglecting the absorption correction is to increase the intensity of large angle reflections in comparison with those of smaller angles and in this respect it acts in a way opposite to that of the temperature factor, which has the effect of reducing the intensities of large angle reflections. This effect is considered in the next section.

6. THE SCALE AND TEMPERATURE FACTORS

If I is the intensity of the spot after making the above corrections, then it can be written in the form

$$I = k^2F^2T, \qquad (1)$$

where F is the structure amplitude of the reflection concerned, T is the temperature factor which is usually of the form exp. $[-B(\sin\theta/\lambda)^2]$ and k^2

is the factor which converts the observed intensities to an absolute scale. The scale factor k and the temperature factor B were determined by using the method of Wilson (1942). He has shown that in the case of a crystal with a large number atoms in the unit cell the relation

$$< | F_{hkl} | >_{av} = \frac{\Sigma_{hkl} | F_{hkl} |^2}{N} = \Sigma_r f_r^2 \qquad (2)$$

holds for a given angle of scattering, where f_r is the scattering factor of the atom r for the scattering angle under consideration and N is the number of reflections observed at this angle. Using equations (1) and (2) we have

$$< I >_{av} = k^2 \Sigma_r f_r^2 T = k^2 \Sigma f_r^2 \exp. [- B (\sin \theta/\lambda)^2]$$

Thus

$$\frac{\Sigma f_r^2}{< I >_{av}} = \frac{1}{k^2} \exp. [- B (\sin \theta/\lambda)^2]$$

and

$$\log \left\{ \frac{\Sigma f_r^2}{< I >_{av}} \right\} = B (\sin \theta/\lambda)^2 + \log k^2. \qquad (3)$$

Hence a graph with $\log (\Sigma f_r^2 / < I >_{av})$ as ordinate and $(\sin \theta/\lambda)^2$ as abscissa should be a straight line, the slope of which is B and the intercept on the y-axis is $\log k^2$, so that both the scale factor and the temperature factor can be obtained from the graph.

For each zone, the reflections were divided into groups having ranges $(\sin \theta/\lambda) \times 10^{-8}$: $0 - 0{\cdot}2$, $0{\cdot}2 - 0{\cdot}4$, $0{\cdot}4 - 0{\cdot}6$, $0{\cdot}6 - 0{\cdot}8$, etc., and using the mean value of $(\Sigma f_r^2 / < I >_{av})$ for each range to correspond to the middle of the range, five or six points were obtained. All these points were found to fall approximately on a straight line, except the one for the smallest value of $(\sin \theta/\lambda)$, *viz.*, $0{\cdot}1 \times 10^8$ which was found to be appreciably above the average line. This was probably due to the large extinction effects occurring for these strong low angle reflections which reduce the value of I and thus lead to an abnormally large value of $\log (\Sigma f_r^2 / < I >_{av})$ in this region. Hence this point was neglected in drawing the graph from which the factors were read off.

By this method, values of $3{\cdot}2 \times 10^{-16}$, $1{\cdot}9 \times 10^{-16}$ and $1{\cdot}5 \times 10^{-16}$ were obtained for the constant B for the *hk*0, *h*0*l* and 0*kl* reflections respectively. The small value of B for 0*kl* and *h*0*l* reflections in comparison with that for the *hk*0 reflections is not surprising for the following reason. As mentioned in Section 6, the absorption correction was neglected for these two zones. The result of this is to effectively reduce the temperature factor as determined by the above method, in these cases.

Using the values of the scale factor k thus obtained the relative set of intensities were placed on an absolute basis to give values of $|F_{hkl}|$ for the various reflections. For the determination of atomic positions by Fourier synthesis, observed F-values uncorrected for temperature effect are preferable so as to avoid large termination errors. The temperature factors obtained by the above method were therefore used only for the comparison between observed structure factors and those calculated on the basis of the proposed structure. On an average an accuracy of 5–10% could be expected for the F_{hkl} values thus obtained, an accuracy which is satisfactory for most analyses.

PART II

Determination of Atomic Co-ordinates

7. Point Positions of Space Group I2/c

The symmetries of the space group I2/c are shown in Fig. 1, the usual nomenclature of International Tables being adopted. The general positions in the unit cell have a multiplicity of eight and the special positions on inversion centres or rotation axes number four. The equivalent point positions are shown in Fig. 2.

The point positions of multiplicity four are

(*a*)	0	0	0,	0	0	$\frac{1}{2}$,	$\frac{1}{2}$	$\frac{1}{2}$	$\frac{1}{2}$,	$\frac{1}{2}$	$\frac{1}{2}$ 0
(*b*)	0	$\frac{1}{2}$	0,	0	$\frac{1}{2}$	$\frac{1}{2}$,	$\frac{1}{2}$	0	$\frac{1}{2}$,	$\frac{1}{2}$	0 0
(*c*)	$\frac{1}{4}$	$\frac{1}{4}$	$\frac{1}{4}$,	$\frac{3}{4}$	$\frac{3}{4}$	$\frac{1}{4}$,	$\frac{3}{4}$	$\frac{3}{4}$	$\frac{3}{4}$,	$\frac{1}{4}$	$\frac{1}{4}$ $\frac{3}{4}$
(*d*)	$\frac{1}{4}$	$\frac{3}{4}$	$\frac{1}{4}$,	$\frac{3}{4}$	$\frac{1}{4}$	$\frac{1}{4}$,	$\frac{3}{4}$	$\frac{1}{4}$	$\frac{3}{4}$,	$\frac{1}{4}$	$\frac{3}{4}$ $\frac{3}{4}$
(*e*)	0	y	$\frac{1}{4}$,	$\frac{1}{2}$	$\frac{1}{2}-y$	$\frac{1}{4}$,	$\frac{1}{2}$	$\frac{1}{2}+y$	$\frac{3}{4}$,	0	$\bar{y}$ $\frac{3}{4}$

and positions of multiplicity eight are

$$x \quad y \quad z, \quad \bar{x} \quad \bar{y} \quad \bar{z}, \quad \bar{x}\ y\ \tfrac{1}{2}-z; \quad x\ \bar{y}\ \tfrac{1}{2}+z$$
$$\tfrac{1}{2}+x \quad \tfrac{1}{2}+y \quad \tfrac{1}{2}+z, \quad \tfrac{1}{2}-x \quad \tfrac{1}{2}-y \quad \tfrac{1}{2}-z,$$
$$\tfrac{1}{2}-x \quad \tfrac{1}{2}+y \quad \bar{z}, \quad \tfrac{1}{2}+x \quad \tfrac{1}{2}-y \quad z,$$

The points listed in (*a*), (*b*), (*c*) and (*d*) have symmetry C_i and in (*e*) symmetry C_2.

8. Preliminary Considerations

Since there are four bariums, four water molecules and eight chlorate ions in the unit cell, we could normally expect the bariums and water oxygens to occupy special positions of multiplicity four and the chlorate

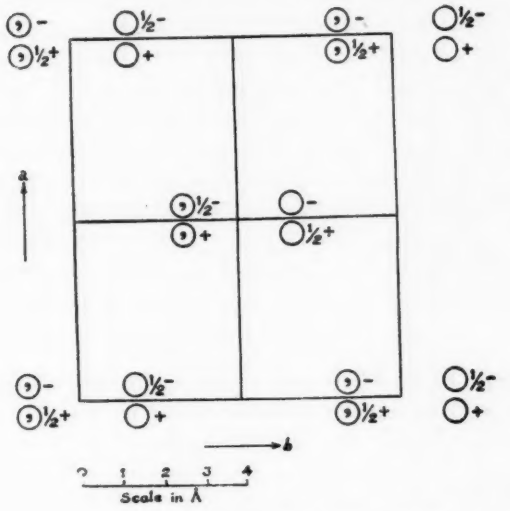

FIG. 1. Point positions in I 2*c*/ unit cell.

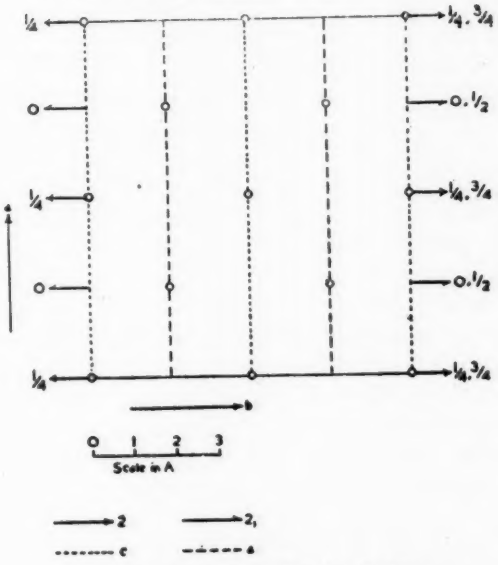

FIG. 2. Symmetries of unit cell I 2/*c*.

ion to occupy the general positions. It was observed that the set of reflections 4 0 0, 8 0 0, 12 0 0, 16 0 0 were very strong and exhibited

a normal decline of intensities. This suggests that the chlorine atoms lie very nearly midway between the (100) planes passing through the barium atoms which are at a distance of $a/2$ apart irrespective of which special positions they occupy. Now, two possibilities arise. The bariums may be either on one of the four sets of centres of inversion or they may be on the rotation axes. In the first case, the barium contribution for each $hk0$ reflection would be zero if h is odd, and a maximum if h is even. Hence we would expect on an average the h even reflections to be stronger than the h odd ones. No such regularity was observed and therefore the second alternative is more likely. However, a final decision can be arrived at only after a detailed examination of the complete intensity data.

9. The c-Axis Patterson Projection

In the absence of any knowledge of the structural arrangement, the best use to which we can put the observational data is to make Patterson synthesis using the observed $|F_{hkl}|^2$ values in the series:

$$AP(u, v) = \sum_{h=-\infty}^{+\infty} \sum_{k=-\infty}^{+\infty} |F_{hk0}|^2 \exp.[(2\pi i(hu + kv)] \tag{4}$$

For this space group (4) can be written in the form

$$AP(u, v) = \sum_{h=0}^{H} \sum_{k=0}^{K} |A_{hk0}|^2 \cos 2\pi hu \cos 2\pi kv, \tag{5}$$

where H and K denote the maximum observed numbers for h and k and

$$|A_{000}|^2 = |F_{000}|^2 = |\Sigma Z_r|^2; \; |A_{h00}|^2 = 2|F_{h00}|^2$$
$$|A_{0k0}|^2 = 2|F_{0k0}|^2 \text{ and } |A_{hk0}|^2 = 4|F_{hk0}|^2$$

The series expressed in the form (5) is suited for calculation using the "Phasenfaktoren Tafel" (Beauclair, Sinogowitz, 1949). This book contains tables of functions $\cos 2\pi hx \cos 2\pi ky$ for h and k varying from 0–20 for points x, y in steps of 1/24. Calculations were first made using these tables but as the net obtained by this method was found to be too coarse for the contours to be drawn accurately, the Beevers-Lipson strip method (1936, *a*, *b*) was later used in evaluating the series. In this case the summation could be done in steps of 1/120 of the unit cell using the recent 3° one-dimensional Fourier strips. For this method of summing, the Fourier series (5) can be put in the more convenient form

$$AP(u, v) = \sum_{k=0}^{K} A(k, u) \cos 2\pi kv, \tag{6}$$

where

$$A(k, u) = \sum_{h=0}^{H} |A_{hk0}|^2 \cos 2\pi hu. \tag{7}$$

Values for the Patterson function P (u, v) are thus obtained at points on a rectangular net of side $a/120 = 0{\cdot}0738$ Å and $b/120 = 0{\cdot}0650$ Å. A quarter of the unit cell was covered by extending the summation for u and v from 0 to 0·500. In fact, by keeping $|A_{h\bar{k}0}|^2$ terms with odd and even values of h and k separate during the summations, the summations need be carried out only in the range 0 to 0·250 for both u and v and the values for the rest of the unit cell could be obtained from these using the symmetry properties of the trigonometric functions and those of the space group under consideration. From the calculated P (u, v) values contours were drawn to show the distribution of the peaks of the Patterson function. The resulting map is shown in Fig. 3 in which only a quarter of the unit cell is drawn. The important peaks are marked in Fig. 4.

The peaks 1 and 1′ at (0, 0) and at $(\frac{1}{2}, \frac{1}{2})$ are of no interest, they being due to the nature of the function used and the space group. The peaks 2, 3, 4 being the most prominent, should enable one to fix the positions of bariums and chlorines in this projected unit cell; because, it is to be expected that the most prominent peaks would be those due to Ba—Ba, Ba—Cl or Cl—Cl vectors whose weights far outweigh those of the other possible vectors. Without any attempt to interpret all the peaks at this stage, though finally all the maxima should be explained in terms of the proposed structure, it is found that two sets of co-ordinates for barium and chlorine agree broadly

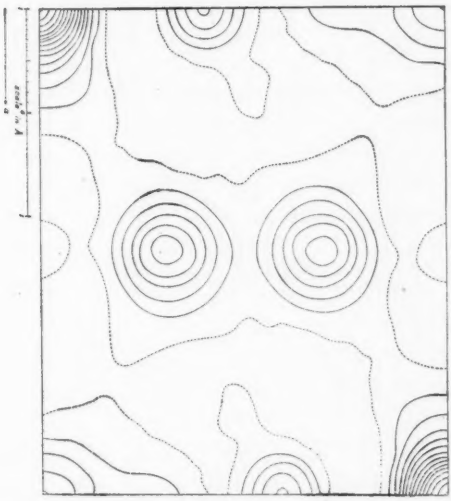

FIG. 3. Patterson projection on (001). Contours at intervals of 100 on an arbitrary scale.

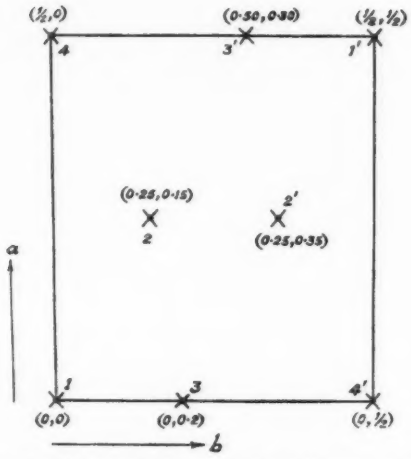

FIG. 4. Positions of Peaks in c-axis Patterson projection.

with the positions of the observed peaks, without considering their relative intensities. The two alternatives, one (I) in which a barium atom is at the centre of inversion and the other (II) in which it is on the rotation axis are diagrammatically shown in Figs. 5 and 6.

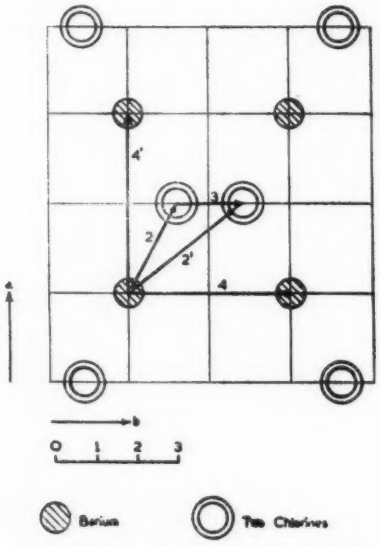

FIG. 5. Alternative I. Barium on centre of inversion.

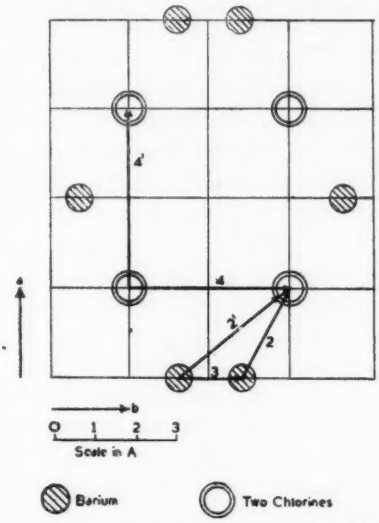

FIG. 6. Alternative II. Barium on rotation axis.

According to Fig. 5 where the barium is at a centre of inversion, the peak 3 corresponds to the superposition of eight Cl—Cl vectors and peak 4 to four Ba—Ba vectors, whereas according to Fig. 6, where barium is on a rotation axis, peak 3 corresponds to two Ba—Ba and peak 4 to sixteen Cl—Cl. Since the vector between atoms of scattering factors f_r and f_s has a weight $f_r f_s$, by putting approximate values for f_{Cl} and f_{Ba}, we find that according to alternative I, peak 4 should be about 4 times larger than peak 3, whereas according to alternative II they have about the same weight. Actually the projection showed that these peaks have approximately the same height. This again strengthens the guess made earlier that the bariums are situated on the rotation axes. In order to finally confirm this, Fourier syntheses were made according to both possibilities.

10. THE *c*-AXIS FOURIER PROJECTION

From the co-ordinates of the Patterson peaks two sets of atomic positions for barium and chlorine atoms are got for the above two alternatives. Assuming the co-ordinates of barium and chlorine to be x_1, y_1 and x_2, y_2 for the first case x_1', y_1' and x_2', y_2' for the second case, the following values are obtained for them:

I. $x_1 = 0{\cdot}25$ $\qquad$ $x_2 = 0{\cdot}50$

$y_1 = 0{\cdot}25$ $\qquad$ $x_2 = 0{\cdot}40$

II. $x_1' = 0{\cdot}00$ $\qquad x_2' = 0{\cdot}25$

$y_1' = 0{\cdot}40$ $\qquad y_2' = 0{\cdot}25$

Since in the above considerations an origin chosen at a centre of inversion was used $F_{hk0} = \pm \mid F_{hk0} \mid$, *i.e.*, the sign alone will have to be determined for these reflections in order to perform the Fourier synthesis. The structure amplitudes for the various reflections could be split up into three parts and written as

$$F_{hk0} = F_{Ba} + F_{Cl} + F_0 \tag{8}$$

the right-hand side denoting the barium, chlorine and oxygen contributions respectively to the structure amplitude. Now, the major part of the contribution to the scattering power of the unit cell is due to the barium and chlorine atoms whose co-ordinates are known to a good degree of accuracy from the Patterson projection, but for the ambiguity of the two alternatives. Thus, we can calculate the contributions $F_{Ba} + F_{Cl}$ to F_{hk0} and use the sign of the total contribution $F_{Ba} + F_{Cl}$ as the sign to be assigned to F_{hk0} in making the synthesis. Thus, using the two alternatives two sets of signs were obtained for the *hk*0 reflections. We could reasonably expect a very large percentage of the signs thus obtained to be correct if the correct alternative has been chosen. Two Fourier syntheses were made using in each case the observed magnitudes for the structure factors and the calculated signs by substituting these in the series:

$$\begin{aligned} A_{ab}\,\sigma(u, v) = F_{000} &+ 2\sum_{h=1}^{H} \pm \mid F_{h00} \mid \cos 2\pi hu \\ &+ 2\sum_{k=1}^{K} \pm \mid F_{0k0} \mid \cos 2\pi kv \\ &+ 4\sum_{h=1}^{H}\sum_{k=1}^{K} \pm \mid F_{hk0} \mid \cos \pi hu \cos 2\pi kv, \end{aligned} \tag{9}$$

where $\sigma(u, v)$ is the electron density per unit area in the projected unit cell. The summations were made just as in the case of the Patterson projection and the contours were drawn.

From the two projections thus obtained it was found that the first alternative was untenable for three reasons:—(*a*) it showed almost the same value for the peaks of barium and chlorine, (*b*) it gave regions of very large negative electron density and (*c*) it showed no indications of the oxygen atoms. The second alternative, where bariums were assumed to be on rotation axes, gave reasonable values for barium and chlorine peaks and showed clearly resolved barium, chlorines and two oxygens in the quarter cell. The peaks of the chlorine atoms, however, left the other oxygen atoms unresolved. The water oxygens were not clearly resolved. Further details could be

obtained only after Fourier refinement and elimination of diffraction effects which are considered later in Section 14.

11. The *b*-Projection

A look at the space group extinctions for I2/*c* shows that all *h*0*l* reflections with either *h* or *l* odd are absent. This implies that in the *b*-projection both *a* and *c* are halved so that the projected unit cell has unit translations *a*/2 and *c*/2 and hence an area one-fourth of the unit cell. The projected unit cell contains one barium, two chlorines, six oxygens and one water oxygen. The scattering power of the barium atoms being much larger than that of any other atoms in the unit cell, the heavy atom method (Robertson and Woodward, 1936) could be used to obtain the Fourier projection. Further, since the barium atom is in a special position, it would project as a centre of inversion in the projected plane group irrespective of whether barium is on a rotation axis or a centre of inversion. For the sake of convenience this point could be taken as the origin in making this projection. (Since the barium is actually on the rotation axis this origin would be at a distance of 0·250 along the *c*-axis from the origin with respect to which the symmetries and point positions have been given earlier.) Thus the heavy barium atom being chosen at the origin which is also a centre of inversion for the plane group, it makes its full positive contribution for each reflection that is not absent on demands of space group. The contribution from barium far outweighs the effect of all other atoms and therefore completely determines the signs of the various reflections, which should therefore be positive throughout. Hence we can assume that $F_{h0l} = |F_{h0l}|$ in making the Fourier projection. This assumption was later justified for every reflection by calculation of the structure amplitudes using the contributions of all atoms in the unit cell.

For the *b*-projection we have the electron density given by

$$A_{ac}\,\sigma(u, w) = \sum_{l=0}^{L} A(l, u) \cos lw + \sum_{l=}^{L} B(l, u) \sin lw, \tag{10}$$

where

$$A_{ac} = \text{Area of the projected unit cell}$$

$$A(l, u) = \sum_{h=0}^{H} A_{h0l} \cos 2\pi hu$$

$$B(l, u) = \sum_{h=0}^{H} B_{h0l} \sin 2\pi hu \tag{11}$$

$$A_{000} = F_{000};\quad A_{h00} = 2F_{h00}$$

$$A_{00l} = 2F_{00l};\quad A_{h0l} = 2\,[F_{h0\bar{l}} + F_{h0l}]$$

$$B_{000} = B_{h00} = B_{00l} = 0;\quad B_{h0l} = 2\,[F_{h0\bar{l}} - F_{h0l}]$$

The summations were made by the strip method and the final sums were multiplied by a suitable factor to give values directly in electrons per Å^2. The projection showed barium, chlorine and sixteen oxygen atoms resolved and indicated the pasitions of the other oxygen atoms. The water oxygen, which presumably is projected on top of the barium atom at the origin, is masked by the latter. The x and z co-ordinates were obtained from this projection and the structure factors for the various $h0l$ reflections were calculated. The calculations showed that all the assumed signs were correct and exhibited a remarkable agreement between the observed and calculated values, except for three very strong reflections of low (sin θ/λ) for which the observed values were too low. The obvious reason for this discrepancy was the neglect of absorption and extinction effects both of which tend to reduce the intensities of the strong low angle reflections.

12. THE a-AXIS PROJECTION

From the c- and b- axis projections, accurate values were obtained for all the co-ordinates of the heavier atoms and fairly good values for most of the oxygen co-ordinates. The other oxygen co-ordinates could not be so satisfactorily fixed due to the overlapping of the atoms in the projections. Since atoms which are unresolved in one projection might be clearly resolved in another, it was decided to make the a-projection also so that the best values for the various co-ordinates could be finally chosen. For this, the signs of the F_{0kl} were obtained by using the atomic co-ordinates got from the other two projections. Choosing the origin at $(00\frac{1}{4})$ so as to correspond to the earlier choices for the c- and b-projections, the structure factors are given by equations.

$$F_{0kl} = 0 \text{ for } k + l \text{ odd}$$

and

$$F_{0kl} = \sum_{r=1}^{6} 8 f_r \cos 2\pi k y_r \cos 2\pi l z_r \text{ for } k, l \text{ even}$$

$$F_{0kl} = \sum_{r=1}^{6} 8 f_r \sin 2\pi k y_r \cos 2\pi l z_r \text{ for } k, l \text{ odd} \qquad (12)$$

The signs got from these equations are used in the series

$$A_{kl}\,\sigma(v, w) \quad \sum_{k,\,l \text{ even}} \sum \pm |F_{0kl}| \cos 2\pi k v \cos 2\pi l w + \sum_{k,\,l \text{ odd}} \sum \pm |F_{0kl}| \sin 2\pi k v \cos 2\pi l w. \qquad (13)$$

This series was summed in the usual way using the Beevers-Lipson strips. The projection exhibited the important peaks, but it also showed very strong diffraction effects around the barium atoms which brought up spurious

peaks and cancelled some of the actual peaks. Hence oxygen positions could not be fixed with any degree of accuracy until this projection was refined and the diffraction effects were reduced.

13. Fourier Refinement of Projections

Having obtained, as described above, an approximate set of atomic co-ordinates, the projections were then refined to give more accurate co-ordinates. The signs of the various structure factors were recalculated using the atomic co-ordinates from the projection and the synthesis was performed with the new sets of signs. In the case of *c*-projection the first refinement revealed the position of the water oxygen also. For the *b*-projection the calculated F_{h0l}'s showed that no change was required in the assumed signs and hence this type of refinement was unnecessary in this case. But, there were a few reflections for which the observed intensities were too low for reasons explained before and the synthesis was therefore repeated using the calculated values (F_c) for these reflections. The effect of using F_c instead of F_0 for these few reflections is only to give zero weight for the observed values of these reflections and no great error is thereby introduced. Fourier refinement of *a*-projection did not improve it appreciably, owing to the enormous diffraction effects around the barium atoms. Hence further improvement of the projection could be done only after eliminating the diffraction effect which we shall consider next.

14. Elimination of Diffraction Effect

In the projections described in the previous section there are regions around the heavy atoms where appreciably large negative electron densities are found. This is to be attributed to the fact that the Fourier syntheses were performed using only reflections up to a $(\sin\theta/\lambda)$ range of about $0{\cdot}8 \times 10^8$ the coefficients of the higher terms in the Fourier series having been taken to be zero. Actually the scattering factors of barium and chlorine are still appreciable in the regions beyond $(\sin\theta/\lambda) = 0{\cdot}8\times10^8$. The effect of the termination of the Fourier series when the coefficients are still large is to introduce strong diffraction effects around the heavier atoms, which appear surrounded by a series of ripples of gradually diminishing amplitude. These rings of positive and negative electron density mask the peaks due to oxygen atoms in some cases and bring out spurious peaks. This difficulty was got over by extending the series as follows: Calculated F values (F_c) were used beyond the region for which F was observed, F_c being calculated from the contributions of only barium and chlorine atoms to the reflections. The positions of these are known very accurately because of two reasons, *viz.*, (1) The diffraction effects do not affect the positions of

maxima of the heavy atoms and (2) the co-ordinates of the heavy atoms could be accurately fixed from the Patterson projections where diffraction effects are negligible due to the large range of values used for the coefficients. The contribution of the oxygen atoms to the structure factor is very small for these large (sin θ/λ) values, because of the relatively faster decline of the atomic scattering factor with angle for oxygen. Further, the purpose of the extension of the Fourier series is to eliminate diffraction effects of the heavier barium and chlorine atoms. For these reasons, it is justifiable to use only the contributions of barium and chlorine atoms in calculating the structure factors F_c.

Thus the series was extended up to h, k, l values equal to twenty. Even then F_c values were not negligibly small and therefore a suitable temperature factor was used to reduce F_c values to a negligible amount beyond these regions. Of course, one could have used a large temperature factor without extending the series such that F values became very small even for (sin θ/λ) $= 0{\cdot}8\times10^{8}$; but this would certainly be detrimental to accuracy because of the accompanying broadening of the peaks. On the other hand, if the temperature factor is too small, the extension of the series will have to be made to such large values of h, k and l that computation would be very laborious. The final choice of the temperature factor B was a compromise between the two opposing considerations. The B values chosen were $3{\cdot}2\times10^{-16}$ for b- and c-projections and $4{\cdot}0\times10^{-16}$ for the a-projection. In the case of projections where the value of the temperature factor used was larger than that actually found, the observed structure factors were multiplied by a suitable factor so as to bring all the F values (both F_0 and F_c) used for a particular summation to have the same effective temperature factor. Using the series thus extended, the projections were made.

15. Final Projections

The final projections obtained after refinement and elimination of diffraction effects are shown in Figs. 7 to 12 together with their key diagrams. These projections were found to be largely free from the diffraction effects. The atomic co-ordinates obtained from them could explain all the peaks in the Patterson projections shown in Figs. 3 and 13.

16. Atomic Co-ordinates

All the three projections together with the Patterson diagrams fixed the barium and chlorine positions to an accuracy of $\pm 0{\cdot}002$ of the unit cell dimensions. Some of the oxygen atoms, though resolved in one projection, were found overlapping with the heavier atoms in another projection

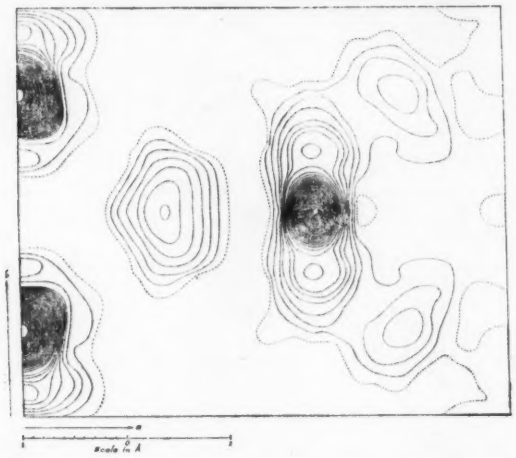

FIG. 7. Final (100) F-projection. Contours at intervals of 2 e. per Å^2 around oxygen, & 4 elsewhere.

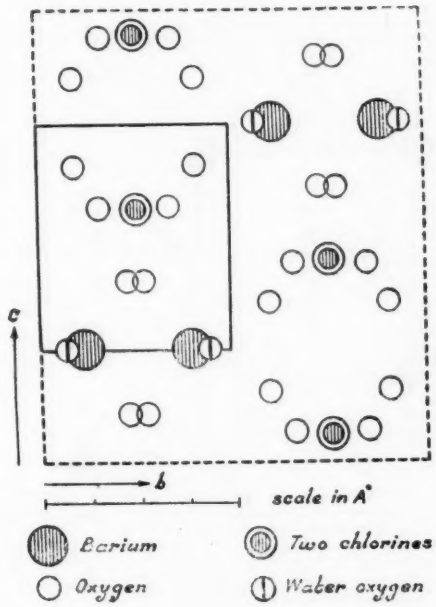

FIG. 8. Atomic positions in *a*-projection.

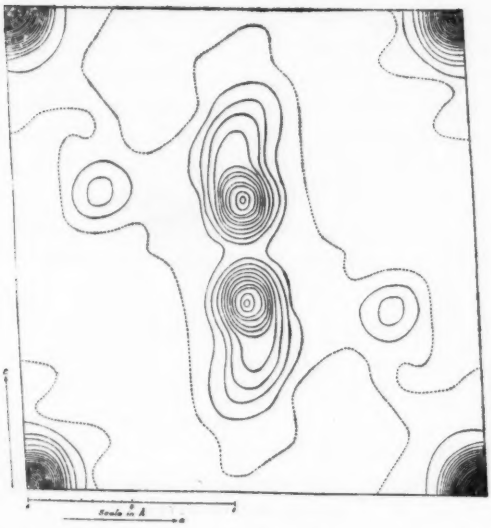

FIG. 9. Final (010) Fourier projection after minimising diffraction errors also. Contours at intervals of 4 electrons per Å².

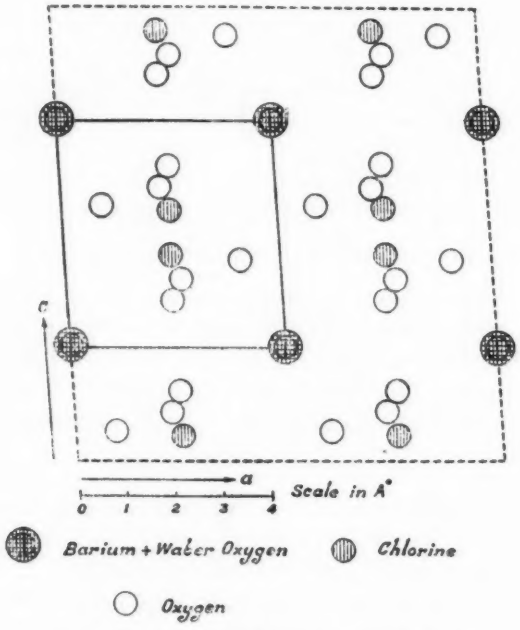

FIG. 10. Atomic positions in *b*-projection.

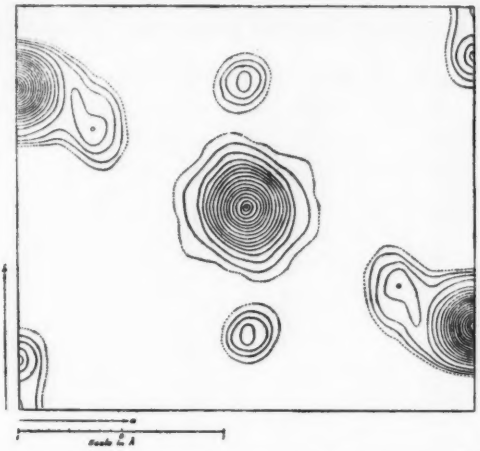

FIG. 11. Final (001) F-projection using F_c values also in synthesis to eliminate diffraction effects. Contours at intervals of 2 *e*. Å^3 around oxygen and 4 *e*, Å^3 elsewhere.

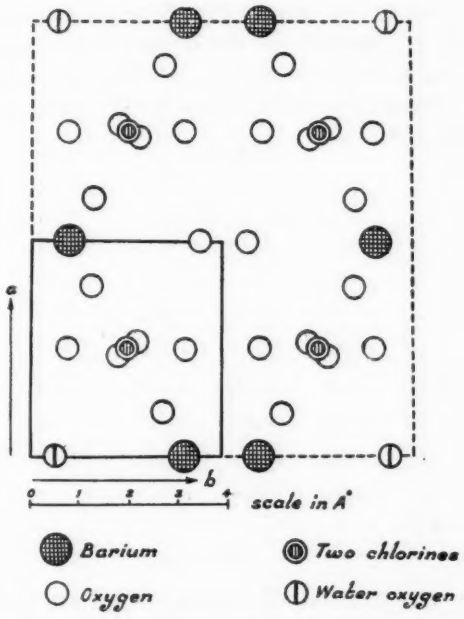

FIG. 12. Atomic positions in c-projection.

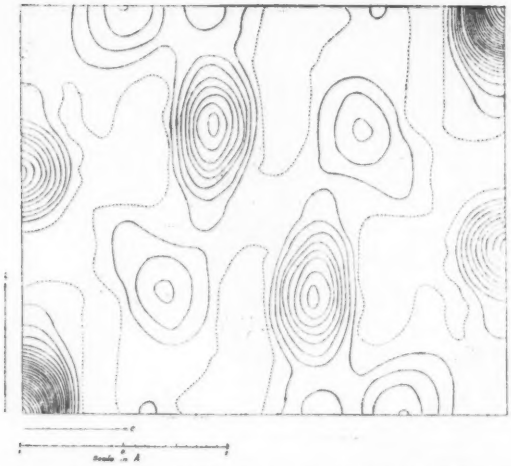

FIG. 13. Patterson projection on (100). Contours at intervals of 50 on an arbitrary scale.

so that the best set of values from all the three projections was finally chosen for these atoms. Due to the comparatively small scattering contribution of the oxygen atoms to the various reflections an accuracy not much better than 0·005 could be expected for the oxygen co-ordinates. The final table of co-ordinates, both fractional and in angstroms, are presented in Table I; the co-ordinates being given with respect to the origin of the space group as given in Section 8.

TABLE I

Atom	Fractional Co-ordinates			Co-ordinates in angstroms		
	u	v	w	x	y	z
1 Barium ..	0·000	0·396	0·250	0·00	3·09	2·34
2 Chlorine ..	0·250	0·250	0·554	2·22	1·95	5·18
3 Oxygen 1 ..	0·092	0·342	0·562	0·82	2·67	5·25
4 Oxygen 2 ..	0·254	0·096	0·650	2·25	0·75	6·08
5 Oxygen 3 ..	0·267	0·225	0·396	2·37	1·76	3·70
6 Water Oxygen ..	0·000	0·062	0·250	0·00	0·48	2·34

17. ACCURACY

The validity of any proposed structure must on the final analysis rest on the agreement between the structure amplitudes F_c calculated on the

TABLE II. *Observed and Calculated Structure Amplitudes*

h	k	l	Fcalc.	Fobs.	h	k	l	Fcalc.	Fobs.
0	0	0	592	..	9	1	0	−52	57
0	2	0	− 74	98	9	3	0	37	37
0	4	0	− 74	85	9	5	0	54	55
0	6	0	−143	135	9	7	0	6	0
0	8	0	74	57	9	9	0	−36	39
0	10	0	23	30	10	0	0	34	40
0	12	0	21	0	10	2	0	48	45
0	14	0	− 28	26	10	4	0	−77	67
1	1	0	−165	166	10	6	0	− 1	0
1	3	0	107	128	10	8	0	− 2	0
1	5	0	134	137	10	10	0	29	32
1	7	0	− 3	0	11	1	0	−41	42
1	9	0	− 57	46	11	3	0	24	22
1	11	0	− 26	27	11	5	0	43	42
1	13	0	16	16	12	0	0	84	87
2	0	0	45	30	12	2	0	− 9	0
2	2	0	162	186	12	4	0	−20	18
2	4	0	−191	199	13	1	0	−31	30
2	6	0	3	0	13	3	0	18	19
2	8	0	− 9	0	13	5	0	28	29
2	10	0	63	42	14	0	0	14	0
2	12	0	− 16	0	14	2	0	23	27
3	1	0	−106	79	14	4	0	−34	40
3	3	0	51	60	15	1	0	−16	19
3	5	0	113	130	15	3	0	6	0
3	7	0	3	0	15	5	0	21	26
3	9	0	− 56	43	16	0	0	31	27
3	11	0	− 27	25	0	0	2	124	90
3	13	0	17	0	0	0	4	133	131
4	0	0	291	290	0	0	6	190	180
4	2	0	− 13	27	0	0	8	66	60
4	4	0	− 56	50	0	0	10	142	119
4	6	0	−144	146	0	0	12	52	39
4	8	0	63	47	0	0	14	49	46
4	10	0	25	42	0	0	16	50	51
4	12	0	17	0	2	0	0	44	21
5	1	0	− 85	67	2	0	2	296	203*
5	3	0	33	35	2	0	4	180	138
5	5	0	93	98	2	0	6	137	111
5	7	0	18	0	2	0	8	139	130
5	9	0	− 54	45	2	0	10	46	44
5	11	0	− 21	19	2	0	12	69	87
6	0	0	13	0	2	0	14	48	35
6	2	0	105	89	2	0	16	38	30
6	4	0	−119	101	4	0	0	302	172*
6	6	0	− 16	32	4	0	2	123	120
6	8	0	− 4	0	4	0	4	104	95
6	10	0	54	35	4	0	6	144	141
7	1	0	− 63	55	4	0	8	71	58
7	3	0	23	27	4	0	10	104	87
7	5	0	80	81	4	0	12	56	37
7	7	0	2	0	4	0	14	48	39
7	9	0	− 41	42	4	0	16	37	35
8	0	0	158	140	6	0	0	13	0
8	2	0	− 18	0	6	0	2	196	149
8	4	0	− 29	25	6	0	4	134	128
8	6	0	− 86	74	6	0	6	65	65
8	8	0	44	39	6	0	8	124	135
					6	0	10	36	25

TABLE II—(*Contd.*)

h	k	l	Fcalc.	Fobs.	h	k	l	Fcalc.	Fobs.
6	0	12	60	60					
6	0	14	48	39	4	0	$\overline{16}$	44	30
8	0	0	182	168					
8	0	2	47	55	6	0	$\overline{2}$	180	150
8	0	4	103	118					
8	0	6	95	96	6	0	$\overline{4}$	138	131
8	0	8	44	39					
8	0	10	93	79	6	0	$\overline{6}$	92	81
8	0	12	37	30					
10	0	0	42	37	6	0	$\overline{8}$	129	132
10	0	2	106	116					
10	0	4	76	67	6	0	$\overline{10}$	32	39
10	0	6	52	51					
10	0	8	71	67	6	0	$\overline{12}$	83	115
10	0	10	29	20					
10	0	12	38	30	6	0	$\overline{14}$	54	39
12	0	0	110	120					
12	0	2	27	14	6	0	$\overline{16}$	26	25
12	0	4	49	60					
12	0	6	66	63	8	0	$\overline{2}$	96	78
12	0	8	20	14					
12	0	10	51	60	8	0	$\overline{4}$	73	67
14	0	0	20	21					
14	0	2	69	78	8	0	$\overline{6}$	104	119
14	0	4	34	25					
14	0	6	30	30	8	0	$\overline{8}$	54	76
16	0	0	51	46					
16	0	2	21	21	8	0	$\overline{10}$	91	98
2	0	$\overline{2}$	216	168*	8	0	$\overline{12}$	44	39
2	0	$\overline{4}$	260	189	8	0	$\overline{14}$	40	35
2	0	$\overline{6}$	124	81	10	0	$\overline{2}$	95	113
2	0	$\overline{8}$	139	134	10	0	$\overline{4}$	77	88
2	0	$\overline{10}$	60	49	10	0	$\overline{6}$	72	74
2	0	$\overline{12}$	80	78	10	0	$\overline{8}$	76	79
2	0	$\overline{14}$	48	42	10	0	$\overline{10}$	27	55
2	0	$\overline{16}$	37	25	10	0	$\overline{12}$	62	87
4	0	$\overline{2}$	128	98	10	0	$\overline{14}$	31	34
4	0	$\overline{4}$	140	112	12	0	$\overline{2}$	45	37
4	0	$\overline{6}$	127	123	12	0	$\overline{4}$	60	71
4	0	$\overline{8}$	98	100	12	0	$\overline{6}$	56	81
4	0	$\overline{10}$	129	112	12	0	$\overline{8}$	32	39
4	0	$\overline{12}$	44	27	12	0	$\overline{10}$	69	65
4	0	$\overline{14}$	55	42	12	0	$\overline{12}$	22	25

TABLE II—(*Contd.*)

h	*k*	*l*	$F_{calc.}$	$F_{obs.}$	*h*	*k*	*l*	$F_{calc.}$	$F_{obs.}$
					0	6	2	−56	40
14	0	$\bar{2}$	50	70	0	6	4	−59	49
					0	6	6	−61	56
14	0	4	54	60	0	6	8	−29	33
					0	8	0	67	48
14	0	6	38	25	0	8	2	3	15
					0	8	4	31	26
14	0	8	48	58	0	1	3	181	154
					0	1	5	11	5
6	0	2	32	25	0	1	7	131	132
0	0	2	124	88	0	1	9	38	23
0	0	4	133	120	0	1	11	5	7
0	0	6	190	167	0	3	1	137	111
0	0	8	66	35	0	3	3	129	118
0	0	10	142	111	0	3	5	199	159
0	2	0	− 71	83	0	3	7	52	31
0	2	2	156	131	0	3	9	64	66
0	2	4	55	48	0	5	1	5	0
0	2	6	− 13	20	0	5	3	14	13
0	2	8	64	74	0	5	5	34	24
0	2	10	− 2	12	0	5	7	24	20
0	4	0	− 75	60	0	5	9	−10	10
0	4	2	−161	123	0	7	1	−64	60
0	4	4	− 93	76	0	7	3	−95	76
0	4	6	− 55	37	0	7	5	−44	51
0	4	8	− 85	88	0	7	7	−76	62
0	4	10	− 33	31	0	9	1	−28	12
0	6	0	−134	91	0	9	3	0	8

basis of the structure and the values F_0 obtained experimentally. To show the extent of agreement between the observed and calculated values the two sets are given in Table II. The F_0's marked with asterisks are the *h0l* reflection for which F_c is far greater than F_0 due to the absorption and extinction effects as mentioned earlier.

As a measure of the agreement between the calculated and observed structure amplitudes the function

$$R = \Sigma \Big| |F_0| - |F_c| \Big| \Big/ \Sigma |F_0|$$

was calculated for the various projections separately and finally for all the reflections taken together, with the results given in Table III.

The function R′ given by $\Sigma \Big| |F_0| - |F_c| \Big| \Big/ \Sigma |F_c|$ had a mean value 0·165, as against 0·178 for R. Unobserved reflections in these ranges of (sin θ/λ) were also taken in calculating the reliability indices R and R′.

TABLE III

Projection	(sin θ/λ) range up to which comparison was made	Number of reflections compared	R
a	$0{\cdot}70\times10^{8}$	46	0·21
b	$0{\cdot}95\times10^{8}$	109	0·16
c	$0{\cdot}85\times10^{8}$	86	0·178
Combined	..	241	0·178

As is to be expected, the agreement is best for the *b*-projection where the largest (sin θ/λ) range and the maximum number of reflections were used; and the least for the *a*-projection where the smallest number of reflections was used and no absorption corrections were made. On the whole, the agreement can be considered to be good especially because the structure determination has been based only on projections 8–9 Å deep. Of course, part of the value of R will be due to errors in measured F values and to neglect of corrections, but a major part must be attributed to the lack of spherical symmetry in the atomic electronic distribution in the crystal and due to the presence of hydrogen atoms whose existence has not been taken into account in calculating the F_c values.

18. DISCUSSION OF THE STRUCTURE

There are eight chlorate ions in the unit cell all of which are obtained from a single ion by the operations of screw axes and inversions. The general arrangement of atoms is shown in Fig. 14 which gives a perspective diagram of the unit cell.

The chlorate ions remain as independent units having the usual distorted low pyramidal structure with an oxygen triangle of average side 2·52 Å and chlorine-oxygen distance 1·57 Å. The chlorine atom is at a distance of 0·45 Å from the oxygen plane. It is interesting to compare these values with the values for the chlorate ions in the case of sodium chlorate and potassium chlorate crystals (Zachariasen, 1929) and these together with the corresponding values for barium chlorate are given in Table IV.

Each chlorine atom is linked to four barium atoms and each barium to eight chlorines at an average distance of 3·89 Å. There is also a barium atom in a line almost normal to the oxygen plane of a chlorate ion at a distance of 5·76 Å from the chlorine. The barium atom is surrounded by ten

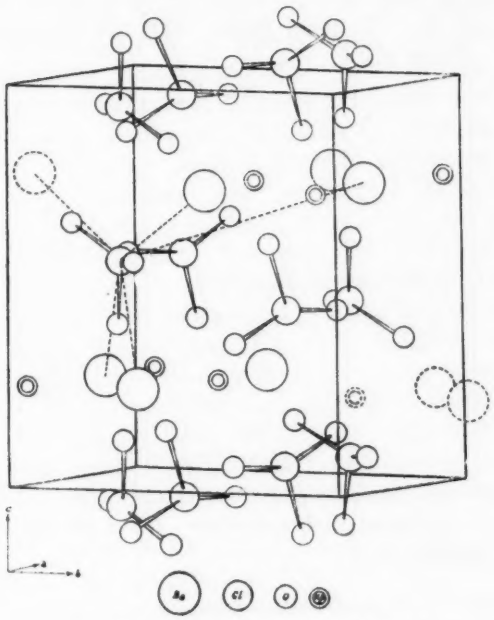

FIG. 14. Barium chlorate monohydrate.

TABLE IV

Crystal		Oxygen–Oxygen	Chlorine–Chlorine	Displacement of Cl atom from O_3 plane
Sodium Chlorate ..	Zachariasen	3*a*, 2·38 Å	1·48 Å	0·48 Å
Potassium Chlorate ..	do	1*a*, 2·48 Å	*a*, 1·60 Å	0·50
		2*b*, 2·33 Å	2*b*, 1·42 Å	
		Mean = 2·43 Å	Mean = 1·48 Å	
Barium Chlorate ..	Author	*a*, 2·52 Å	*a*, 1·60 Å	0·45 Å
		b, 2·59 Å	*b*, 1·51 Å	
		c, 2·45 Å	*c*, 1·59 Å	
		Mean = 2·52 Å	Mean = 1·57 Å	

oxygen atoms at a mean distance of 2·87 Å and by a water oxygen on the rotation axis at a distance of 2·60 Å. This average barium-oxygen distance

2·87 Å is slightly greater than the value 2·75 Å given as the sum of crystal radii for Ba^{++} and O^{--} (Pauling, 1948). The various interatomic distances are collected in Table V.

TABLE V

Atoms	Cl—O	O—O	Ba—O	Ba-Water Oxygen
	..	..	3·02	
	1·60	2·52	2·97	
Distance in Å ..	1·51	2·59	2·78	2·60
	1·59	2·45	2·74	
	..	..	2·84	
Mean ..	1·57 Å	2·52 Å	2·52 Å	2·60 Å

19. OPTICAL PROPERTIES

We shall now consider the explanation of the strong positive birefringence of the crystal on the basis of this structure. The optical properties of the crystal are summarised in Fig. 15.

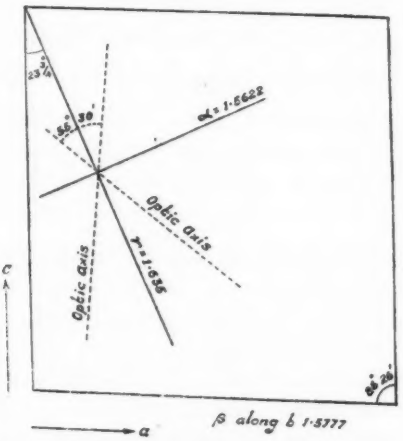

FIG. 15. Optical constants of barium chlorate.

It is well known that a flat molecule, or a polyatomic ion in which all atoms lie in a plane, has a higher refractive index when the electric vector lies in the plane of the group of atoms than when it is perpendicular to the plane. In crystals these ions are surrounded by others and the interaction

between them introduces complication, but the distances between atoms in the neighbouring molecules are in general much greater than those linked by direct bonds. Since the induction effects fall off rapidly with increasing distance, the interaction between different molecules may be neglected as a first approximation. Hence the main factor contributing to the birefringence of crystals containing strongly anisotropic ions is the relative orientation of these units. When they are all parallel as in the case of most nitrates and carbonates the anisotropy is almost the same as that of the units; but when these units are inclined to each other in the unit cell their individual effects cancel out particularly, or sometimes completely as in cubic crystals. When such ions have their planes inclined at an appreciable angle to each other but are all parallel to a line, the refractive index along this line will be high, but in other directions it will be comparatively low corresponding to an average value for the other two principal directions of the molecule and hence the birefringence would be positive. These ideas enable one to explain the optical properties of barium chlorate from the orientations of the chlorate ions in the unit cell as indicated below.

In barium chlorate, the bulk of the contribution to the refractivity is from the chlorate ions, in particular from the O_3 groups. The planes of these groups have only two types of orientations in the crystal, the two being related to each other by a rotation of 180° about the *b*-axis. If we denote by *l*, *m*, *n* the direction cosines of the normals to the two types of oxygen planes with reference to the co-ordinate axes parallel to *b*, *c* and the third mutually perpendicular direction, then it can be shown that they have the following values for the structure determined here

$$l = 0{\cdot}674 \qquad m = 0{\cdot}652 \qquad n = 0{\cdot}348$$

$$l = 0{\cdot}674 \qquad m = -0{\cdot}652 \qquad n = 0{\cdot}348$$

Thus the line of intersection of the two planes (*i.e.*, common direction to the oxygen planes) lies in the *a*-*c* plane (Fig. 16). If A is the angle made by this line with the *c*-axis, then $\cot A = l/n = 1{\cdot}937$, so that $A = 27° 18'$. Thus the common direction makes an angle approximately 27° with the *c*-axis in the acute angle between *c* and *a*. Being a direction common to the two O_3 groups, this will be the direction of maximum refractive index (γ). Further, the normal to the oxygen planes of the chlorate ions make an angle $\theta = \cos^{-1} m = 49° 17'$ with the *b*-axis and this angle remains the same for all the ions. Thus the angle made by the oxygen planes with the *b*-axis is smaller than 45°, and hence the refractive index along the *b*-direction will be the larger of the two smaller refractive indices (α and β).

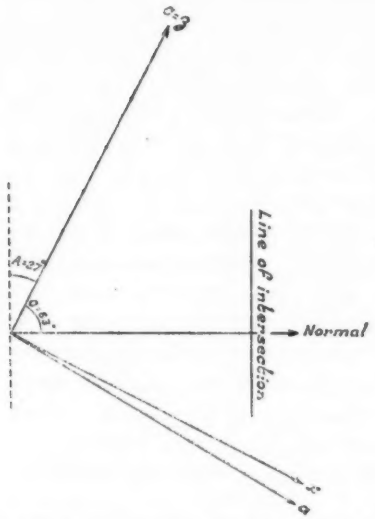

FIG. 16. Line of intersection of oxygen plane and (010) plane.

To summarise, the structure enables us to predict the following: (1) The largest refractive index (γ) will be in a direction making an angle $A = 27°$ with the c-axis. (2) The middle refractive index (β) will be along the b-direction and β will be nearer to α than to γ. These are in agreement with the observed data $\alpha = 1{\cdot}5622$, $\beta = 1{\cdot}5777$, $\gamma = 1{\cdot}635$ and $A = 23\frac{3}{4}°$.

In conclusion, the author has great pleasure in recording his best thanks to Professor R. S. Krishnan for his kind interest and to Dr. G. N. Ramachandran for his guidance and help throughout the investigation.

SUMMARY

The crystal structure of barium chlorate monohydrate has been completely determined. The crystals are monoclinic with space group $I2/c$–C_{2h}^6 and four molecules in a unit cell with edges $a = 8{\cdot}86$ Å, $b = 7{\cdot}80$ Å, $c = 9{\cdot}35$ Å and $\beta = 93° 26'$. The heavy atom positions were first fixed from Patterson projections and the atomic co-ordinates of all atoms were obtained from Fourier projections along the three axes. In the structure, chlorate ions retain their usual low pyramidal form. Each chlorine is surrounded by four bariums and each barium by eight chlorines. Tables are given for the various atomic co-ordinates and the interatomic distances. The structure is able to explain qualitatively the known optical properties of the crystal.

References

Beauclair, I. W. de and Sinogowitz, U.	..	"Phasenfaktoren Tafel," Akademie Verlag, Berlin, 1949.
Beevers, C. A. and Lipson, H.	..	*Nature*, 1936, **137**, 825.
Bradley, A. J.	..	*Proc. Phy. Soc.*, 1935, **47**, 879.
Buerger, M. J.	..	*X-Ray Crystallography*, John Wiley, 1942.
—— and Klein, G. E.	..	*Jour. App. Phy.*, 1945, **16**, 408.
Eakle, A. S.	..	*Z. Krist.*, 1896, **26**, 586.
Groth, P.	..	*Chemische Crystallographic*, 1908, **2**, 114.
Kartha, G.	..	*Curr. Sci.*, 1951, **20**, 151.
————	..	*Acta. Cryst.*, 1952 **5**, 549.
Lipson, H. and Beevers, C. A.	..	*Proc. Phy. Soc.*, 1936, **48**, 772.
Pauling, L.	..	*Nature of the Chemical Bond*, 1948, 346, Cornell University Press.
Robertson, J. M.	..	*Journ. Sci. Inst.*, 1943, **20**, 175.
—— and Woodward, I.	..	*Journ. Chem. Soc.*, 1940, **1**, 36.
Wilson, A. J. C.	..	*Nature*, 1942, **150**, 152.
Zachariasen, W. H.	..	*Z. Krist.*, 1929, **71**, 501, 517.
—— and Barta, F. A.	..	*Phys. Rev.*, 1931, **37**, 1626.

STUDIES IN IRON OXIDE SOLS

Part I. Electrical Conductivity of Iron Oxide Sol

By A. K. M. Trivedi, A. S. Divatia and M. J. Patani

(L. D. Arts College and M. G. Science Institute, Ahmedabad)

Received December 13, 1951

(Communicated by Dr. R. D. Desai, F.A.SC.)

In an investigation on the equivalent conductivity of colloidal sulphur sols, Bolam and Trivedi,[1] have shown that the equivalent conductivity of the bound polythionate *increases* with increase in the concentration. Thus the behaviour of sulphur sol is similar to the behaviour of soap solutions and paraffin chain electrolytes, in that at relatively high concentrations, the equivalent conductivity increases with the increase in the concentration. McBain[2] remarks: ".... any colloid which carries electrical charges will in some measure approach the behaviour of a typical colloidal electrolyte." Hartley[3] points out that the micelles may be regarded as highly polyvalent ions and the increase in conductivity is ascribed to the smoothing out of the variations in the distribution of oppositely charged ions. In the present investigation an attempt was made to see whether iron oxide sols show the anomalous increase in conductivity similar to sulphur sol and soap solutions.

Concentrated iron oxide sol was prepared. The conductivity of the sol with dilution as well as the concentrations of the various constituents were determined. Like the sulphur sol, the relative proportions of the colloid and the crystalloid constituents are not likely to change significantly on dilution; hence, the detailed study of sols of this type may throw light on the anomalous conductivity of colloidal electrolytes.

Experimental

Concentrated iron oxide sol was prepared by a modification of Graham's method.[4] Iron hydroxide was freshly precipitated from 500 ml. of a normal solution of ferric chloride by 4 N ammonia. The precipitate was thoroughly washed with water and suspended in 500 ml. of water. 4 N hydrochloric acid was gradually added while stirring. The sol obtained in this way was concentrated to about one-fourth the volume, and subjected to hot intermittent dialysis in a parchment paper bag for a period of one month. The diffusate was changed every day, distilled water at 60°–70° C. being used throughout. The dialysis was continued until the diffusate failed to give turbidity with silver nitrate.

Analysis of the Sol

The iron oxide content of the sol was estimated by evaporating the sol to dryness. The total chloride was estimated as follows:—To an aliquot portion of the sol, excess of sodium hydroxide was added and the precipitate obtained was digested for three hours on a water-bath. An equivalent quantity of sulphuric acid was then added and after a further digesting of three hours on a water-bath, the precipitate was filtered. One gram of calcium carbonate was then added to neutralise the acid, and the solution was titrated with N/10 silver nitrate by Mohr's method. Duplicate experiments showed that the method was quite reproducible. Fixed and free hydrogen ions were estimated as follows:—To an aliquot portion of the sol, exactly one gram of sodium sulphate was added. The precipitate obtained was allowed to settle for three hours on a water-bath and kept at room temperature for several hours. The precipitate was then filtered and washed. The filtrate and the washings were titrated with N/10 sodium hydroxide. This method gives the free hydrogen ions in the sol. The results obtained were fairly reproducible.

The determination of the fixed hydrogen ions in the sol had to be done in an indirect manner, by determining the total hydrogen-ion concentration and the free hydrogen-ion concentration in the sol. The difference between the two gives fixed hydrogen-ion concentration in the sol. The method however was not very sensitive. The total hydrogen-ion concentration was estimated as follows:—To an aliquot portion of the sol, a definite quantity of standardised sodium hydroxide was added and the contents were heated on a water-bath to coarsen the particles. An amount of hydrochloric acid equivalent to the previously added sodium hydroxide was then added (this is done to avoid the filtration of the alkaline solution). After a further digestion of one hour iron oxide was filtered off, and the filtrate and the washings were titrated with standard sodium hydroxide. This gives the total hydrogen-ion concentration of the sol. The composition of the sol is given in Table I.

Table I

Sol	Concentration				Fixed H per gm. Fe_2O_3	$Fe^{\cdots}$ per gm. Fe_2O_3
	Iron oxide gm./l	Free H m.e./l	Fixed H m.e./l	Total Cl m.e./l		
Fe_2O_3	105·0	1·20	7·20	96·0	0·068	0·2781

THE DETERMINATION OF THE CONDUCTIVITY OF THE SOL

The conductivity of the sol was determined by using a Leeds and Northrup Potentiometer. The conductivity cell was specially platinized (Findlay[5]), and it was placed in a thermostat maintained at 34·5° C. An audiofrequency oscillator was used to supply 500 cycle A.C. current. The sol was diluted by mixing with conductivity water. 50 ml. of sol was taken and 50 ml. of conductivity water was added. This was termed 0·5 C. sol. Similarly 0·9 C., 0·8 C., etc., sols were prepared. The conductivity of the diluted sols was determined in two series. In one case, starting from the most concentrated sols, the conductivity was determined by proceeding to the diluted ones. In second case, the conductivity of the most dilute sol was first determined followed by the determination of the conductivity of the more concentrated sols. For every observation, several readings were taken which agreed fairly closely with one another. The specific conductivity of the conductivity water was also determined, but as it was very low ($1 \cdot 5 \times 10^{-6}$) in comparison with that of the sol, it was neglected. The specific conductivity of the sol is obtained after determining the resistance of N/10 KCl at 34·5° C. The value of the specific conductivity of N/10 KCl at 34·5° C. is obtained graphically by plotting the values of the conductivity of N/10 KCl at different temperatures (Jones and Bradshaw[6]). In Table II are given the relative concentrations of the sol and their resistances.

TABLE II

C	(Resistances)	Mean Resistance	R_c	$(1/R_c) \times 10^3$
1·0	(133·9, 133·8, 133·7)	133·8	133·8	7·475
0·9	(154·5, 154·5, 154·6)	154·5	139·0	7·194
0·8	(175·6, 175·7, 175·5)	175·6	140·5	7·119
0·7	(202·0, 202·0, 202·0)	202·0	141·4	7·073
0·6	(236·6, 236·7, 237·0)	236·7	142·0	7·042
0·5	(265·7, 265·6, 265·5)	265·6	132·8	7·532
0·4	(311·8, 311·6, 311·3)	311·5	124·6	8·026
0·3	(365·6, 365·6, 365·6)	365·6	109·7	9·110
0·2	(431·2, 430·8, 430·4)	430·8	86·2	11·600

DISCUSSION

The data in Table II show that when the iron oxide sol is diluted, the value of the product R_c (resistance × concentration) increases. The fourth column gives the value of $(1/R_c) \times 10^3$ which is therefore proportional to the specific conductivity of the sol. The value of R_c first increases with

dilution and then decreases *rapidly* with further dilution. This is shown graphically in Fig. 1.

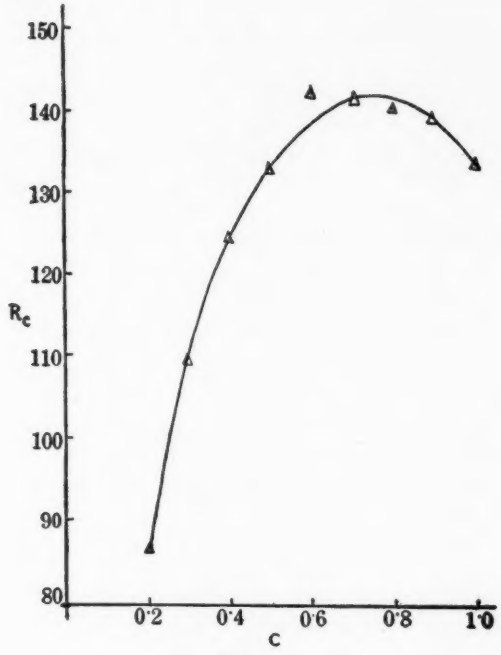

FIG. 1

The conductivity of the sol may be due to (*a*) free hydrochloric acid, (*b*) free ferric chloride, (*c*) fixed hydrochloric acid and (*d*) fixed ferric chloride. The qualitative test indicated that free ferric chloride was absent. Hence the specific conductivity of the sol minus the specific conductivity of the free hydrochloric acid may be taken as the conductivity of the iron oxide sol; *i.e.*, of the colloid with the absorbed gegenions. The specific conductivity of free hydrochloric acid was obtained by assuming the same temperature coefficient for hydrochloric acid as that for potassium chloride solution and obtaining the values of the specific conductivity of hydrochloric acid at 25° C. from the literature (Harned and Owen[7]).

The composition of the micelles can be calculated as follows:—From the total chloride content (m.e./l) the concentration of the hydrogen-ion, both fixed and free, is deducted. The concentration of fixed ferric ions is then equal to the residual chloride divided by three. It is obvious that in the case of dialysed sols, the stabilizing ions consist mostly of ferric ions.

The equivalent conductivity of the micelles is obtained on dividing the specific conductivity of the micelles by its concentration in terms of equivalents per litre. In Table III are given the concentration of chloride in m.e./1, the specific conductivity and the equivalent conductivity of the micelles.

TABLE III

Concentration of the sol	Concentration of Cl in the micelles (m.e./1)	Specific conductivity of the micelles ($\cdots \times 10^4$)	Equivalent conductivity of the micelles
1·0	96·0	9·982	10·40
0·9	86·4	8·440	9·691
0·8	76·8	7·367	9·592
0·7	67·2	6·373	9·482
0·6	57·6	5·420	9·410
0·5	48·0	5·041	10·510
0·4	38·4	4·452	11·630
0·3	28·8	4·039	14·030
0·2	19·2	3·754	19·550

It is obvious that the conductivity of the micelles is only a fraction of the conductivity of the stabilizing ions, if dissolved in pure water. Even if it is assumed that the stabilizing electrolyte is wholly ferric chloride, its equivalent conductivity at the dilution and the temperature used in the experiments will be at least 90 to 100.* Thus the conductivity of the micelles is only of the order of 10%, *i.e.*, the bulk of the stabilizing ions is fixed, because they adhere to the micelles and hence their individuality with respect to charge, osmotic pressure, etc., is considerably reduced. This conclusion is in harmony with the results of McBain and Thomas,[8] who determined the transference numbers of ferric ions and chloride ions in ferric hydroxide sol. They conclude that 89·5 per cent. of the chloride counterions travel towards the cathode. Similar conclusions are reached by Bjerrum[9] in the case of colloidal chromium hydroxide sol; Ghosh[10] in the case of stannic oxide and Bolam and Trivedi[1] in the case of sulphur sols. In Fig. 2 is given the graph of the equivalent conductivity against the square root of the concentration of the bound chloride. The nature of the graph resembles very closely to the nature of the curve obtained in the case of soap

* According to *International Critical Tables* [p. 233, Vol. VI (1929) McGraw Hill Books] the equivalent conductivity of ferric chloride is 66·5 at 18° C. when the concentration in, *milliformulaweight* is 500. The equivalent conductivity at 34·5° C. for the concentration used in the experiments will be considerably higher.

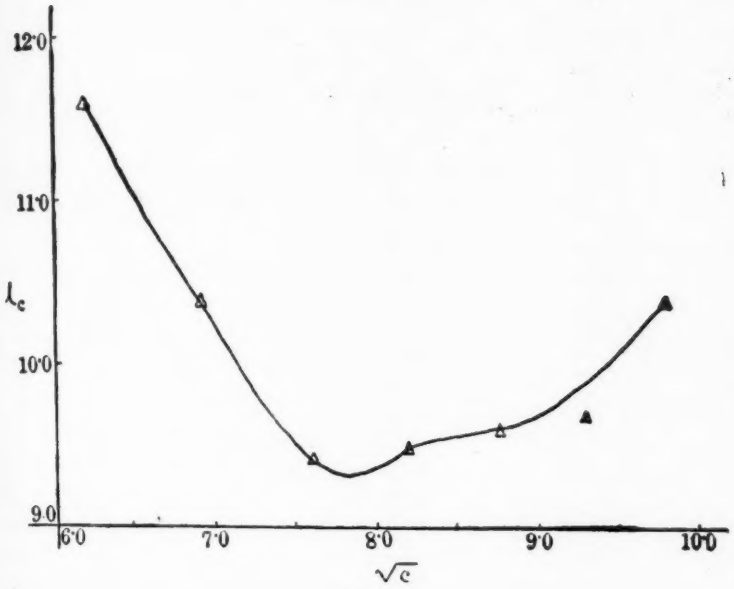

FIG. 2

solutions (McBain and Coworkers[2]). On dilution the equivalent conductivity first decreases and then increases *rapidly* (W. Kopczewski[11]). The curve thus passes through a minimum. It may be remarked that in the case of sulphur sols (Bolam and Trivedi[1]), the rapid increase in conductivity on further dilution was not obtained, as the electrodes adsorbed sulphur in some form or the other, making the measurement of the conductivity of the dilute sol difficult. The behaviour of iron oxide sol, like that of sulphur sol, may therefore be considered to give qualitative support to Hartley's theory.[3]

SUMMARY

Concentrated iron oxide sol of Graham type has been prepared and subjected to hot intermittent dialysis for a period of one month. The composition of the sol as well as the variation of the conductivity with dilution were determined. It has been found that the bulk of the stabilizing ions adhere to the micelles and the variation of the conductivity with dilution shows that the iron oxide sol behaves as a typical colloidal electrolyte.

ACKNOWLEDGEMENT

Our thanks are due to the Ahmedabad Education Society for generous grant towards chemicals and apparatus.

REFERENCES

1. Bolam and Trivedi .. *Trans. Far. Soc.*, 1943, **39**, 247.
2. McBain and Coworkers .. *J.C.S.*, 1919, **115**, 1279.
3. Hartley .. *Aqueous Solutions of Paraffin-Chain Salts*, 1936, p. 32; *Trans. Far. Soc.*, 1938, **34**, 1284; *Kolloid-Z.*, 1939, **88**, 22.
4. Graham .. *Phil. Trans.*, 1861, **151**, 208; *J.C.S.*, 1862, **15**, 249.
5. A. Findlay .. *Practical Physical Chemistry*, 1943, p. 161, Longmans, Green & Co. (*vide* Jones and Bollinger, *J.A.C.S.*, 1935, **57**, 280).
6. Jones and Bradshaw .. *J.A.C.S.*, 1933, **55**, 1780.
7. Harned and Owen .. *Physical Chemistry of Electrolytic Solutions*, 1943, p. 537, Reynolds Books.
8. McBain and Thomas .. *J. Phy. Chem.*, 1936, **40**, 997.
9. Bjerrum .. *Zeitschr. Phy. Chem.*, 1924, **110**, 676.
10. Ghosh .. *J.C.S.*, 1929, 2290.
11. W. Kopczewski .. *Compt. Rend.*, 1924, **179**, 628.

STUDIES IN THE CHEMICAL BEHAVIOUR OF SOME COMPOUNDS OF SULPHUR

Part III. Formation of Disulphur Monoxide by the Reaction Between Hydrogen Sulphide and Sulphur Dioxide

By A. R. Vasudeva Murthy

(Indian Institute of Science, Bangalore)

Received August 12, 1952

(Communicated by Dr. B. Sanjiva Rao, F.A.SC.)

While studying the kinetics of the reaction between hydrogen sulphide and sulphur dioxide, it was found that certain metallic sulphides, in presence of moisture, would function as efficient catalysts for the reaction.[1] The mechanism of the reaction could be explained on the basis that thiosulphurous acid ($H_2S_2O_2$) was the primary product of the union. Thiosulphurous acid however, is exceedingly unstable. Attempts to prepare the acid have not so far been successful. The lower oxides of sulphur are, in general, more stable than their corresponding oxyacids. Disulphur monoxide, the anhydride of thiosulphurous acid, can therefore be expected to be more stable than the acid and it may be practicable to isolate it as a product of the reaction between hydrogen sulphide and sulphur dioxide.

The reaction between the two compounds in non-aqueous media has been investigated by a number of workers.[2–5] In their attempt to prepare suspensions of sulphur in organic solvents, Garard and Colt[6] passed sulphur dioxide and hydrogen sulphide in the form of moist gases into solvents such as benzene and toluene and obtained yellow solutions which appeared to be quite stable. Bary[7] observed that when solutions of sulphur dioxide and hydrogen sulphide in toluene were mixed together, a clear yellow liquid was obtained, which became turbid on keeping and finally deposited sulphur.

Goehring and Wiebusch[8] studied recently the reaction between hydrogen sulphide and sulphur dioxide in inert organic solvents, in the presence of moisture. They claimed that the yellow solutions formed by the reaction contained "polysulphur oxides". The yellow solutions were similar to those obtained by B. S. Rao,[9] by dissolving in carbon tetrachloride the products of combustion of sulphur, in oxygen under reduced pressure. Goehring and Wiebusch investigated the yellow solution employing as the analytical reagent, a solution of potassium iodide in anhydrous formic acid.

It has been shown by the present author in a previous paper[10] that a solution of potassium iodide in formic acid, as used by Goehring and Wiebusch, and by Stamm and Wiebusch,[11] is not a suitable reagent for the study of the lower oxides of sulphur. The appropriate technique to be employed in such investigations, as developed in this laboratory, has therefore been used in the present investigation on the yellow solutions formed by the union of hydrogen sulphide and sulphur dioxide in moist carbon tetrachloride.

EXPERIMENTAL

Preparation of the yellow solution.—In obtaining the yellow solution by the method of Goehring and Wiebusch,[8] a saturated solution of water in carbon tetrachloride was diluted with the solvent, to give 120 g. of solution containing about 5 mg. of water. This was cooled to $-16°$ C. and sulphur dioxide was passed to saturation. Three litres of a mixture of dried sulphur dioxide and hydrogen sulphide (ratio of SO_2 to $H_2S = 2:1$) was then bubbled into the solution for about 30 minutes. The yellow solution obtained was dried over phosphorus pentoxide and filtered, and the residual reactants in the filtrate were pumped off, their complete removal being confirmed by appropriate tests.

Decomposition of the yellow solution by mercury.—An aliquot of the yellow solution was treated with mercury in an all-glass apparatus and the sulphur dioxide and mercury sulphide formed were estimated by methods indicated in an earlier paper.[10] The results are presented in the following table.

TABLE I. *Decomposition of the Yellow Solution by Mercury*

1 Expt. No.	2 *a* SO_2* liberated	3 *b* HgS formed	4 *b*/*a* S : SO_2	5 % S_2O	6 % Elemental sulphur
1	6·85	24·10	3·52	88·5	11·5
2	9·45	32·60	3·45	89·9	10·1
3	13·00	45·98	3·54	88·2	11·8
4	24·20	82·75	3·42	90·4	9·5
5	27·65	97·12	3·51	88·7	11·4
6	23·15	79·90	3·45	89·8	11·2
		Average	3·48	89·2	10·9

* Quantities of sulphur and its compounds have been expressed in terms of g. atom of $S \times 10^6$ per g. of solution.

It will be noticed that the average ratio of elemental sulphur to sulphur dioxide (Column 4) is 3·48. For pure disulphur monoxide (*cf.* Part II, present series) the ratio is 3 : 0. It is, therefore, concluded that the sulphur compound present in the yellow solution is disulphur monoxide and that 10% of the sulphur content of the solution is in the elemental form. This is to be expected as the moisture present in carbon tetrachloride would promote the decomposition of the disulphur monoxide as also its union with hydrogen sulphide (*cf.* Goehring,[8] B. S. Rao and M. R. A. Rao[12]). For the production of disulphur monoxide by the reaction between hydrogen sulphide and sulphur dioxide the ratio of the two gases must be 1 : 1, in terms of the equation

$$SO_2 + H_2S \rightarrow H_2S_2O_2 \rightarrow H_2O + S_2O.$$

It is however found that sulphur dioxide should be in large excess (6 SO_2 : 1 H_2S) to obtain a satisfactory yield of disulphur monoxide. With a smaller proportion of sulphur dioxide there is decomposition of the yellow solution to sulphur and sulphur dioxide. Sulphur dioxide thus appears to have stabilising influence on disulphur monoxide. As already stated, disulphur monoxide reacts with hydrogen sulphide in presence of moisture. When sulphur dioxide however is also present in the system, part of the hydrogen sulphide will be diverted for the reaction with sulphur dioxide. Furthermore, the reaction between the two gases increases the concentration of disulphur monoxide. These two factors are probably responsible for the observed stabilising effect. It is of interest to note that barely 3% of the reactants used, combine to give disulphur monoxide.

Reaction between the yellow solution and hydrogen iodide.—An aliquot of the yellow solution was sucked into a bulb containing hydrogen iodide under reduced pressure. The iodine and hydrogen sulphide formed were estimated, as also the elemental sulphur in the carbon tetrachloride. The results are given in Table II.

It can be seen from the results presented in Table II that the hydrogen sulphide and the iodine liberated correspond to disulphur monoxide. The results confirm the conclusions arrived at, from the data given in Table I.

Reaction of the yellow solution with alkali.—The reaction of the yellow solution with alkali was studied using the technique of Rao.[9] The experimental results (Table III) gave further confirmatory evidence of the presence of disulphur monoxide. For purposes of comparison, action of alkali on

TABLE II. *Reaction between the Yellow Solution and Hydrogen Iodide*

1 Expt. No.	2 H_2S* obtained	3 Iodine (g. atom $\times 10^6$ per g.)	4 Ratio I: H_2S	5 S in CCl_4	6 % S_2O	7 % S
1	26·15	79·25	3·03	3·17	89·2	10·8
2	35·46	106·40	3·00	4·56	88·6	11·3
3	51·50	154·20	2·99	6·81	88·3	11·6
4	93·20	280·20	3·01	11·45	89·0	10·9
5	91·12	272·80	2·99	16·98	84·3	15·7
6	49·23	150·20	3·05	6·76	87·9	12·0
		Average	3·01		87·9	12·0

* Quantities of sulphur and its compounds are expressed in terms of g. atom of S $\times 10^6$ per g. of solution.

TABLE III. *Reaction of Yellow Solution with 2 N Alkali*

Reaction between SO_2 and alkali	1	2	3	4
Sulphide	4·20	8·32	11·46	6·78
Sulphite	4·57	9·96	13·52	7·86
Thiosulphate	8·96	15·63	21·56	13·58
Elemental sulphur	17·70	33·06	46·54	31·98
% Hydrolysis (H)	26·4	30·7	30·0	29·0
% Thionisation (T)	18·7	19·2	18·8	19·4
% Decomposition (D)	54·8	50·1	51·2	51·6
% Total S accounted for	99·9	100·0	100·0	100·0
S_2O (as calcd. from reaction with alkali)	31·80	54·25	76·30	46·74
S_2O* taken (as detd. by HI reaction)	30·83	52·32	75·82	46·29

* Quantities of sulphur and its compounds are expressed in terms of g. atoms of S $\times 10^6$ per g. of solution.

the disulphur monoxide solution obtained by combustion of sulphur was also studied (Table IV).

TABLE IV. *Reaction of Disulphur Monoxide Solution with 2 N Alkali Containing Cadmium Hydroxide*

Reaction between alkali and disulphur monoxide	1	2	3	4
S_2O* taken (as detd. by HI reaction)	95·50	53·25	30·15	84·05
Sulphide	14·52	7·39	4·86	12·44
Sulphite	17 08	9·65	5·26	14·50
Thiosulphate	27·96	14·61	9·36	25·50
Elemental sulphur	35·64	21·38	10·55	31·52
Total sulphur	95·20	53·03	30·03	83·96
% Hydrolysis (H)	30·5	27·9	32·4	29·7
% Thionisation (T)	19·5	18·4	20·8	20·0
% Decomposition (D)	49·9	53·8	46·9	50·4
Total	99·9	100·1	100·1	100·1

* Quantities of sulphur and its compounds are expressed in terms of g. atoms of S $\times 10^6$ per g. of solution.

As already indicated (Part I, present series[13]), a solution of disulphur monoxide in carbon tetrachloride when treated with alkali, produces sulphide, sulphite, thiosulphate and sulphur, as a result of three simultaneous reactions: Hydrolysis (H), Thionisation (T), and Decomposition (D). The extent of each reaction as calculated from the analytical results (*cf.* B. S. Rao[9]) has been given in Tables III and IV.

At concentration of the same magnitude, solutions of disulphur monoxide obtained by the two methods undergo 30% hydrolysis, 20% thionisation and 50% decomposition. Values for disulphur monoxide in the solutions as determined by treatment with alkali agree with those obtained by the hydrogen iodide method of analysis.

The effect of dilution and of certain catalysts, on the reaction between alkali and the disulphur monoxide solutions obtained by both the methods was studied. The observations made by B. S. Rao[9] were confirmed.

The reaction between disulphur monoxide and water or buffer solutions of low alkalinity was found to be very complicated. The products formed were sulphur, sulphite, thiosulphate and polythionates (tri, tetra and pentathionates). No sulphide was obtained.

Disulphur monoxide solutions were obtained in a number of organic solvents employing the combustion method as well as the sulphur dioxide hydrogen sulphide reaction. The solvents employed were chloroform, chlorobenzene, cyclohexane, toluene, xylene and decalin. The disulphur monoxide content of each solution was determined by the reaction with alkali as also by the hydrogen iodide method. In all these solvents the behaviour of the disulphur monoxide was the same as in carbon tetrachloride solution. In polar solvents like ethylene glycol, cyclohexanol and dioxane there was considerable decomposition of disulphur monoxide and stable solutions could not be obtained.

Spectrophotometric study of the decomposition of the disulphur monoxide solutions.—It was found both by B. S. Rao[9] and by Goehring and Wiebusch[8] that solutions of disulphur monoxide in carbon tetrachloride or chloroform, when freshly prepared, gave a characteristic absorption spectrum, there being absorption of light from the ultra-violet end upto a wavelength of 4700 Å. Absorption spectra of the two types of solutions of disulphur monoxide obtained by the present author were studied employing the Coleman Universal Spectrophotometer. The solutions obeyed Beer's Law and the absorption spectra were identical (Fig. 1). Concentration of solution 1 was $28{\cdot}5\times10^{6}$ and of solution 2, $13{\cdot}6\times10^{6}$ g. atoms of sulphur per g. of solution.

The rate of decomposition at 25° C. of disulphur monoxide in the two solutions was also studied. The results are expressed graphically in Fig. 2.

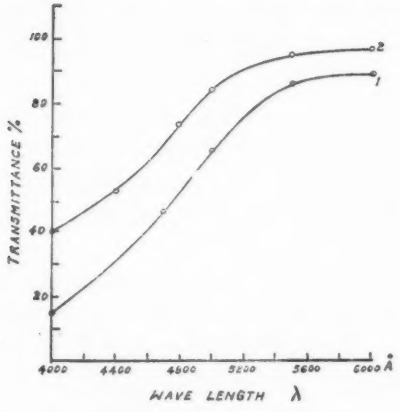

FIG. 1

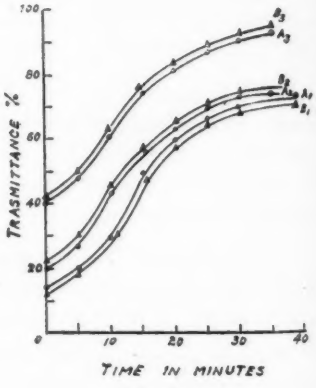

FIG. 2

FIG. 1 Absorption spectra of S_2O solutions in carbon tetrachloride.
FIG. 2 Rate of decomposition of S_2O solutions in carbon tetrachloride.

The disulphur monoxide decomposed at the same rate in the two solutions. The transmittance measurements were for the wavelength 4000 Å. Concentrations of disulphur monoxide in the solutions employed were 28·5, 23·4 and $13·6 \times 10^6$ g. atoms of sulphur per g. of solutions A_1, A_2 and A_3 respectively. All these solutions were obtained from oxide produced by the combustion method. In solutions B_1, B_2 and B_3 of the oxide formed by the hydrogen sulphide-sulphur dioxide reaction, the disulphur monoxide concentrations were 30·2, 22·2 and $12·8 \times 10^6$ g. atoms of sulphur per g. of solution.

Summary

1. Hydrogen sulphide and sulphur dioxide react in carbon tetrachloride (kept at − 16° C.), in presence of moisture, to give a yellow solution which contains disulphur monoxide—the anhydride of the hypothetical thiosulphurous acid. For the formation of the oxide, sulphur dioxide has to be in large excess.

2. The chemical behaviour of disulphur monoxide in the yellow solution was identical with that of the oxide obtained by the combustion of sulphur, under oxygen at low pressure.

3. A spectrophotometric study showed identical behaviour of disulphur monoxide in the two solutions.

Acknowledgment

The author wishes to acknowledge his grateful thanks to Dr. B. Sanjiva Rao for his keen interest in the work and for his valuable criticism. He is also thankful to Dr. M. R. A. Rao for his helpful suggestions. His sincere thanks are also due to Prof. K. R. Krishnaswami for kind encouragement,

References

1. A. R. Vasudeva Murthy and B. Sanjiva Rao .. *Proc. Ind. Acad. Sci.*, 1951, **34**, 283.
2. Klein .. *J. Phy. Chem.*, 1910, **15**, 1.
3. Matthews .. *J. Chem. Soc.*, 1926, 2270.
4. Sarason .. *German Patent*, 1912, 262467 (cited from *C. A.*, 1913, **7**, 3532).
5. B. Sanjiva Rao and M. R. A. Rao *Nature*, 1931, **128**, 413.
6. Garard and Colt .. *J. Am. Chem. Soc.*, 1927, **49**, 630.
7. Bary .. *Rev. gén. Caoutchouc*, 1931, **8**, 71, 25 (cited from *C. A.*, 1931, **25**, 5796).
8. Goehring and Wiebusch .. *Z. anorg. Chem.*, 1948, **257**, 227.
9. B. Sanjiva Rao .. *Proc. Ind. Acad. Sci.*, 1939, **10**, 491.
10. A. R. Vasudeva Murthy .. *Ibid.*, 1952, **36**.
11. Stamm and Wiebusch .. *Naturwissenschaften*, 1944, **32**, 42.
12. B. Sanjiva Rao and M. R. A. Rao *Curr. Sci.*, 1943, **12**, 323.
13. A. R. Vasudeva Murthy .. *Proc. Ind. Acad. Sci.*, 1952, **36**, 388.

MAGNETIC STUDY OF DOUBLE SALTS IN SOLUTION

By Mata Prasad, F.A.Sc., D. D. Khanolkar and M. G. Datar
(*Chemical Laboratories, Institute of Science, Bombay*)

Received January 21, 1952

When two salts, each primarily formed by the union of a base and an acid, are dissolved in water and the solution evaporated, it sometimes happens that they combine in a definite molecular proportion to form a compound of greater complexity which is called a molecular compound or a double salt. On solution a double salt yields the same ions as the single salts from which it is derived, but the physical properties of the salt are not necessarily additive. Various physical properties, such as solubility, viscosity, rates of diffusion of the constituents, volume change and others of the binary mixtures of the component salts have been used to investigate the formation of double salts in solution. Schonrock[1] has reported that the rotation of the polarised light is additive for solutions of mixtures of salts which do not form double salts while there is a marked deviation from additivity for the mixtures known to form double salts. The measurements of the heats of solutions of the mixture of the constituents of double salts led Graham,[2] and Berthelot[3] to establish the existence of double salts in solution. The temperature-concentration curves of a number of binary mixtures of salts having the same anion but different cations show that more than one double salt is formed in solution. Thus, ammonium chloride unites with the chlorides of magnesium, zinc, cadmium and mercury to form as many as three salts with each one of them. In some cases these salts have been isolated in the solid state while in others their presence has been inferred from the phase rule study of the systems.

Recently Nair and Pande[4] have carried out measurements of pH, viscosity, transport number and magnetic susceptibility of $Pb(NO_3)_2$—KNO_3—H_2O and $Pb(NO_3)_2$—NH_4NO_3—H_2O systems. They have reported the formation of three different double salts in each system. In the present communication the authors have investigated some ternary systems by the magnetic method with the idea of examining the formation of double salts in these systems.

Experimental

All the substances used for studying the ternary systems were of Merck's pure quality. They were crystallised twice from distilled water before use

and their purity was ascertained by estimating the amount of cation in them. The following five systems were chosen for investigation: (i) NH_4NO_3—$Pb(NO_3)_2$—H_2O, (ii) NH_4NO_3—$AgNO_3$—H_2O, (iii) NH_4Cl—$ZnCl_2$—H_2O, and (iv) NH_4Cl—$CdCl_2$—H_2O. The procedure followed for preparing these systems was as follows: Stock solutions of one molar concentration of the components of the systems were prepared by the standard method. In the case of the first two systems 20 c.c. of the stock solution of NH_4NO_3 were pipetted out into a standard flask of 50 c.c. capacity, the requisite amount of the other component was added by means of a standard burette and the whole mixture was made upto 50 c.c. with distilled water. 20 such mixtures were prepared in which the amount of the other component varied from 0 c.c. to 30 c.c. In the last three systems varying amounts of the second component were added to 20 c.c. of NH_4Cl solution.

Magnetic susceptibilities of the mixtures were measured on a modified form of Gouy's balance by the method described by Prasad, Dharmatti and Gokhale.[5] The values of the specific susceptibilities (χa) of the several mixtures are given in columns 2 and 5 of Tables I–IV. In columns 3 and 6 of the same tables are given the changes in the values of specific susceptibilities of the mixtures per addition of 1 c.c. of the second component and are denoted by $\Delta\chi a$. The susceptibility values are expressed in terms of -1×10^{-6} c.g.s. units. The experimental error was found to be within $\pm$ 1%.

TABLE I

NH_4NO_3—$Pb(NO_3)_2$—H_2O

c.c. of $Pb(NO_3)_2$ solution	χa	$\Delta\chi a$	c.c. of $Pb(NO_3)_2$ solution	χa	$\Delta\chi a$
0	0·7018	..	12	0·6610	0·0025
1	0·6987	0·0031	14	0·6560	0·0025
2	0·6954	0·0033	16	0·6506	0·0027
3	0·6918	0·0036	18	0·6440	0·0033
4	0·6878	0·0040	20	0·6366	0·0037
5	0·6832	0·0046	22	0·6326	0·0020
6	0·6801	0·0031	24	0·6287	0·0020
7	0·6771	0·0030	26	0·6251	0·0018
8	0·6739	0·0032	28	0·6214	0·0019
9	0·6702	0·0037	30	0·6176	0·0019
10	0·6660	0·0042			

TABLE II

$NH_4NO_3—AgNO_3—H_2O$

c.c. of $AgNO_3$ solution	χa	$\Delta\chi a$	c.c. of $AgNO_3$ solution	χa	$\Delta\chi a$
0	0·7018	..	12	0·6767	0·0015
1	0·7003	0·0015	14	0·6736	0·0016
2	0·6987	0·0016	16	0·6702	0·0017
3	0·6969	0·0018	18	0·6664	0·0019
4	0·6950	0·0019	20	0·6619	0·0023
5	0·6929	0·0021	22	0·6587	0·0016
6	0·6906	0·0023	24	0·6554	0·0017
7	0·6881	0·0025	26	0·6521	0·0017
8	0·6855	0·0026	28	0·6487	0·0017
9	0·6827	0·0028	30	0·6456	0·0015
10	0·6797	0·0030			

TABLE III

$NH_4Cl—ZnCl_2—H_2O$

c.c. of $ZnCl_2$ solution	χa	$\Delta\chi a$	c.c. of $ZnCl_2$ solution	χa	$\Delta\chi a$
0	0·7089	..	12	0·6857	0·0016
1	0·7079	0·0010	14	0·6825	0·0016
2	0·7066	0·0013	16	0·6789	0·0018
3	0·7049	0·0017	18	0·6747	0·0021
4	0·7027	0·0022	20	0·6693	0·0027
5	0·6998	0·0029	22	0·6661	0·0016
6	0·6976	0·0022	24	0·6629	0·0016
7	0·6953	0·0023	26	0·6599	0·0015
8	0·6933	0·0020	28	0·6570	0·0015
9	0·6912	0·0021	30	0·6542	0·0014
10	0·6888	0·0024			

TABLE IV

$NH_4Cl—CdCl_2: 2H_2O—H_2O$

c.c. of $CdCl_2$ solution	χa	$\Delta\chi a$	c.c. of $CdCl_2$ solution	χa	$\Delta\chi a$
0	0·7089	..	12	0·6922	0·0015
1	0·7076	0·0013	14	0·6885	0·0019
2	0·7061	0·0015	16	0·6842	0·0022
3	0·7044	0·0017	18	0·6792	0·0025
4	0·7026	0·0018	20	0·6736	0·0028
5	0·7005	0·0021	22	0·6694	0·0021
6	0·6996	0·0009	24	0·6654	0·0020
7	0·6986	0·0010	26	0·6614	0·0020
8	0·6976	0·0010	28	0·6573	0·0021
9	0·6965	0·0011	30	0·6533	0·0020
10	0·6952	0·0013			

Values of the specific susceptibilities (χa) of mixtures of different concentrations for each system were plotted against the volume of the second component added to 20 c.c. of the ammonium salt and the curves obtained are shown in full lines in Figs. 1–4. It will be seen that these curves are non-linear and show breaks at some points. In order to bring out the breaks in the curves more clearly, the changes in the susceptibility value per addition of 1 c.c. of the second component ($\Delta\chi a$) were plotted against the number of c.c. of the second component added to the fixed quantity of the ammonium salt and the curves obtained are shown in Figs. 1–4 in dotted lines.

DISCUSSION OF RESULTS

(*a*) *NH_4NO_3—Pb $(NO_3)_2$—H_2O.*—The curves (Fig. 1) obtained for this system show breaks at three points, corresponding to the addition of 5 c.c., 10 c.c. and 20 c.c. of Pb $(NO_3)_2$ solution. These breaks indicate the formation of 4 $NH_4NO_3 \cdot Pb(NO_3)_2$, 2 $NH_4NO_3 \cdot Pb(NO_3)_2$ and $NH_4NO_3 \cdot Pb(NO_3)_2$, in solution. These observations are in agreement with those of Nair and Pande.[4] None of these compounds has been isolated so far. Bogitch[6] dissolved lead nitrate in molten ammonium nitrate but did not get any evidence for the formation of the double salt with mixtures containing up to 55% lead nitrate.

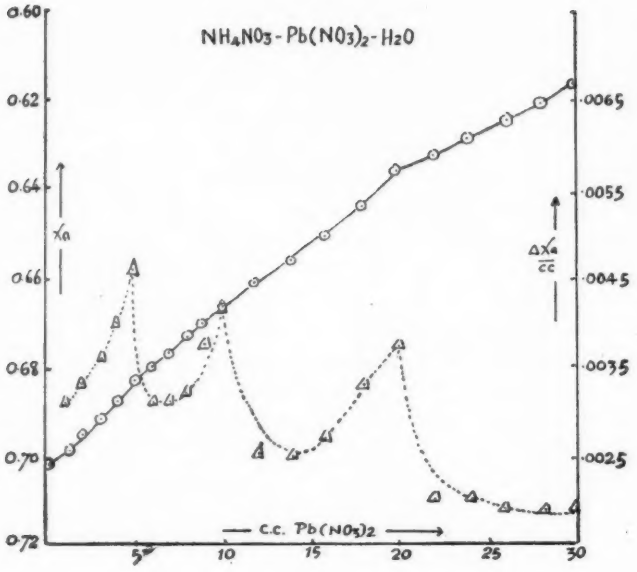
NH4NO3 - Pb(NO3)2 - H2O
0·60
0·62
0·64
0·66
0·68
0·70
0·72
Xa
ΔXa/cc
·0065
·0055
·0045
·0035
·0025
c.c. Pb(NO3)2
5
10
15
20
25
30

FIG. 1

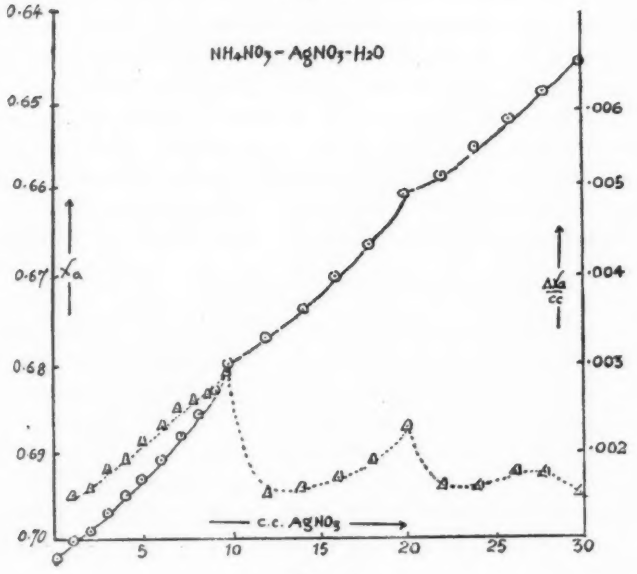
NH4NO3 - AgNO3 - H2O
0·64
0·65
0·66
0·67
0·68
0·69
0·70
Xa
ΔXa/cc
·006
·005
·004
·003
·002
c.c. AgNO3
5
10
15
20
25
30

FIG. 2

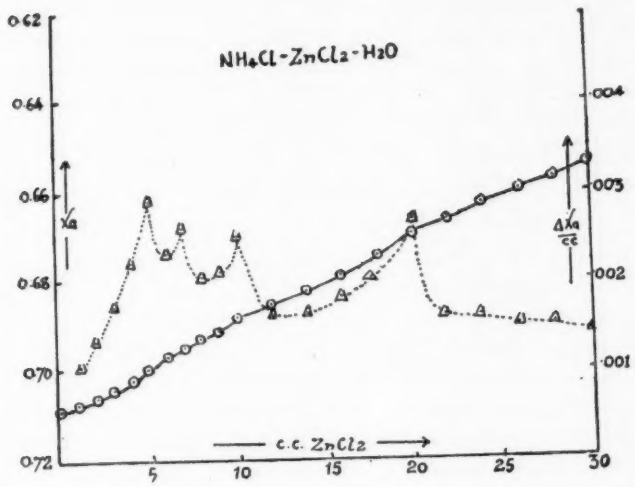
NH4Cl-ZnCl2-H2O
χa
Δχa/cc
c.c. ZnCl2
0·62
0·64
0·66
0·68
0·70
0·72
·004
·003
·002
·001
5
10
15
20
25
30

FIG. 3

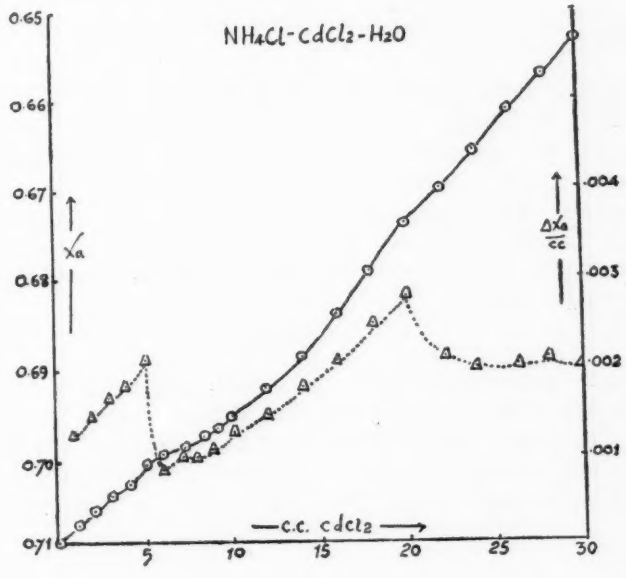
NH4Cl-CdCl2-H2O
χa
Δχa/cc
c.c. cdcl2
0·65
0·66
0·67
0·68
0·69
0·70
0·71
·004
·003
·002
·001
5
10
15
20
25
30

FIG. 4

(*b*) *NH_4NO_3.$AgNO_3$—H_2O.*—The curves (Fig. 2) obtained for this system show definite breaks at the points corresponding to the addition of 10 c.c. and 20 c.c. of $AgNO_3$ solution, indicating the formation of $2\,NH_4NO_3.AgNO_3$ and $NH_4NO_3.AgNO_3$. The existence of $NH_4NO_3.AgNO_3$ has been confirmed by Zawadsky and Flavitzky[7] and Russell and Maskelyne[8] from freezing point curves of the mixtures of NH_4NO_3 and $AgNO_3$. The existence of $2\,NH_4NO_3.AgNO_3$ has not been reported so far.

(*c*) *NH_4Cl—$ZnCl_2$—H_2O.*—The breaks observed in the curves (Fig. 3) for this system occur for the addition of 5 c.c., 6·67 c.c., 10 c.c. and 20 c.c. of $ZnCl_2$ solution, indicating that as many as four compounds, namely, $4\,NH_4Cl.ZnCl_2$, $3\,NH_4Cl.ZnCl_2$, $2\,NH_4Cl.ZnCl_2$ and $NH_4Cl.ZnCl_2$, exist in solution. Grunauer[9] measured the melting points of nine different mixtures of $ZnCl_2$ and NH_4Cl and obtained a V-shaped curve with eutectics at three different points corresponding to three different double salts. From the study of freezing, melting and boiling points of the binary mixtures of NH_4Cl and $ZnCl_2$, Hachmeister[10] has shown that NH_4Cl and $ZnCl_2$ combine in the ratio 4: 1, 3: 1, 2: 1 and 1: 2. Though Hachmeister has not reported the existence of the salt $NH_4Cl.ZnCl_2$, Mellor[11] states that it is obtained by the fractional crystallisation of a solution containing equimolecular parts of $ZnCl_2$ and NH_4Cl. Marignac[12] has reported the isolation of $2\,NH_4ClZn.Cl_2$ and $3\,NH_4Cl.ZnCl_2$.

(*d*) *NH_4Cl—$CdCl_2$—H_2O.*—The formation of $4\,NH_4Cl.CdCl_2$ and $NH_4Cl.CdCl_2$ in solution is indicated by the breaks in the curves (Fig. 4) occurring for the addition of 5 c.c. and 20 c.c. of $CdCl_2$ solution. These observations support the results obtained by Hachmeister[10] from the study of the freezing, boiling and melting points of the binary mixtures of these two salts. Croft,[13] Crossman[14] and Rimbach[15] have reported the isolation of $CdCl_2.NH_4Cl$. Von Hauver[16] has prepared the compound $CdCl_2.4NH_4Cl$, as a crystalline solid.

SUMMARY

Magnetic susceptibilities of ternary systems consisting of (i) ammonium nitrate and the nitrates of lead and silver and (ii) of ammonium chloride and the chlorides of zinc and cadmium have been measured in solution on a modified form of Gouy's balance. The results obtained have been utilised to reveal the formation of double salts in solution in each system.

References

1. Schonrock .. *Zeit. Phys. Chem.*, 1893, **11**, 753.
2. Graham .. *Phil. Mag.*, 1844, (3) **24**, 401.
3. Berthelot .. *Ann. Chem. Phys.*, 1883, (5) **29**, 202.
4. Nair and Pande .. *Proc. Ind. Acad. Sci.*, 1949, **30**, 251.
5. Prasad, Dharmatti and Gokhale *Ibid.*, 1944, **20**, 224.
6. Bogitch .. *Compt. Rend.*, 1915, **161**, 790.
7. Zawadsky and Flavitzky .. *Zeit. Phys. Chem.*, 1904, **47**, 721 ;
   .. *J. Russian Chem. Soc.*, 1909, **41**, 739.
8. Russell and Maskelyne .. *Proc. Roy. Soc*, (*Lond.*), 1877, **41**, 739.
9. Grunauer .. *Zeit. Anorg. Chem.*, 1904, **39**, 409.
10. Hachmeister .. *Ibid.*, 1919, **109**, 145.
11. Mellor .. *A Comprehensive Treatise on Theoretical and Inorganic Chemistry*, **4**, 551.
12. Marignac .. *Ann. Mines*, 1857, (5) **12**, 1.
13. Croft .. *Phil. Mag.*, 1842, (3) **21**, 356.
14. Crossman .. *Zeit. Anorg. Chem.*, 1902, **33**, 149 ; 1905, **38**, 1569.
15. Rimbach .. *Ber.*, 1897, **30**, 3075 ; 1902, **35**, 1298; 1905, **38**, 156°.
16. Von Hauver .. *Sitzbar Akad. Wein.*, 1854, **13**, 449.

SYNTHETICAL EXPERIMENTS IN THE CHROMONE GROUP

Part XXVI. Synthesis of 5: 7: 2′-Trihydroxyisoflavone, 5: 7: 2′-Trihydroxy-8-methylisoflavone and 5-Hydroxyisoflavone

By S. S. Karmarkar, K. H. Shah and K. Venkataraman, F.A.Sc.
(*From the Department of Chemical Technology, University of Bombay*)

Received December 2, 1952

Nineteen natural colouring matters have been assigned isoflavone structures, and six of these have been isolated from soya bean. Walz showed that two constituents of soya bean meal were glucosides of genistein (5: 7: 4′-trihydroxyisoflavone) and daidzein (7: 4′-dihydroxyisoflavone).[1] Okano and Beppu have described four isoflavones (isogenistin, methylisogenistin, methylgenistein and tatoin), three flavones, and a "red colouring matter like resene" as constituents of soya bean.[2] Isogenistin and methylisogenistin were glucosides yielding the aglucones isogenistein and methylisogenistein, the constitution of which is discussed in the present paper. Methylgenistein was regarded as 5: 7: 4′-trihydroxy-8-methylisoflavone, since alkaline hydrolysis gave methylphloroglucinol, formic acid and *p*-hydroxyphenylacetic acid, and this structure has been supported by Shriner and Hull,[3] who found that the product of the condensation of ethyl formate with 2: 6-dihydroxy-4-methoxy-*m*-tolyl 4-methoxybenzyl ketone in presence of sodium, followed by demethylation with hydriodic acid, resembled the methylgenistein of Okano and Beppu. However, no direct comparison of the synthetic and natural substances was made and, in view of the difficulties[4] of applying the Joshi-Venkataraman modification[5] of Späth and Lederer's isoflavone synthesis to *o*-hydroxyphenyl benzyl ketones carrying further unprotected hydroxyl groups, we have undertaken a new synthesis of 5: 7: 4′-trihydroxy-8-methylisoflavone.

The structures assigned by Okano and Beppu to isogenistein as 5: 7: 2′-trihydroxyisoflavone (I) and to methylisogenistein as the 8-methyl derivative (II) were based on the results of alkaline fission; (I) gave phloroglucinol, formic acid and *o*-hydroxyphenylacetic acid, while (II) gave C-methylphloroglucinol and the same two acids. The isoflavones (I) and (II) have now been synthesized, and their properties do not correspond with those described for Okano and Beppu's isogenistein and methylisogenistein.

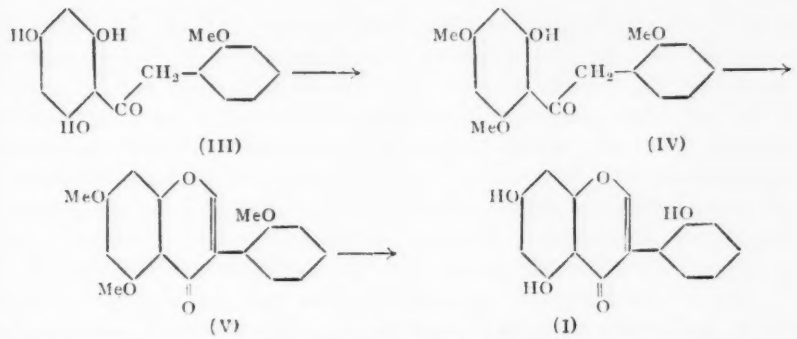

The ketone (III), m.p. 170°, prepared by a Hoesch reaction between phloroglucinol and *o*-methoxybenzyl cyanide, was dimethylated to (IV), m.p. 116°, by means of dimethyl sulphate and potassium carbonate in acetone. Condensation of (IV) with ethyl formate and sodium, following the procedure of Joshi and Venkataraman, gave 5:7:2′-trimethoxyisoflavone (V), m.p. 138°, which was finally demethylated to 5:7:2′-trihydroxyisoflavone (I), m.p. 187°, by the action of aluminium bromide in boiling benzene. The triacetyl derivative melted at 151°. The melting points cited by Okano and Beppu for isogenistein and its triacetate are 302° and 189° respectively. Baker, *et al.*,[6] have very recently reported the synthesis of (I) from (III) by their method involving cyclization to the corresponding 2-carbethoxyisoflavone by means of the chloride of monoethyl oxalate, hydrolysis and decarboxylation[7]; their results are in agreement with ours, proving that Okano and Beppu's isogenistein cannot possess the structure (I). Baker, *et al.*, have further stated that similar synthetic evidence has been obtained by Mr. S. Varadarajan in Professor T. R. Seshadri's laboratory (private communication).

5:7:2′-Trihydroxy-8-methylisoflavone (II) has been synthesized by the following route:—

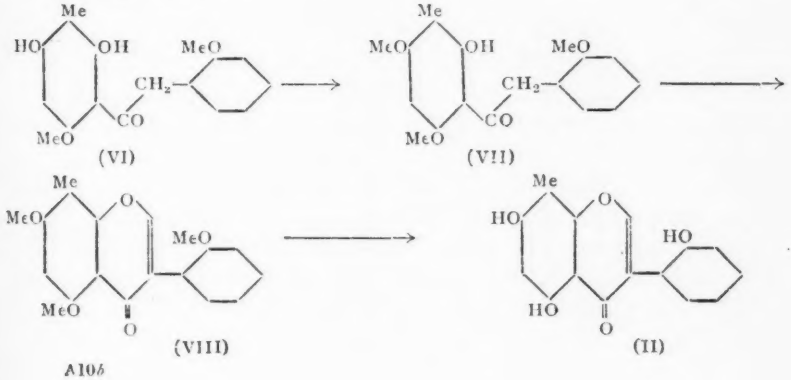

2:6-Dihydroxy-4-methoxy-*m*-tolyl 2-methoxybenzyl ketone (VI), m.p. 194°, was prepared from 2:6-dihydroxy-4-methoxytoluene[3] and *o*-methoxybenzyl cyanide by the Hoesch reaction. The ketone (VI) could not be converted to the isoflavone by the ethyl formate-sodium or ethyl orthoformate-pyridine reactions;[8] but the trimethyl ether (VII), m.p. 150°, in which the only unprotected hydroxyl was *ortho* to the carbonyl group, cyclized readily to the isoflavone (VIII), m.p. 183–84°, on treatment with ethyl formate and sodium; Okano and Beppu obtained from "methylisogenistein" a trimethyl ether melting at 152–53°. Aluminium bromide demethylation of (VIII) yielded (II), m.p. 234°, which gave a green colouration with alcoholic ferric chloride; Okano and Beppu's "methylisogenistein" melted at 301–02°, and the ferric colouration was violet-red. The triacetate of (II) melted at 105° (139° after dehydration), while the corresponding derivative prepared by Okano and Beppu melted at 188°.

Tatoin, m.p. 318°, one of the colouring matters isolated by Okano and Beppu from soya bean, was regarded by them to be probably constituted as 5:4′-dihydroxy-8-methylisoflavone; alkaline fission yielded 4-methylresorcinol, formic acid and *p*-hydroxyphenylacetic acid. The same products can result from 5:4′- and 7:4′-dihydroxy-6-methylisoflavone; and Bhandari, Bose and Siddiqui[9] synthesized the latter by the condensation of ethyl formate with 4:6-dihydroxy-*m*-tolyl *p*-methoxybenzyl ketone, followed by demethylation, and they found that the properties differed from those of tatoin. They also isolated from the fresh germs of soya beans a colouring matter which was apparently identical with tatoin. As a preliminary to the synthesis of 5:4′-dihydroxy-8-methylisoflavone we have now synthesized 5-hydroxyisoflavone (IX), m.p. 102°, by the action of ethyl orthoformate in pyridine-piperidine on 2:6-dihydroxyphenyl benzyl ketone (X), m.p. 170°. The ketone (X) was obtained by a Friedel-Crafts reaction

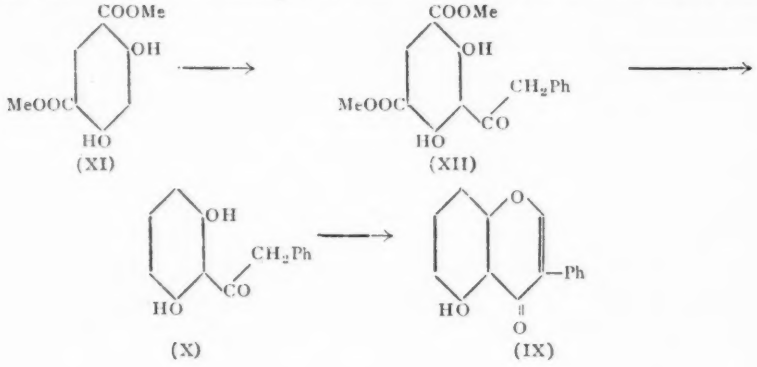

between 4: 6-dicarbomethoxyresorcinol (XI) and phenylacetyl chloride, followed by hydrolysis and decarboxylation of the ketonic ester (XII).

Experimental

2: 4: 6-*Trihydroxyphenyl* 2-*methoxybenzyl ketone* (*III*).—A slow stream of dry hydrogen chloride was passed for 5 hours through an ice-cooled solution of dry phloroglucinol (5 g.), *o*-methoxybenzyl cyanide (5 g.), fused zinc chloride (6 g.) and anhydrous ether (100 c.c.). The reaction mixture was kept in a refrigerator for 48 hours. The ether was decanted off and the solid ketimine hydrochloride was washed with ether, and treated with water (500 c.c.) under reflux for 2 hours; the ketone crystallised from water in pale yellow needles, m.p. 170° (Found: C, 65·4; H, 5·1. $C_{15}H_{14}O_5$ requires C, 65·7; H, 5·1%). An alcoholic solution of the substance gives a violet-brown colouration with ferric chloride.

2-*Hydroxy*-4: 6-*dimethoxyphenyl* 2-*methoxybenzyl ketone* (*IV*).—The ketone (III) (2 g.) was dissolved in dry acetone (50 c.c.) and treated with dimethyl sulphate (1·4 c.c.; 2 mols.) and freshly ignited potassium carbonate (6 g.). After refluxing for 14 hours, acetone was removed and water was added. The precipitate (1·9 g.) crystallized from alcohol in colourless needles, m.p. 116° (Found: C, 67·0; H, 5·8. $C_{17}H_{18}O_5$ requires C, 67·6; H, 5·9%). The alcoholic solution gives a deep red colour with ferric chloride.

5: 7: 2′-*Trimethoxyisoflavone* (*V*).—To a solution of the ketone (IV) (1 g.) in freshly distilled ethyl formate (20 c.c.), cooled to 0°, sodium dust (1·5 g.) was added. The mixture was left in the refrigerator for 22 hours, and then at room temperature for 2 hours, poured into ice and hydrochloric acid and allowed to stand. The solid that separated (1 g.) crystallized from water in colourless needles, m.p. 138° (Found: C, 69·0; H, 5·4. $C_{18}H_{16}O_5$ requires C, 69·2; H, 5·1%). Cyclization of the ketone (IV) to the isoflavone (V) was indicated by the insolubility of the substance in aqueous caustic soda and the absence of ferric chloride colouration. The yield of this substance (V) is low if the reaction is carried out at room temperature.

5: 7: 2′-*Trihydroxyisoflavone* (*I*).—The ether (V) (1 g.) in dry benzene (50 c.c.) was added to a solution of freshly distilled aluminium bromide (5·12 g.; 6 mols.) in benzene (50 c.c.), when immediate separation of a complex was noticed. The mixture was refluxed for 3 hours, poured over ice and hydrochloric acid, and extracted with ether. The ether layer was washed with water and then extracted with 1% caustic soda solution. On acidifying the alkaline extract a colourless precipitate was obtained (0·80 g.), which crystallized from dilute alcohol in colourless needles, m.p. 187° (Found: C, 66·3; H, 4·1. $C_{15}H_{10}O_5$ requires C, 66·7; H, 3·7%). With alcoholic

ferric chloride it gives a brownish violet colour. The *triacetyl* derivative separated from dilute acetic acid as colourless needles, m.p. 151° (Found: C, 64·0; H, 4·3. $C_{21}H_{16}O_8$ requires C, 63·6; H, 4·0%).

2: 6-*Dihydroxy*-4-*methoxy-m-tolyl* 2-*methoxybenzyl ketone* (*VI*).—The ketone (VI) was prepared in the same manner as (III) from 2: 6-dihydroxy-4-methoxytoluene (4 g.), *o*-methoxybenzyl cyanide (4 g.), fused zinc chloride (6 g.) and ether (150 c.c.). It crystallized from dilute alcohol in pale yellow needles (2·8 g.), m.p. 194° (Found: C, 67·5; H, 6·2. $C_{17}H_{18}O_5$ requires C, 67·6; H, 5·9%). The ferric reaction in alcohol is dark violet-brown.

2-*Hydroxy*-4: 6-*dimethoxy-m-tolyl* 2-*methoxybenzyl ketone* (*VII*).—The ketone (VI) (1·5 g.), dimethyl sulphate (0·5 c.c., 1 mol.) and anhydrous potassium carbonate (5 g.) and acetone (50 c.c.) were refluxed for 14 hours, and worked up as usual. The product crystallized from dilute alcohol in colourless needles (1·4 g.), m.p. 150° (Found: C, 68·2; H, 6·4. $C_{18}H_{20}O_5$ requires C, 68·4; H, 6·5%). An alcoholic solution of the substance gives a greenish brown colour with ferric chloride.

5: 7: 2′-*Trimethoxy*-8-*methylisoflavone* (*VIII*).—A solution of the ketone (VII) (2 g.) in freshly distilled ethyl formate (150 c.c.), cooled to 0°, was gradually added to sodium dust (3 g.). An immediate reaction ensued, which soon became vigorous; the mixture turned reddish brown in colour. After 4 hours, the reaction mixture was poured over ice and hydrochloric acid with stirring. Next day the separated solid (1·7 g.) was filtered and crystallized from dilute alcohol; the colourless needles had m.p. 183–84° (Found: C, 70·2; H, 5·7. $C_{19}H_{18}O_5$ requires C, 69·9; H, 5·5%). Cyclization of the ketone (VII) to the isoflavone (VIII) was indicated by the absence of ferric reaction and the insolubility in aqueous caustic soda.

5: 7: 2′-*Trihydroxy*-8-*methylisoflavone* (*II*).—The trimethyl ether (VIII was treated with aluminium bromide in benzene under the conditions described for the demethylation of (V). The product crystallized from dilute alcohol in colourless needles, m.p. 234° (Found: C, 68·0; H, 4·6. $C_{16}H_{12}O_5$ requires C, 67·6; H, 4·2%). The alcoholic solution of the substance gives an intense green colour with ferric chloride.

On acetylation with acetic anhydride and a few drops of pyridine in the usual manner the *triacetyl* derivative crystallized from alcohol in colourless needles, m.p. 105° (Found: C, 63·2; H, 4·8. $C_{22}H_{18}O_8$, 1/2 H_2O requires C, 63·0; H, 4·5). On drying at 120° and 2 mm. pressure over P_2O_5 for 4 hours, the m.p. rose to 139° (Found: C, 64·7; H, 4·8. $C_{22}H_{18}O_8$ requires C, 64·4; H, 4·4%).

3: 5-*Dicarbomethoxy*-2: 6-*dihydroxyphenyl benzyl ketone* (*XII*).—Dimethyl resorcinol-4:6-dicarboxylate (5 g.) in dry nitrobenzene (75 c.c.) at 5–10° was treated with powdered aluminium chloride (10 g.). Phenylacetyl chloride (5 c.c.) was gradually added, the reaction mixture stirred for 3 hours and left at room temperature for 24 hours. It was then heated on a steam-bath for an hour and poured over ice and hydrochloric acid. After steam distillation of nitrobenzene and unreacted ester, the product (5·75 g.) was filtered and crystallized thrice from dilute alcohol. The colourless needles had m.p. 131° (Found: C, 63·2; H, 4·6. $C_{18}H_{16}O_7$ requires C, 62·8; H, 4·6%). An alcoholic solution of the substance gives a blood-red ferric chloride colour. The 2: 4-*dinitrophenylhydrazone*, prepared as usual, crystallized from dilute acetone in yellow plates, m.p. 215° (Found: N, 10·3. $C_{24}H_{20}O_{10}N_4$ requires N, 10·6%).

2: 6-*Dihydroxyphenyl benzyl ketone* (*X*).—The ester (XII) (1 g.) was treated with boiling 10% alcoholic caustic soda (200 c.c.) for 3 hours, alcohol was distilled off, and the solution acidified and extracted with ether. The ether extract was extracted with sodium bicarbonate solution, the aqueous extract acidified and filtered. The precipitate was a carboxylic acid, but decarboxylation occurred during crystallization from water. The precipitate was decarboxylated by boiling with water for 3 hours, and the product (X) (0·5 g.) crystallized from dilute alcohol in faint yellow plates, m.p. 170° (Found: C, 74·0; H, 5·7. $C_{14}H_{12}O_3$ requires C, 73·7; H, 5·3%). The substance gives a green colour with alcoholic ferric chloride.

5-*Hydroxyisoflavone* (*IX*).—The ketone (X) (1 g.), dry pyridine (20 c.c.), piperidine (1 c.c.) and ethyl orthoformate (1·9 g.; 3 mols.) were refluxed for 8 hours, and poured into dilute hydrochloric acid. The separated solid was filtered (1 g.) and crystallized from dilute alcohol. The colourless needles had m.p. 102° (Found: C, 75·6; H, 4·4. $C_{15}H_{10}O_3$ requires C, 75·6; H, 4·3%). The alcoholic solution gives a dark violet colour turning immediately to dark olive with ferric chloride. The substance dissolves in aqueous caustic soda very slowly with a faint yellow colour. Acetylation by refluxing with acetic anhydride and pyridine for 2 hours gave the *acetyl* derivative which crystallized from dilute acetic acid in colourless needles, m.p. 144° (Found: C, 72·6; H, 4·5. $C_{17}H_{12}O_4$ requires C, 72·9; H, 4·3%).

Summary

5: 7: 2′-Trihydroxyisoflavone and 5: 7: 2′-trihydroxy-8-methylisoflavone have been synthesized, and have been found to be different respectively from "isogenistein" and "methylisogenistein" isolated by Okano and Beppu from soya bean.

As a preliminary to the synthesis of 5: 4′-dihydroxy-8-methylisoflavone, which Okano and Beppu have stated to be the probable structure of tatoin, another constituent of soya bean, 5-hydroxyisoflavone has been synthesized.

Our thanks are due to Dr. T. S. Gore for carrying out the microanalyses recorded in the paper.

REFERENCES

1. Walz .. *Ann.*, 1931, **489**, 118.
2. Okano and Beppu .. *J. Agri. Chem. Soc. Japan*, 1939, **15**, 645; 1940, **16**, 369.
3. Shriner and Hull .. *J. Org. Chem.*, 1945, **10**, 228.
4. Iyer, Shah and Venkataraman *Curr. Sci.* (*India*), 1949, **18**, 404.
5. Joshi and Venkataraman .. *J. Chem. Soc.*, 1934, 513; Späth and Lederer, *Ber.*, 1930, **63**, 745.
6. Baker, Harborne and Ollis .. *Chemistry and Industry*, 1952, 1058.
7. ——— and Ollis .. *Nature*, 1952, **169**, 706.
8. Sathe and Venkataraman .. *Curr. Sci.* (*India*), 1949, **18**, 373;
   Iyer, Shah and Venkataraman *Proc. Ind. Acad. Sci.*, 1951, **33 A**, 116.
9. Bhandari, Bose and Siddiqui *J. Sci. Ind. Research* (*India*), 1949, **8 B**, 217.

1140-52 Printed at the Bangalore Press, Bangalore City, by G. Srinivasa Rao, Superintendent and Published by The Indian Academy of Sciences, Bangalore.

INDEX TO VOL. XXXVI (A)

AUTHORS' INDEX

Anantakrishnan, S. V. .. Kinetic studies in ester hydrolysis, VII, 201.

Anantakrishnan, S. V. and Pai, K. V. Srinivasa — The Kjeldahl method of nitrogen determination, 299.

Balakrishna, S. .. Sound velocities in some Indian rock specimens, 375.

Bannerjee, N. R. and Seshadri, T. R. — Synthetic experiments in the benzopyrone series, XVIII, 134.

Batra, P. C. .. *See* Puntambeker and Batra.

Beri, R. M. .. *See* Rao and Beri.

Bhatnagar, C. and Bhawalkar, D. R. — Studies in electrets, I, 170.

Bhawalkar, D. R. .. *See* Bhatnagar and Bhawalkar.

Chandrasekhar, S. .. Some remarks on the optical rotary dispersion of quartz, 118.

Chowdhuri, B., Saxena, R. C. and Subramanian, A. — On the penetrating component in air showers, 457.

Datar, M. G. .. *See* Prasad and others.

Deshpande, S. M. .. *See* Sahasrabudhey and others.

Divatia, A. S. .. *See* Trivedi and others.

Doss, K. S. G. and Gupta, S. L. — Behaviour of surface-active substances at the dropping mercury electrode, 493.

Doss, K. S. G. and Saraswat, H. C. — Surface films of invertase, 343.

Gakhar, K. L. .. *See* Rao and Gakhar.

Gupta, S. L. .. *See* Doss and Gupta.

Ishaq, Mohd. .. *See* Shah and Ishaq.

Jain, A. C., Seshadri, T. R. and Thiruvengadam, T. R. — Nuclear oxidation in flavones and related compounds, XL, 217.

Jha, S. .. On the formation of alpha-particles in radioactive nuclei, 472.

Karmarkar, S. S., Shah, K. H. and Venkataraman, K. — Synthetical experiments in the chromone group, XXVI, 552.

Kartha, Gopinath .. Structure of halogenates of the type A $(BO_3)_2 H_2O$, I, 501,

Khanolkar, D. D. .. *See* Prasad and others.

Krishnamoorthy, P. N. .. *See* Taylor and others.

Krishnamurti, D. .. *See* Raman and Krishnamurti.

Lal, B. B. .. Photochemical after-effect in the bromine-oxalate reaction, 148.

Photochemical after-effect in H_2O_2-$K_4Fe.(CN)_6$ reaction, 244.

Lal, D., Pal, Yash, Peters, B. and Swami, M. S. — Production and interaction of mesons at very high energies, 75.

Manikarnikamma, S. N. — The second curvature of a geodesic on a hypersurface of a Riemannian space, 175.

Murthy, A. R. Vasudeva — Studies in the chemical behaviour of some compounds of sulphur, I, II, III, 388, 425, 537.

Muthuswami, T. N. .. Niggli's principles of igneous petrogenesis, 1.

Naranan, S. .. *See* Srikantan and Naranan.

Narasimhachari, N., Rajagopalan, D. and Seshadri, T. R. — A new effect of hydrogen bond formation (chelation), IV, 231.

Narasimhachari, N., Seshadri, T. R. and Sethuaraman, S. — Synthetic experiments in the benzopyrone series, XIX, 194.

Neelakantam, K. and Parthasarathi, K. — Volumetric determination of manganese with 8-hydroxy-quinoline, 123.

Pai, K. V. Srinivasa .. *See* Anantakrishnan and Pai.

Pal, Yash .. *See* Lal and others.

Panicker, A. R. .. *See* Singh and others.

Pankajamani, K. S. and Seshadri, T. R. — Survey of anthoxanthins, I, 157.

Parameswaran, M. R. .. Some converse theorems on summability, 363.

Parthasarathi, K. .. *See* Neelakantam and Parthasarathi.

Patani, M. J. .. *See* Trivedi and others.

Peters, B. .. *See* Lal and others.

Prasad, Mata, Khanolkar, D. D. and Datar, M. G. — Magnetic study of double salts in solution, 544.

Prasad, Raghu .. Preliminary observations on the temperature gradients and light penetration in the upper 200 feet of water of the Bay of Bengal, 61.

Puntambekar, S. V. and Batra, P. C. .. Chemical examination of the fatty oil from the seeds of *Steculia urens* Roxb., 284.

Rabindran, K., Sunthankar, A. V. and Tilak, B. D. A new synthesis of thiophenes and thiapyrans, VII, 405.

Rabindran, K. and Tilak, B. D. Thiophenes and thiopyrans, VIII, 411.

Raizada, P. S. .. *See* Saksena and Raizada.

Rajagopalan, D. .. *See* Narasimhachari and others.

Ramakrishna, B. S. .. *See* Rao and Ramakrishna.

Raman, C. V. and Krishnamurti, D. On the iridescence of potassium chlorate crystals, I, II, III, 315, 321, 330.

On the polarisation and spectral character of the iridescence of potassium chlorate crystals, 419.

Ramaseshan, S. and Suryan, G. Paramagnetic resonance in some cupric salts, 211.

Ramdas, A. K. .. The infra-red absorption spectrum of potassium chlorate crystals, II, 55.

Ranganathan, M. K. .. *See* Singh and others.

Rao, G. Venkat and Seshadri, T. R. A note on the biogenesis of pedicin, 130.

Rao, P. S. and Beri, R. M. Analysis of amino acids using paper chromatography (horizontal migration), 370.

Rao, P. S. and Gakhar, K. L. Studies on tuber hemicelluloses, II, 70.

Rao, R. V. Gopal .. *See* Sahasrabudhey and others.

Rao, S. K. Lakshmana, and Ramakrishna, B. S. Certain trigonometric summations, 208.

Sahasrabudhey, R. H., Deshpande, S. M., and Rao, R. V. Gopal Oxidation of ethanol under silent electric discharge, 258.

Saksena, B. D. and Raizada, P. S. Ring frequencies of dioxane and trioxane, 267.

Saraswat, H. C. .. *See* Doss and Saraswat.

Aging of surfaces of invertase solutions, 381.

Saxena, R. C. .. *See* Chowdhuri and others.

Sehgal, J. M. and Seshadri, T. R. Nuclear oxidation in flavones and related compounds, XLI, 355.

Seshadri, T. R. .. *See* Rao and Seshadri.

See Bannerjee and Seshadri,

		See Pankajamani and Seshadri.
		See Narasimhachari and others.
		See Jain and others.
		See Sehgal and Seshadri.
Sethuraman, S.	..	*See* Narasimhachari and others.
Shah, K. H.	..	*See* Karmarkar and others.
Shah, S. M. and Ishaq, Mohd.		Quasi-monotone series and an extension of Dvoretzky's theorem, 402.
Singh, B. K., Panicker, A. R. and Ranganathan, M. K.		Studies on the nature of the racemic modifications of optically active compounds in the solid state, IX, 440.
Sitaramaswami, M.	..	*See* Taylor and others.
Sreedhar, A. K.	..	Thermal expansion of crystals at low temperatures, I, 141.
Sreekantan, B. V.	..	Life-time of μ-mesons, 289.
Srikantan, B. V. and Naranan, S.		Cosmic rays underground, 97.
Srinivasan, N. R.	..	Studies on niobium and tantalum, IV, V, 185, 278.
Subramanian, A.	..	*See* Chowdhuri and others
Sunthankar, A. V.	..	*See* Rabindran and others.
Suryan, G.	..	*See* Ramaseshan and Suryan.
Swami, M. S.	..	*See* Lal and others
Taylor, H. J., Sitaramaswami, M., and Krishnamoorthy, P. N.		High altitude balloon experiments and measurement of the heavy primary radiation flux at the geometric equator, 41.
Thiruvengadam, T. R.	..	*See* Jain and others.
Thosar, Y. V.	..	On recurrence relations involving Legendre's associated functions of one kind only, 128.
Tilak, B. D.	..	*See* Rabindran and others.
		See Rabindran and Tilak.
Trivedi, A. K. M., Divatia, A. S. and Patani, M. J.		Studies in iron oxide sols, I, 530.
Udgaonkar, B. M.	..	Relativistic field quantization, 482.
Venkataraman, K.	..	*See* Karmarkar and others.
Viswanatham, B.	..	On the asymptotic behaviour of solutions of non-linear differential equations, 335.
Viswanathan, K. S.	..	The characteristic vibrations of a rectangular lattice, 306.

TITLE INDEX

Alpha-particles in radioactive nuclei, on the formation (Jha), 472.

Amino acids, analysis, using paper chromatography (horizontal migration) (Rao and Beri), 370.

Anthoxanthins, survey, I (Pankajamani and Seshadri), 157.

Benzopyrone series, synthetic experiments, XVIII (Bannerjee and Seshadri), XIX (Narasimhachari and others), 134, 194.

Biogenesis of pedicin, a note (Rao and Seshadri), 130.

Chromone group, synthetical experiments, XXVI (Karmarkar and others), 552.

Cosmic rays underground (Srikantan and Naranan), 97.

Differential equations, non-linear solutions, on the asymptotic behaviour (Viswanathan), 335.

Electrets, studies, I (Bhatnagar and Bhawalkar), 170.

Ethanol, oxidation, under silent electric discharge (Sahasrabudhey and others), 258.

Halogenates of the type A $(BO_3)_2.H_2O$, structure, I (Kartha), 501.

High altitude balloon experiments and measurement of the heavy primary radiation flux at the geomagnetic equator (Taylor and others), 41.

Hydrogen bond formation (chelation), a new effect, IV (Narasimhachari and others), 231.

Infra-red absorption spectrum of potassium chlorate crystals, II (Ramdas), 55.

Iridescence of potassium chlorate crystals, I, II, III (Raman and Krishnamurti), 315, 321, 330.

Iridescence of potassium chlorate crystals, on the polarisation and spectral character (Raman and Krishnamurti), 419.

Iron oxide sols, studies, I (Trivedi and others), 530.

Kinetic studies in ester hydrolysis, VII (Anantakrishnan), 201.

Optically active compounds in the solid state, racemic modifications, studies on the nature, IX (Singh and others), 440.

Optical rotary dispersion of quartz, some remarks (Chandrasekhar), 118.

Magnetic study of double salts in solution (Prasad and others), 544.

Manganese, volumetric determination, with 8-hydroxy-quinoline (Neelakantam and Parthasarathi), 123.

Mesons, production and interaction, at very high energies (Lal and others), 75.

μ-Mesons, life-time (Sreekantan), 289.

Niggli's principles of igneous petrogenesis (Muthuswami), 1.

Niobium and tantalum, studies, IV, V (Srinivasan), 185, 278.

Nitrogen determination, kjeldahl method (Anantakrishnan and Pai), 299.

Nuclear oxidation in flavones and related compounds, XL (Jain and others), XLI (Sehgal and Seshadri), 217, 355.

Paramagnetic resonance in some cupric salts (Ramaseshan and Suryan), 211.

Penetrating component in air showers (Chowdhuri and others), 457.

Photochemical after-effect in the bromine-oxalate reaction (Lal), 148.

Photochemical after-effect in H_2O_2–$K_4Fe(CN)_6$ reaction (Lal), 244.

Quasi-monotone series and an extension of Dvoretzky's theorem (Shah Ishaq), 402.

Rectangular lattice, the characteristic vibrations (Viswanathan), 306.

Recurrence relations involving Legendre's associated functions of one kind only (Thosar), 128.

Relativistic field quantization (Udgaonkar), 482.

Riemannian space, hypersurface, the second curvature of a geodesic (Manikarnikamma), 175.

Ring frequencies of dioxane and trioxane (Saksena and Raizada), 267.

Sound velocities in some Indian rock specimens (Balakrishna), 375.

Steculia urens Roxb., seeds of, fatty oil from, chemical examination (Puntambekar and Batra), 284.

Sulphur, some compounds, chemical behaviour, studies, I, II, III (Murthy), 388, 425, 537.

Summability, some converse theorems on (Parameswaran), 363.

Surface-active substances, behaviour, at the dropping mercury electrode (Doss and Gupta), 493.

Surfaces, aging, invertase solutions (Saraswat), 381.

Surface films of invertase (Doss and Saraswat), 343.

Temperature gradients and light penetration in the upper 200 feet of water of the Bay of Bengal, preliminary observations (Prasad), 61.

Thermal expansion of crystals at low temperatures, I (Sreedhar), 141.

Thiophenes and thiapyrans, a new synthesis, VII (Rabindran and others), VIII (Rabindran and Tilak), 405, 411.

Trigonometric summations, certain (Rao and Ramakrishna), 208.

Tuber hemicelluloses, studies, II (Rao and Gakhar), 70.

NOTICE TO AUTHORS

Scientific papers intended for publication in the *Proceedings of the Indian Academy of Sciences* can be accepted only when they are communicated by a Fellow of the Academy whose duty shall be to satisfy himself that such communications are fit to be read at the Meeting of the Academy and published in its *Proceedings*.

Papers should not ordinarily exceed fifty pages of foolscap. MSS. should be either typewritten or written in legible hand on one side of the paper. All papers should be carefully revised by the authors and should be absolutely in final form for printing. Position for text-figures should be indicated. Each paper shall conclude with a critical summary not exceeding 350 words.

Drawings, diagrams or other illustrations should be made on larger scale (preferably) twice the size than the ones in which they are intended to appear. They should be done in Indian ink on bristol board with lettering in pencil. Scale of magnification of camera lucida tracings should be indicated by the side of drawings. In certain special cases arrangements will also be made for monochrome lithographic and other colour plates. Reduction of illustrations desired should be indicated in pencil. Appropriate legends should accompany all drawings. Names of authors are to be marked in pencil on the left-hand corner of drawing sheets. Photomicrographs should be securely mounted with colourless paste.

All tables, quotations and footnotes which will be set hereafter (beginning from Vol. I, No. 2) in types smaller than the text, should be typewritten on separate sheets and placed with the text in proper sequence. Footnotes should be numbered in Arabic numerals.

References to literature in the text should be given, whenever possible, in chronological order, only the names of authors and years of publication, in brackets, being given. They should be cited in full after the summary, the authors' names following in alphabetical order. Thus,

Name or Names of author; Name of Journal (abbreviation) with a single underline; Year of publication; Number of Volume with a double underline, and lastly page. The following would be a useful illustration:—

Bergmann and Stather . . . . . Z. Physiol. Chem., 1926, 152, 189.

Two copies of slip-proof and wherever possible, a page proof for final revision will be sent to authors. All corrections are best made on the slip-proof which should be transmitted to the Office of the Academy. All proof corrections involve heavy expenses which would be negligible if the papers are carefully revised by the authors before submission.

Authors will be supplied with reprints of their papers at cost price, if intimation is given at the time of returning the slip-proof.

All the blocks printed in the *Proceedings* will be offered to the respective authors at a price of 25% of the actual cost of preparing the blocks *plus* the packing and postal charges or railway freight to be incurred for despatching them, it being understood that authors should give due acknowledgment to the Academy whenever such blocks are reproduced in other journals.

The original drawings and plates of blocks appearing in the *Proceedings* will be returned to such of the authors as may require them provided the cost of despatching such originals is borne by them.

CONTENTS

PAGE

On the Polarisation and Spectral Character of the Iridescence of Potassium Chlorate Crystals . . . . Sir C. V. Raman and D. Krishnamurti 419

Studies in the Chemical Behaviour of Some Compounds of Sulphur. Part II. Reaction Between Disulphur Monoxide and Hydrogen Iodide . . . . . A. R. Vasudeva Murthy 425

Studies on the Nature of the Racemic Modifications of Optically Active Compounds in the Solid State. Part IX. Camphor-β-Sulphonamides, Camphor-β-Sulphonanhydramides, Camphor-β-Sulphon-phenyl, *o*-tolyl-, *m*-tolyl-, *p*-tolyl-, α-naphthyl-, and β-naphthyl-amides (*d* and *dl*) . . . . . Bawa Kartar Singh, A. R. Panicker and M. K. Ranganathan 440

On the Penetrating Component in Air Showers . . . . . B. Chowdhuri, R. C. Saxena and A. Subramanian 457

On the Formation of Alpha-Particles in Radioactive Nuclei . . . .S. Jha 472

Relativistic Field Quantization . . . . . B. M. Udgaonkar 482

Behaviour of Surface-Active Substances at the Dropping Mercury Electrode . . . . . K. S. G. Doss and S. L. Gupta 493

Structure of Halogenates of the Type A $(BO_3)_2.H_2O$. I. Barium Chlorate Monohydrate Ba $(ClO_3)_2.H_2O$ . . . . . Gopinath Kartha 501

Studies in Iron Oxide Sols. Part I. Electrical Conductivity of Iron Oxide Sol . . . . . A. K. M. Trivedi, A. S. Divatia and M. J. Patani 530

Studies in the Chemical Behaviour of Some Compounds of Sulphur. Part III. Formation of Disulphur Monoxide by the Reaction Between Hydrogen Sulphide and Sulphur Dioxide . . . . A. R. Vasudeva Murthy 537

Magnetic Study of Double Salts in Solution . . . . . Mata Prasad, D. D. Khanolkar and M. G. Datar 544

Synthetical Experiments in the Chromone Group. Part XXVI. Synthesis of 5 : 7 : 2′-Trihydroxyisoflavone, 5 : 7 : 2′-Trihydroxy-8-methylisoflavone and 5-Hydroxyisoflavone . . . . . S. S. Karmarkar, K. H. Shah and K. Venkataraman 552

PAGE
um
rti 419
II.
thy 425
ive
es,
yl-,
an 440
ian 457
Jha 472
kar 482
pta 493
ate
tha 501
Sol
ani 530
III.
gen
thy 537
tar 544
esis
one
nan 552